LABORATORY INVESTIGATION OF INFILTRATION PROCESS OF NON-NEWTONIAN FLUIDS THROUGH POROUS MEDIA IN A NON-ISOTHERMAL FLOW REGIME FOR EFFECTIVE REMEDIATION OF ADSORBED CONTAMINANTS

By

Fawad Naseer, B.S.

A Thesis Submitted in Partial Fulfillment for the Degree of

Master of Science

in

Geological Engineering

University of Alaska Fairbanks

December 2019

APPROVED:

Debasmita Misra, Committee Chair
Paul Metz, Committee Member
Obadare Awoleke, Committee Member
Majdi Abou Najm, Committee Member
Tathagata Ghosh, Chair
Department of Mining and Geological Engineering
Bill Schnabel, Dean
College of Engineering and Mines
Michael Castellini, *Dean of the Graduate School*

Abstract

Contamination of soil and groundwater have serious health implications for man and environment. The overall goal of this research is to study a methodology of using non-Newtonian fluids for effective remediation of adsorbed contaminants in porous media under non-isothermal flow regimes. Non-Newtonian fluids (Guar gum and Xanthan gum solutions) provide a high viscous solution at low concentration and these fluids adjust their viscosities with applied shear rate and change in temperature. Adjustment of viscosity with an applied rate of shear is vital for contaminant remediation because non-Newtonian shear thinning fluids can penetrate to low permeability zones in subsurface by decreasing their viscosities due to high shear rates offered by low permeability zones.

The application of non-Newtonian shear thinning fluids for contaminant remediation required the improvement in understanding of rheology and how the factors such as concentration, temperature and change in shear rate impacted the rheology of fluids. In order to study the rheology, we studied the changes in rheological characteristics (viscosity and contact angle) of non-Newtonian fluids of different concentrations (i.e., 0.5g/l, 1g/l, 3g/l, 6g/l and 7g/l) at different temperatures ranging from 0 ºC to 30 ºC. OFITE model 900 viscometer and Tantec contact angle meter were used to record the changes in viscosity of fluids for an applied range of shear rate (i.e., 17.02 s^{-1} to 1021.38 s^{-1}) and contact angles, respectively, for different concentrations of non-Newtonian fluids.

Understanding the flow characteristic of non-Newtonian fluids under low temperature conditions could help in developing methods to effectively remediate contaminants from soils. Results of rheological tests manifested an increase in the viscosity of both polymers with concentration and decrease in temperature. Mid (i.e., 3g/l) to high (i.e., 6g/l and 7g/l) concentrations of polymers manifested higher viscosities compared to 0.5g/l for both polymers. Flow of high viscous solutions required more force to pass through a glass-tube-bundle setup which represented a synthetic porous media to study the flow characteristic and effectiveness of Newtonian and non-Newtonian fluids for contaminant remediation. Low concentrations of 0.5g/l were selected for flow and remediation experiments because this concentration can flow through porous media easily without application of force. The 0.5g/l of Xanthan gum and de-ionized water were used to conduct the infiltration experiments to study the flow characteristics of Newtonian and non-Newtonian fluids at 0.6°C, 5°C and 19°C in synthetic porous media.

Infiltration depth of both Newtonian and non-Newtonian fluids would decrease with the decrease in temperature because of the change in their properties like dynamic viscosity, density and angle of contact.

The result of comparison of Newtonian and non-Newtonian fluids showed water to be more effective in remediating a surrogate adsorbent contaminant (Dichlobenil) from the synthetic porous media at 19°C. This result was counter-intuitive to what we began with as our hypothesis. However, it was also observed later that 0.5 g/l concentration of Guar gum behaved more like a Newtonian fluid and 0.5 g/l concentration of Xanthan gum had not shown strong non-Newtonian behavior compared to higher concentrations of Xanthan gum. Hence more analysis needs to be done to determine what concentration of non-Newtonian fluid should be more effective for remediation.

This thesis is dedicated to my dear parents for their eternal love, support and care.

Table of Contents

List of Figures

List of Tables

List of Abbreviations

APRE	Absolute percent relative error
D_z	Infiltration depth
d_{adj}	Minimum ratio between the ith and (i+1) th representative radius
d_{range}	Maximum ratio between the largest and smallest radius
g	Gravitational acceleration
$\frac{\partial h}{\partial z}$	Head gradient per unit length.
K	Consistency index
MDD	Maximum displacement distance
NSE	Nash-Sutcliffe efficiency coefficient
Pr	Prandtl number
N	Power law index
Q	Flow
Q	Velocity
R	Representative radius
t	Time
v	Velocity for fluid
w	Weights
PBIAS	Percent bias
Y^{mean}	Mean of the observed data
Y^{obs}	Observation value
Y^{sim}	Simulation value
Greek symbols	
α	Power law index
β	Consistency index
ρ	Density
τ	Shear stress
γ	Shear rate

Acknowledgments

I am grateful to Dr. Debasmita Misra for his constant guidance, support, and motivation throughout the research work. His encouragement in my many moments of crisis helped me to accomplish my research. I would also like to thank my committee member Dr. Majdi Abou Najm for his assistance during the entire duration of this research. Many thanks to Dr. Obadare Awoleke for guiding me with the rheological experiments during the beginning of my experimental work. Thanks to Dr. Paul Metz for his valuable suggestions and comments to guide me in the correct direction. Thanks to Nabil Michel Atallah for providing me the Matlab solver and helping me to get familiar with solver through discussions. I greatly appreciate the help provided by Shane Billings, Tauseef Mahmood and staff of machine shop for experiments.

This work would not have been possible without the financial support of USGS-National Institute of Water Resources (NIWR), National Institute of Food and Agriculture (NIFA) USDA Hatch program, University of Alaska Fairbanks Clarence Berry fellowship and Alaskan Section of American Water Resources Association scholarship. I am thankful to all the funding agencies for the financial support.

Heartfelt thanks to my parents, sisters, brother, and wife for their unconditional love, care, and infinite prayers. You are my constant source of inspiration I would not have achieved this without your support.

Chapter 1 Introduction

Contamination of soil and groundwater by adsorbed contaminants such as phosphates, carbon tetrachloride, chlorinated aliphatic hydrocarbons (CAH), certain emerging contaminants (e.g., PFAS), or certain heavy metals have been of major concern lately (e.g., Jung et al., 2016; Palaniappan et al., 2010; Barnes et al., 2007; Gillham and O'Hannesin, 1994). Quality of water is increasingly threatened as human populations grow, industrial and agricultural activities expand, and as climate change threatens to cause major alterations of the hydrologic cycle. Inadequately treated sewage, industrial and agricultural or food wastes, dissolved metals and many emerging contaminants, enter through the soil to pollute the groundwater on a daily basis. Additionally, mining, oil and gas exploration and production, industrial and nuclear plants are adding to the problem. A lack of understanding of fate and transport of contaminant within soil matrix and groundwater makes the situation worse.

Preferential flow of contaminants through soil to groundwater is defying the conceptual understanding of flow and transport through porous media. Adding to the complexity are the highly adsorbed contaminants that do not travel at a rate proportional to the flux rate of water in the porous media. Experimental and field observations show that the infiltration of water does not necessarily move downward at a uniform rate in a specific direction. In reality, water and contaminant travel in a wide range and at varying velocities. Hence, contaminant remediation methods need to be adapted to their distribution within the soil matrix and flow pathways.

Non-Newtonian fluids are gaining interest for contaminant remediation because these fluids exhibit viscosity change with change in shear rate. Jung et al. (2016 and references therein) provide a comprehensive review of "important characterization and remediation techniques that have been developed to deal with the contamination of soils and sediments. Soil remediation technologies such as excavation, soil vapor extraction, bioremediation, surfactants enhanced remediation, and steam injection have been used for many years. The excavation of contaminated soil is a simple solution. However, this method has become less popular owing to its high cost and the lack of available landfill sites. Instead, soil flushing methods such as soil vapor extraction, surfactant-enhanced remediation, and steam injection have been more popular in recent years. Among these, surfactant-enhanced remediation facilitates an enhanced rate of remediation by exploiting the low surface tension of the surfactants. Oil-contaminated sites have

been remediated by in-situ flushing using biosurfactants (e.g., D'Cunha and Misra; 2005; D'Cunha et al., 2009), that is, surface-active substances synthesized by living cells. Biopolymers synthesized from plants can also be used instead of biosurfactants as an eco-friendly soil remediation method. Biopolymer flushing was originally developed for petroleum-enhanced oil recovery, and subsequently, it has been used for the remediation of petroleum waste at contaminated sites."

A biopolymer is a non-Newtonian fluid that has recently experienced growing interest in many petroleum and environmental engineering applications. Besides enhanced oil recovery, recently, fracturing agents and drilling muds with complex rheologic behavior are being used in low permeability formations in the oil and gas industry. This non-Newtonian flow through porous media accomplishes fracture cleanup operation that follows hydraulic fracturing during oil-well completion (Balhoff and Thompson, 2006). In environmental applications, liquid pollutants and wastes such as suspensions, solutions and emulsions of various substances, certain asphalts and bitumen, greases, sludges, and slurries may migrate in the subsurface and penetrate into underground reservoirs, leading to groundwater contamination. Non-Newtonian fluid (biopolymer) flow in porous media is also relevant in soil remediation processes involving the removal of liquid pollutants via chemical (often polymerization) reactions (Di Federico et al., 2010).

The basic principle of biopolymer flushing is that the addition of a biopolymer to the flushing water leads to increased viscosity and capillary number, decreased mobility, and contact with a larger volume of the reservoir (Lake, 2008). The capillary number of a fluid is related to the fluid velocity, fluid viscosity, and surface tension. Mobility is a relative measure of how easily a fluid moves through porous media. Apparent mobility is defined as the ratio of the effective permeability to the fluid viscosity (Sorbie, 1991). The physical properties of biopolymers, such as viscosity, surface tension, and contact angle, are important to determine when using biopolymer solutions is feasible for the remediation of contaminated soils (Jung et al., 2016).

Biopolymers such as polyacrylamide (PAM) and Xanthan gum have shown great promise for enhanced oil recovery (EOR) because they lead to an increase in the viscosity of water, decrease in the mobility of water, and contact with a larger volume of the reservoir (Blokker, 2014; Pollock et al., 1994; Hove et al., 1990). Xanthan gum was tested to deliver remedial

amendments (e.g., phosphate, sodium lactate, ethyl lactate) for subsurface remediation (Zhong et al., 2013). Xanthan gum is a microbial polysaccharide discovered in the 1950s by the U.S. Department of Agriculture with high molecular weight and high solubility. Xanthan gum shows viscosity synergy with Guar gum.

The biopolymer Guar gum is also an excellent candidate for remediation of contaminated soils (Velimirovic et al., 2014). Guar gum is the natural material obtained from the Guar seeds. It is a non-Newtonian shear thinning (viscosity decreases with an increase in stress) fluid (Figure 1.1). The shear offered by the low permeability zones is high, which allow the shear thinning fluid to decrease its viscosity with increase in shear rate. This decrease in viscosity helps penetration of shear thinning fluid into hard-to-reach low permeability zones in the subsurface porous media. The mixture of Guar gum with water increases the viscosity and allow better transportation and suspension of the fluid. Guar gum is naturally biodegradable and thus has almost no environmental impacts on the soil. Guar gum and Xanthan gum solutions were used as the non-Newtonian fluids in this research.

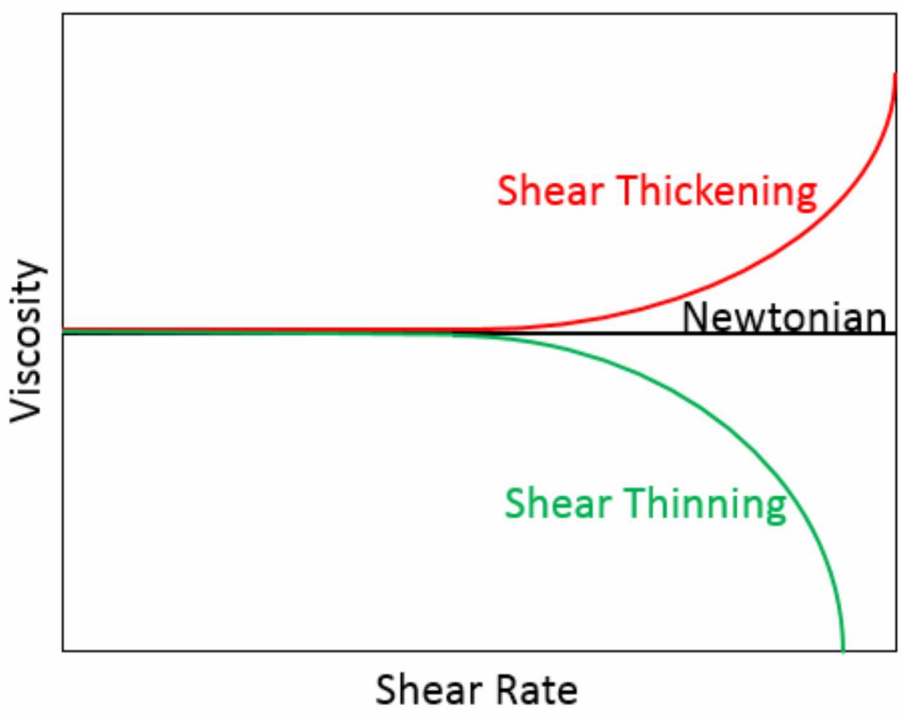

Figure 1.1. Viscosity vs shear rate relationship for Newtonian and non-Newtonian (shear thickening and shear thinning) fluids

While laboratory and field scale studies including modeling of non-Newtonian fluid flow in porous media as a remediation agent has been studied, but such studies have been limited to porous media temperatures of approximately 30°C. According to Jung et al. (2016), previous work on biopolymers were limited to the evaluation of the shear strength, stiffness, and erosion resistance properties of soils saturated with biopolymer solutions. Little is known about the flow characteristics of biopolymer solutions through a porous medium, especially at the range of low temperatures that are experienced in cold regions such as Alaska.

Complexities associated with the pore structures hinder the flow model development for a porous media. The proper understanding of the complex pore structures and flow pattern in the media is most important. A knowledge of such complexity will provide an opportunity to study and compare the behavior of non-Newtonian fluid and Newtonian fluid under different temperature regimes in the soil. It is critical to understand the impact of temperature on the flow or rheology of Guar gum and Xanthan gum solutions in soil because the adsorption kinetic of each adsorbent contaminant is different. Understanding of the flow characteristic of non-Newtonian fluids will help us to investigate its effectiveness in remediation of adsorbed contaminants such as Dichlobenil, Phosphates and Carbon Tetrachloride.

Our hypothesis is that the difference in rheological characteristics between Newtonian and non-Newtonian fluids make the latter a better candidate for fluid flow and remediation of adsorbed contaminants from soils at different thermal regimes. The major goal of this research is to determine a method for effective remediation of adsorbed contaminants in soils of cold regions using non-Newtonian fluids. In order to accomplish the goal, we have completed the following objectives using a synthetic porous media in laboratory settings.

- Study the effect of temperature on rheological properties of Guar gum and Xanthan gum of different concentrations. (Chapter 2)
- Study the flow characteristics of Newtonian and non-Newtonian fluids under different thermal regimes. (Chapter 3)
- Comparison of Newtonian and non-Newtonian fluid for remediation of adsorbed contaminant. (Chapter 4)

Chapter 2 Effect of temperature on rheological properties of Guar gum and Xanthan gum of different concentrations[1]

Abstract

The overall goal of this research is to study a methodology of using non-Newtonian fluids for effective remediation of adsorbed contaminants in porous media under non-isothermal flow regimes. Different concentrations of non-Newtonian fluids (Guar gum and Xanthan gum solutions) were exposed to temperatures ranging from 0.6 ºC to 30.6 ºC to study the changes in viscosity, contact angle and shear stress with change in shear rate. Separate sample solutions for Guar gum and Xanthan gum having concentrations of 0.5g/l, 1g/l, 3g/l, 6g/l, and 7g/l were prepared. OFITE model 900 viscometer and Tantec contact angle meter were used to record the changes in viscosity and contact angle at 0.6 °C, 5 ° C, 15 °C, 19 °C and 30.6 °C. The range of shear rate applied varied from 17.02 s^{-1} to 1021.38 s^{-1}. It was observed that the sample solutions of Xanthan gum behaved as **non-Newtonian** shear-thinning fluid for the selected range of temperature and concentration. Guar gum also displayed non-Newtonian shear thinning behavior for mid to high concentrations but was asymptotic to Newtonian behavior for low concentrations. Increase in temperature increased the shear thinning behavior of Xanthan gum solutions. At 5 ºC the addition of salt in low to mid Guar gum concentrations increased the viscosity, whereas, a higher concentration of 7g/l exhibited viscosity decrease. With the increase in temperature to 30.6°C, low to mid Guar gum concentrations also displayed decrease in viscosity.

Keywords: Non-Newtonian, Rheology, Guar gum, Xanthan gum, Temperature

2.1 Introduction

Soil and groundwater contamination is emerging as a great concern. Soil contamination in urban and rural environments maybe caused at industrial sites such as mining heaps, dumps, filled natural depressions, and quarries (Meuser, 2010). Mine drainage water contains metals, salts, coal and other minerals that may be highly adsorbed to soils and within the saturated porous media. According to Palaniappan et al. (2010), there are approximately 500,000

[1]Naseer et al. Effect of temperature on rheological properties of Guar gum and Xanthan gum of different concentrations. Unpublished Manuscript 2019.

abandoned mines alone in the United States. The state of Colorado alone has 23,000 abandoned mines that have polluted 2,300 km of streams. Oil and gas industrial processes like hydraulic fracturing, oil purification, oil and gas storages, pipelines and oil spills are contributing to soil and water contamination (Jung et al., 2016). With such adsorbed contaminants in soils and aquifers having a potential of increased prevalence in a rapidly changing climatic environment, it is critical that effective remediation measures be tested and developed to clean the soil and aquifer environments. The major goal of this research is to determine a method for effective remediation of adsorbed contaminants in soils of cold regions using non-Newtonian fluids.

In recent years, use of non-Newtonian fluids are gaining interest for soil and groundwater remediation. These fluids exhibit change in viscosity with applied shear rate. Non-Newtonian shear thinning fluids are characterized by decrease in viscosity with increase in rate of shear. Non-Newtonian shear thinning fluids penetrate into low permeability zone because these zones offer higher shear rates to fluid, which results in decrease of fluid viscosity and thus facilitates its penetration in low permeability zones (Zhong et al., 2013).

The two most common non-Newtonian fluids are solutions of Guar gum and Xanthan gum. Guar gum solution has been investigated for the treatment of drinking water, industrial effluent, and transportation of microscale zero-valent iron particles in porous media (Mukherjee et al., 2017, Gupta and Ako, 2005, Tosco et al., 2014). Xanthan gum solution has been tested to deliver remedial amendments (e.g., phosphate, sodium lactate, ethyl lactate) for subsurface remediation (Zhong et al., 2013). These industrial applications of polymers are possible due to their unique property of producing a high viscous solution with low concentration. Moreover, both gums are non-toxic, cheap and biodegradable (Brunchi et al., 2016, Yang et al., 2015). The unique property of producing high viscous aqueous solutions of these gums are influenced by concentration, temperature, and salt. Thus, it is important to understand how these three factors influence rheology to know the potential of these polymers in a variety of engineering applications, including remediation of soils.

2.1.1 Chemistry of Guar Gum

The Guar gum solution, as a non-Newtonian fluid, is an excellent candidate for the remediation of contaminated soils (Velimirovic et al., 2014). Guar gum is galactomannan (mannose backbone with galactose side groups) polysaccharide mainly extracted from the Cyamopsis Tetragonolobus (Torres et al., 2014), which is cultivated in the Indian subcontinent

from ancient times (Mudgil et al., 2014). These polysaccharides are formed by molecules of galactose and mannose. The principal backbone is the chain of (1-4) - β-D-mannopyranosyl units with (1-6) α-D-galactopyranosyl units linked to the principal chain (Figure 2.1; McCleary et al., 1981; Wientjes et al., 2000; KÕk et al.,1999). The mannose to galactose ratio in solution is temperature dependent (Casas et al., 2000). Guar gum dissolves in a polar solvent by forming strong hydrogen bonds. The greater branching of Guar is believed to be responsible for greater hydrogen bonding activity. Hydrogen bonding activity of Guar gum is due to the presence of hydroxyl group in the Guar gum molecule (Mudgil et al., 2014).

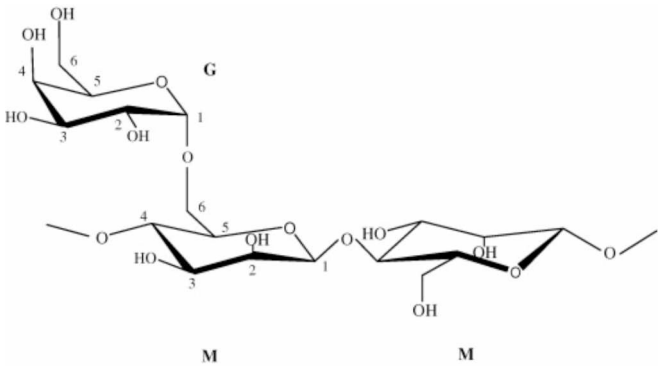

Figure 2.1. Chemical representation of Guar gum molecule, showing the positions of Galactose (G) and Mannose (M) on the polysaccharide chain (Ding et al., 2008)

Low concentration of Guar gum that has a higher molecular weight manifests high viscosity, which changes with shear rate. Extensive intermolecular entanglement through hydrogen bonding and higher molecular weight provides high viscosity of Guar gum solution (Sandolo et al., 2009). Variation of molecular weight depends on the chain length of the polysaccharide. As mentioned earlier, mannose to galactose ratio in a solution is temperature dependent. Molecules with high molecular weight and high galactose to mannose ratio have greater probability of solubility when temperature is raised. (Casas et al., 2000).

Guar gum dispersion in water leads to the intermolecular chain entanglement causing the viscosity of aqueous solution (Srichamroen, 2007). Higher concentrations enhance the molecular entanglement, limiting the length to which the molecules will be extended. The presence of entanglement leads to the formation of a gel-like structure (Martin-Alfonso et al., 2018, Torres et al., 2014). High viscous solutions exhibit the non-Newtonian shear thinning behavior in which the apparent viscosity decreases with the increase in shear rate. This shear-thinning behavior of

Guar gum aqueous solution was reported by many researchers (e.g., Torres et al., 2014, Chenlo et al., 2010, Bourbon et al., 2010) at temperature above 20°C.

Our experiments revealed that low concentration of Guar gum solution showed inconsistency in viscosity with the increase in shear rate, as illustrated in Figure A1. During the 2017 American Geophysical Union annual meeting (Naseer et al., 2017), it was recommended to us that addition of salt to low concentrations of Guar gum may resolve the issue of inconsistence changes to viscosity with change in shear rate, as observed in Figures A1a and A1b. Rheological experiments were conducted by adding NaCl (10g/l) or KCl (10g/l) separately to Guar gum solutions to investigate the effect of salt concentration on viscosity of the polymer solution. Reviewing the literature, we found Gittings et al., (2001) reported that the addition of salts results in a decrease in viscosity with the possible explanation that presence of salt ions in solution disrupts the covering of water molecules around the Guar chain which results in a decrease in solubility of Guar gum in water. We have studied the effect of temperature on the sheath of water molecules around Guar gum chain for saline Guar gum solutions by conducting the rheological experiments at different temperatures.

2.2.2 Chemistry of Xanthan Gum

Xanthan gum is a microbial polysaccharide discovered in the 1950s by the U.S. Department of Agriculture. It has a high molecular weight and high solubility. Xanthan gum shows viscosity synergy with Guar gum. Primary structure of Xanthan gum consists of β- (1-4) -D-glucose (cellulose) backbone that is substituted at every C_3 second glucose residues by charged trisaccharide side chain namely a D-glucuronic acid unit between two D-mannose units. One D-mannose unit is linked to the main chain and contains an acetyl group at position O_6 and other one contains a pyruvic acid residue linked via keto group to the 4 and 6 positions. Xanthan secondary structure of double helix is dependent on temperature, concentration and salinity conditions (Figure 2.2; Brunchi et al., 2014; Martin-Alfonso et al., 2018).

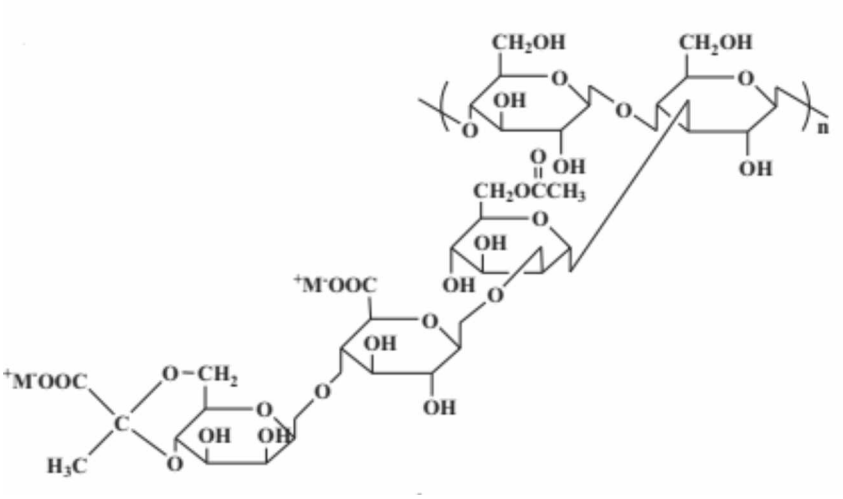

Figure 2.2. Structure of Xanthan gum (Xu et al., 2013)

Similar to Guar gum, Xanthan gum shows non-Newtonian shear thinning behavior resulting from molecular entanglement. This molecular entanglement is concentration dependent. Thus, higher concentrations would impact the shear thinning behavior of Xanthan gum solution.

In water, the Xanthan backbone is disordered and highly extended due to the electrostatic repulsions exhibited between charged groups that belong to the side chains. The high extended structure favors the hydrogen bonding and a randomly broken helix is formed (Brunchi et al., 2014). In temperatures between 25°C to 40°C, Xanthan gum maintained ordered conformation stabilized by the hydrogen bonding but destabilized by electrostatic repulsion between negatively charged groups (Casas et al., 2000).

2.2.3 Rheology

Rheology is the science of deformation and flow behavior of fluid under applied stress. Viscosity is the important rheological term associated with the rheology study which determines how the fluid will flow under a variety of conditions, including temperature and shear rate. Viscosity of Newtonian fluids does not change with the shear rate. However, viscosity of non-Newtonian fluid changes with change in shear rate. Knowledge of rheological properties of fluid and how the factor like temperature and shear rate would affect the rheological properties are essential to understand the flow and contaminant remediation in the subsurface porous media. For example, temperature affects the viscosity of non-Newtonian fluids, which will impact the flow of and the scouring (can be useful in remediation of the residual contaminant from the porous media surface) property of the non-Newtonian fluid.

Many researchers have investigated the rheological properties of Guar gum and Xanthan gum. Most of these studies (e.g., Casas et al., 2000; Brunchi et al., 2016; Chenlo et al., 2010) were conducted at temperatures above 20°C. Little is known about the impact of low (i-e., 0.6°C, 5°C, 15°C) temperature, such as those experienced in cold regions soils, on rheological properties of these polymers. We are aware of only one study conducted by Srichamroen, (2007) for Guar gum at 4°C.

To achieve our broad objective of studying the methodology of non-Newtonian fluids for contaminant remediation, it is important to understand the impact of environmental factors (i.e., the temperature of porous media (soil), the salinity and shear offered by low and high permeability zones) on fluid rheology. Viscosity and contact angle are most important aspects associated with non-Newtonian fluids that can affect flow and contaminant remediation in the subsurface porous media.

To understand the changes in rheology of non-Newtonian fluids with change in temperature, we studied the change in viscosity, contact angle and shear stress with change in shear rate at 0.6 °C, 5 ° C, 15 °C, 19 °C and 30.6 °C for Guar gum and Xanthan gum solutions. Some questions addressed in this research work are as follow:

- How would selected temperature range affect the viscosity of Guar gum and Xanthan gum solutions of different concentrations?
- How would the effect of temperature affect the non-Newtonian behavior of these polymers?
- How would the addition of salts (10,000 mg/L) impact the rheological properties of Guar gum? Does the type of salt (NaCl or KCl) influence the rheological properties differently?

2.2 Methodology

Commercial food grade Guar gum (Derived from Cyamopsis Tetragonolobus) and Xanthan gum were used without any further purification. Experimental aqueous solutions were prepared for concentrations of 0.5g/l, 1g/l, 3g/l, 6g/l and 7g/l by slowly dispersing defined amounts (0.5g, 1g, 3g, 6g, and 7g) of Guar gum or Xanthan gum into a rapidly swirling vortex of one liter of distilled water (Patel et al., 1987; Venugopal et al., 2010). Sample solutions were prepared by using food blender for two minutes to avoid the formation of clumps and later stirred at 1000 rpm for thirty minutes at 19°C temperature. Changes in viscosity and contact angles of prepared Guar gum and Xanthan gum solutions were recorded at 0.6 °C, 5 ° C, 15 °C, 19 °C and

30.6 °C with application of different shear rates. To attain these temperatures, sample solutions were kept in a cold chamber for 3 hours. Sodium Chloride (10g/l) and Potassium Chloride (10g/l) were added separately to different concentrations of Guar gum to study the impact of salinity on change in viscosity of Guar gum solutions with change in applied shear rates. Concentration of salts (Swann, 2017) and polymers (Casas et al., 2000; Chenlo et al., 2010; Torres et al., 2014; Bradley et al., 1989) were selected based on the specifications provided in available literature.

Rheological tests were conducted by using the OFITE model 900 viscometer to record changes in viscosity and shear stress of the solutions at different shear rates at a particular temperature. Tantec contact angle meter was used to record the contact angle of solutions at different temperatures. The sample container was wrapped by insulated material to maintain the temperature of the solution during each measurement. The temperature of the sample was recorded before and after each rheological test. A maximum of ±2 °C change was observed amongst all rheological analyses. A minimum of three replicates were conducted for each test. Figure 2.3 provides set up of rheological tests.

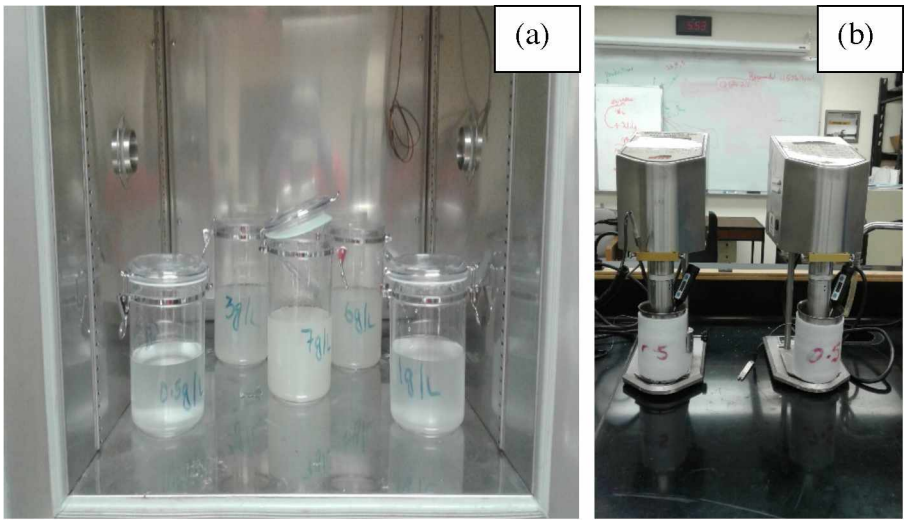

Figure 2.3. (a) Samples of different concentration are in Thermotron temperature chamber to attain the desired temperature. (b) OFITE Model 900 viscometer used to find the apparent viscosity of Guar gum and Xanthan gum samples at different shear rates.

2.3 Results and Discussion

2.3.1 Rheological Study of Guar Gum

Guar gum solutions of different concentrations were investigated for a change in viscosity depending on the level of shear rate. Figure 2.4 summarizes the variation of the apparent viscosity with increase in shear rate for Guar gum solutions at different temperatures. Mid (i.e., 3g/l) to high (i.e., 6g/l and 7g/l) Guar gum concentrations showed decrease in viscosity with an increase in shear rate (Figure 2.4). Temperature had a lesser effect on viscosity change when the shear rate was increased. Thus, difference in viscosity is more prominent at low shear rates compared to high shear rates. Low concentrations of Guar gum solutions did not show decrease in the viscosity with increase in shear rate (Figure 2.5). The viscosity was approximately constant at all shear rates for low concentrations.

The temperature of the polymer aqueous solution at which the viscosity was recorded influenced the apparent viscosity of the solution. Decrease in the viscosity was observed with an increase in temperature for all investigated concentrations (Figure 2.4). According to Srichamroen (2007), temperature causes the water molecules to lose their ordering around the Guar molecules, thus affecting the conformation and resulting in reduced-viscosity behavior. High Guar gum concentrations in solutions resulted in higher viscosity, and the temperature effect on viscosity was found to be less prominent (Figures 2.4b and 2.4c), especially at 7g/l concentration.

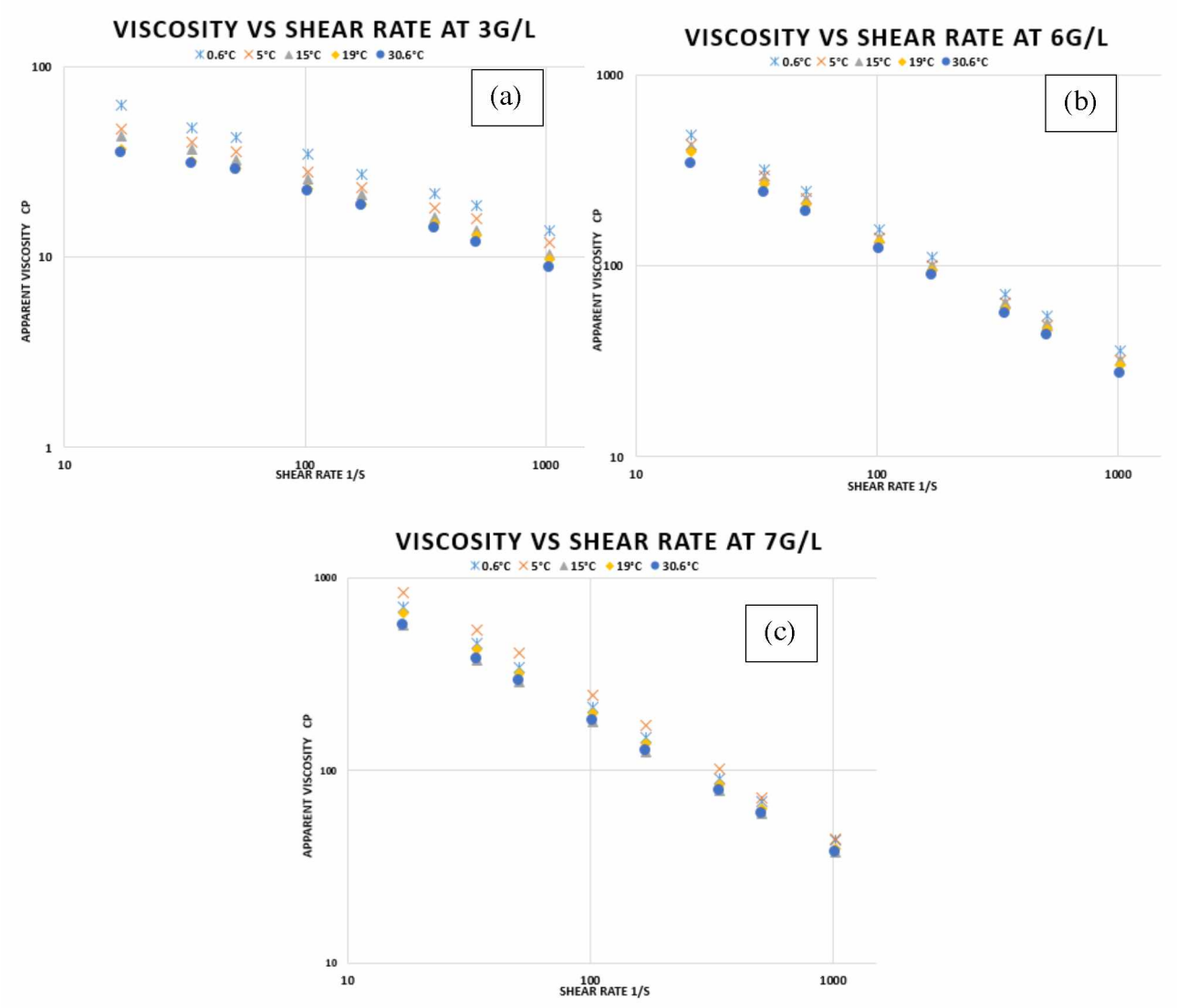

Figure 2.4. Variation of apparent viscosity of Guar gum solutions with increase in shear rate at different temperatures

Table 2.1 summarizes the percentage decrease in apparent viscosity (i.e., relationship between viscosity or the fluid's resistance to flow and the shear rate) for different Guar gum solutions when temperature of solutions were increased from 5°C to 30.6°C. Decrease in viscosity was observed for all concentrations under consideration.

The decrease in the viscosity at particular shear rate and temperature for different concentrations of Guar gum solutions are critical for flow of non-Newtonian fluids in the subsurface porous media. Variable temperature and shear rate offered by different permeability zones in the subsurface would impact the fluid viscosity, which would result in change in the fluid velocity flowing through the porous media. Highly viscous fluids need more force to move through the pore space as compared to less viscous fluid. By knowing the percent decrease in the viscosity at particular temperature and shear rate, it would be easier to understand the flow of non-Newtonian fluid in regions experiencing those conditions of temperature and the porous media offering such shear rate.

Table 2.1. Percentage decrease in apparent viscosity of Guar gum solutions when temperature was raised from 5°C to 30.6 °C.

Shear rate(1/s)	Guar gum Solutions				
	0.5g/l	1g/l	3g/l	6g/l	7g/l
17.02		-37±16%	-25±2%	-21±1%	-32±0%
34.05	-9±4%	-40±4%	-22±4%	-18±0%	-30±0%
51.07	-19±6%	-24±6%	-20±3%	-15±0%	-29±0%
102.14	-28±2%	-27±3%	-21±1%	-12±0%	-27±0%
170.23	-32±0%	-27±4%	-20±0%	-12±0%	-26±0%
340.46	-36±2%	-30±5%	-23±0%	-12±0%	-23±1%
510.69	-40±2%	-32±3%	-25±0%	-11±0%	-17±1%
1021.38	-37±2%	-30±4%	-27±0%	-14±0%	-14±0%

When Guar gum is dispersed in water, the galactose side chain of the molecule interacts with the water molecule, leading to inter-molecular chain entanglement of the Guar gum in aqueous solutions, rendering viscosity to the solution. With the increase in the concentration of Guar gum, the degree of inter-molecular chain interaction or entanglement would be enhanced, which would result in increased viscosity (Srichamroen, 2007; Zhang et al., 2005). Figure 2.5 shows the variation of the apparent viscosity with change in the shear rate at constant

temperatures for different concentrations of Guar gum. Higher concentrations showed high viscosity at all temperatures under consideration.

Non-Newtonian shear thinning of Guar gum increases with the increase in concentration. Shear thinning was demonstrated by mid to high concentrations at all investigated temperatures (Figure 2.5). High Guar gum concentrations showed steep decrease in the apparent viscosity with an increase in the shear rate at all investigated temperatures (Figure 2.5). This is evidence of strong shear-thinning as reported by Chenlo et al. (2010) and Torres et al. (2014) for high concentrations. Mid (3g/l) concentration showed a less steep decrease in viscosity with an increase in shear rate. At low concentrations the shear thinning did not respond similar to those of mid or high concentration solutions, as is evidenced in Figure 2.5 at any particular temperature.

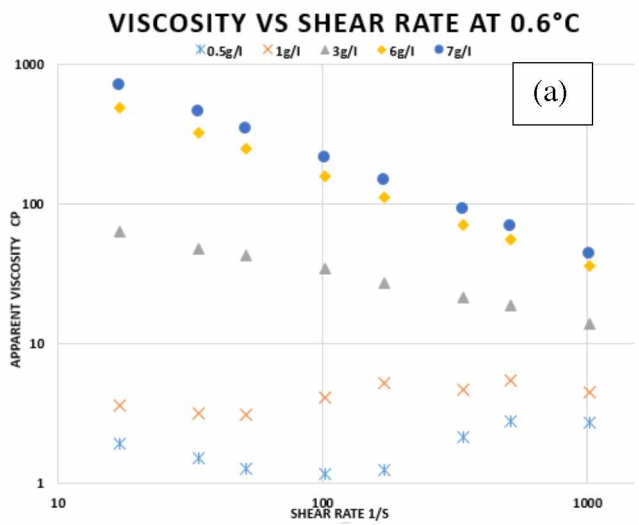
VISCOSITY VS SHEAR RATE AT 0.6°C
0.5g/l 1g/l 3g/l 6g/l 7g/l
(a)
APPARENT VISCOSITY CP
SHEAR RATE 1/S

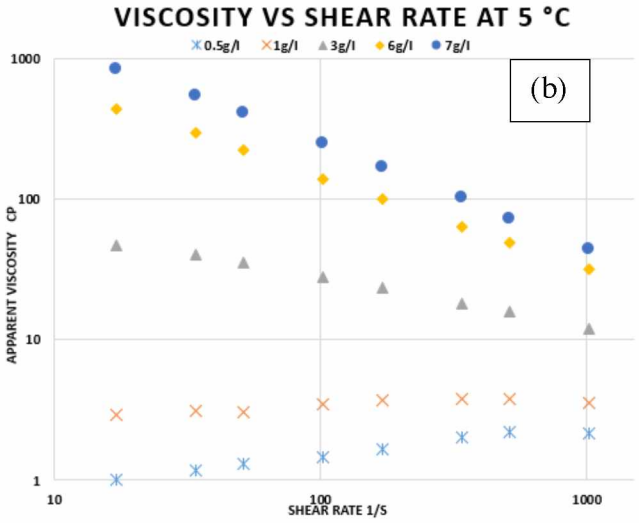
VISCOSITY VS SHEAR RATE AT 5 °C
0.5g/l 1g/l 3g/l 6g/l 7g/l
(b)
APPARENT VISCOSITY CP
SHEAR RATE 1/S

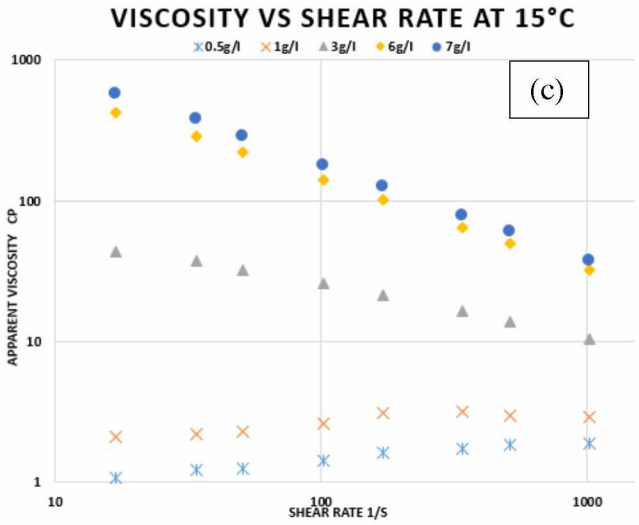
VISCOSITY VS SHEAR RATE AT 15°C
0.5g/l 1g/l 3g/l 6g/l 7g/l
(c)
APPARENT VISCOSITY CP
SHEAR RATE 1/S

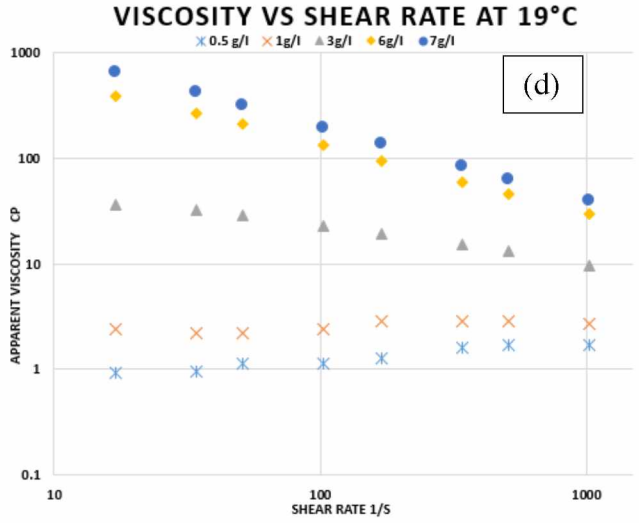
VISCOSITY VS SHEAR RATE AT 19°C
0.5 g/l 1g/l 3g/l 6g/l 7g/l
(d)
APPARENT VISCOSITY CP
SHEAR RATE 1/S

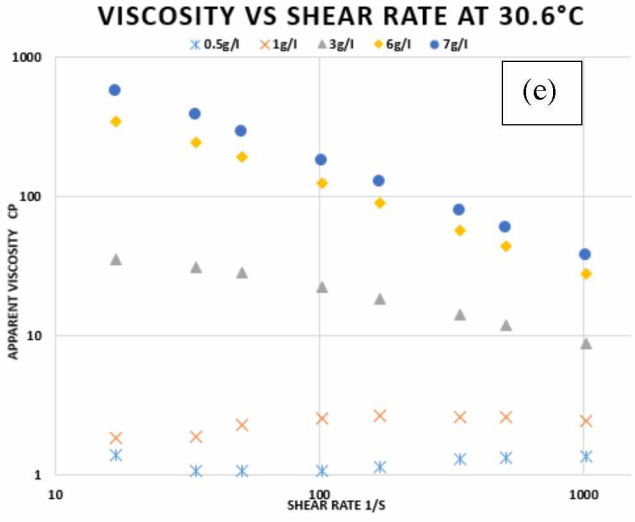
VISCOSITY VS SHEAR RATE AT 30.6°C
0.5g/l 1g/l 3g/l 6g/l 7g/l
(e)
APPARENT VISCOSITY CP
SHEAR RATE 1/S

Figure 2.5. Variation of apparent viscosity of Guar gum solution with an increase in shear rate at different concentrations

2.3.2 Non-Newtonian Rheological Model for Guar Gum

Power law model is one of the simplest model used to describe the flow behavior of the non-Newtonian shear-thinning fluids. The non-Newtonian behavior of polymer aqueous solutions was quantified by the power law relationship.

$$\tau = K\gamma^n \quad (1)$$

Here, τ is used for shear stress. The power law consistency index (K) is related to the fluid viscosity at low shear rate and is important for field applications. For example, fluid with a higher value of K would enhance the hole cleaning and suspension effectiveness of drilling muds in petroleum industry (Yang et al., 2010).

The power law index (i.e., n) represents the degree of non-Newtonian behavior over a given range of shear rate (i.e., γ). At $n < 1$, the fluid is non-Newtonian shear thinning, and at $n = 1$, the fluid is Newtonian. Lower value of n indicates the fluid is more shear thinning. The velocity profile of the fluid having lower value of n will be flatter (Figure 2.6). This shear thinning behavior of the non-Newtonian fluid increases the fluid velocity over a large area of the annulus (Yang et al., 2010) and greatly improves the hole cleaning operations in petroleum industry. Better performance of lower n value fluid can be useful in cleaning the contaminants from soils as demonstrated using a glass-tube-bundle model (synthetic porous media) in Chapter 4. Power law was used to find the degree of shear thinning behavior offered by all solutions of non-Newtonian fluids (Guar gum and Xanthan gum) at different temperatures.

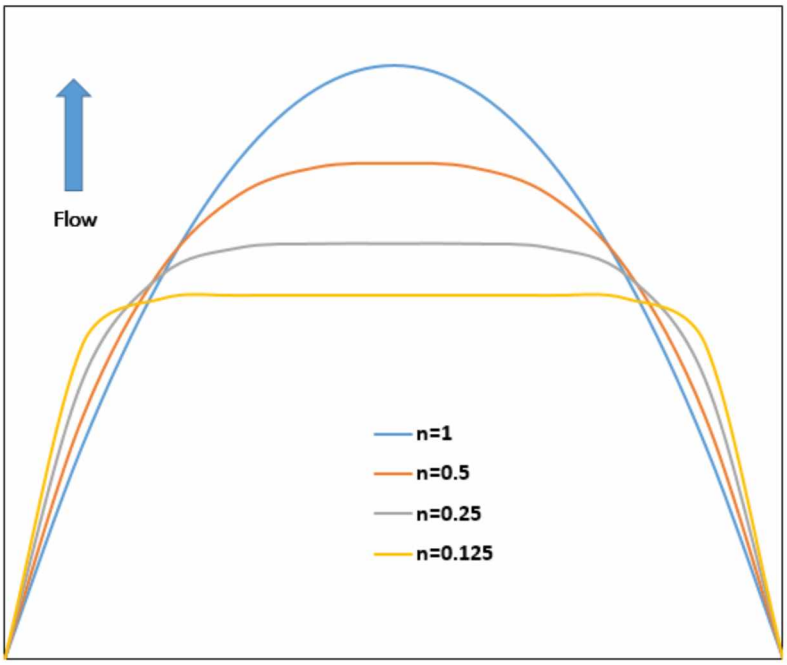

Figure 2.6. Effect of power law index (n) on velocity profile of fluid

Figure 2.7 summarizes the consistency curves (shear stress vs shear rate curves) for different Guar gum concentrations at different temperatures that are computed using equation 1. Lines represent fitting of power law relationship to experimental data. The fitted K and n along with coefficient of determination are listed in Table 2.2.

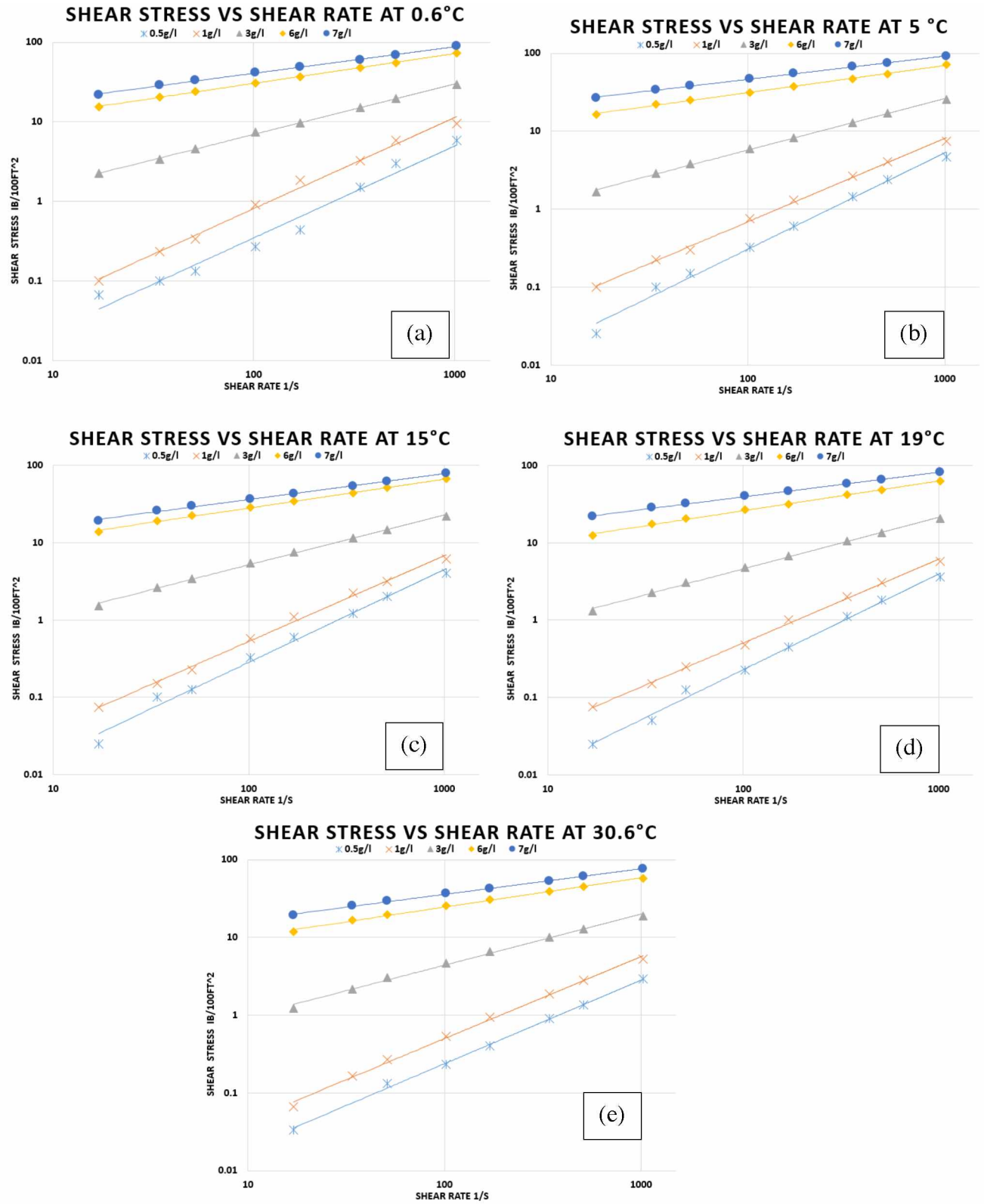

Figure 2.7. Shear stress and shear rate relationship for different concentrations of Guar gum.

The high coefficient of determination suggests that the Guar gum solutions at different temperatures had a good fit with the power law model. Hence, it is evident that they may be characterized as non-Newtonian fluids. However, no significant change in n was observed with a change in temperature (Table 2.2) at a specific Guar gum concentration. This indicates that the temperature effect on non-Newtonian behavior of Guar gum solutions is insignificant. Decrease in the value of n was observed with the increase in polymer concentration. This suggests that shear thinning of Guar gum solution increased with the increase in concentration.

Table 2.2. Effect of temperature and concentration on non-Newtonian behavior of Guar gum. Fitted K and n values according to power law relationship.

Concentration g/l	Temperature °C	Power law consistency index, K (Pa*s^n)	Power Law index, n	R^2
3	0.6	1.793E-01	0.63	0.999
	5	1.307E-01	0.66	0.999
	15	1.273E-01	0.64	0.998
	19	1.022E-01	0.67	0.998
	30.6	1.021E-01	0.66	0.995
6	0.6	2.597E+00	0.37	0.999
	5	3.028E+00	0.35	0.999
	15	2.398E+00	0.37	0.998
	19	2.109E+00	0.39	0.998
	30.6	2.065E+00	0.38	0.996
7	0.6	4.190E+00	0.33	0.998
	5	4.190E+00	0.33	0.998
	15	4.190E+00	0.33	0.998
	19	4.190E+00	0.33	0.998
	30.6	4.190E+00	0.33	0.9981

Table 2.2 data indicates that concentration had a greater influence on the power law consistency index K than change in temperature. K value increases with an increase in concentration level under the studied temperature range. A small decrease in K with increase in temperature was observed for 3g/l and 6g/l solutions whereas K remained constant for the 7g/l solution.

2.3.3 Effect of Salt on Guar Gum

As discussed in section 2.1.1, Low concentration of Guar gum solution showed inconsistency in viscosity with the increase in the shear rate as seen in Figure A1. To resolve the inconsistency in viscosity salts were added to the separate solutions of Guar gum. We studied the effect of increase in ionic strength on viscosity of Guar gum by adding Sodium Chloride and Potassium Chloride.

The influence of Sodium Chloride (10g/l) and Potassium Chloride (10g/l) on the viscosity of Guar gum at temperatures of 5 °C and 30.6 °C are summarized in Figures 2.8 and 2.9. Figure 2.8 provides the comparison between salt free and salt containing Guar gum solutions and Figure 2.9 provides the percent change in viscosity at studied range of shear rate with addition of salt. At 5°C, addition of 10g/l of Sodium Chloride resulted in increase in apparent viscosity for low to mid concentration of Guar gum solutions (Figures 2.8a and 2.9a). The possible reason for increase in viscosity is that the salt disrupts the existing positive-negative charge attractions, which allows chain expansion by enhanced solvation (Zhang et al., 2005). The 6g/l Guar gum solution revealed no change in the apparent viscosity with the addition of Sodium Chloride whereas the 7g/l Guar gum solution manifested a decrease in the apparent viscosity (Figures 2.8a and 2.9a).

At 30.6°C, the change in the apparent viscosity was not very prominent with the addition of Sodium Chloride (Figures 2.8b and 2.9b) apart from little variation observed at low shear rate for the 0.5g/l solution. Magnitude of change is less in apparent viscosity with increase in temperature when salt containing Guar gum solutions were compared to salt free Guar gum solutions (Figures 2.8a, 2.8b, 2.9a and 2.9b). The highest change in magnitude of viscosity was observed at 5 °C and least change in magnitude of viscosity was observed at 30.6 °C. According to Srichamroen (2007), at 37 °C the viscosity of 0.25 % (w/w) (i.e., 2.5g/l) Guar gum with Krebs bicarbonate (i.e., aqueous mixture of salts having higher concentration of Sodium Chloride) decreases compared to Guar gum in water whereas the viscosity of 0.5% (w/w) (i.e., 5g/l) Guar

gum with Krebs bicarbonate increases compared to Guar gum in water. The decrease or increase in viscosity with addition of Sodium chloride for different concentrations of Guar gum solutions would depend on the particular temperature under considerations (Figure 2.8a, 2.8b, 2.9a and 2.9b).

The addition of 10g/l Potassium Chloride at 5°C resulted in the increase in the apparent viscosity for low to mid concentration of Guar gum solutions. This increase in viscosity due to addition of Potassium Chloride (Figure 2.8c and 2.9c) was less prominent compared to Sodium Chloride's impact on viscosity (Figure 2.8a and 2.9a). Similarly, decrease in viscosity of 7g/l Guar gum solution with addition of Potassium Chloride was comparatively less to Sodium Chloride decrease in viscosity. Thus, type of salt clearly influenced the amount of viscosity change.

It is important to note the behavior of 6g/l Guar gum solution (Figures 2.8 and 2.9). No significant change in viscosity was observed regardless of temperature and salt type. A concentration less than 6g/l exhibited increase in viscosity at 5°C whereas a concentration greater than 6g/l exhibited a decrease in viscosity with the addition of salt (Figures 2.8a, 2.8c, 2.9a and 2.9c).

These results provide us valuable insight into how the viscosity of Guar gum changed at low temperature of 5°C. The addition of the remedial amendments (e.g., phosphate, sodium lactate, ethyl lactate for subsurface remediation) in low to mid concentration solution can increase the viscosity of solutions which would help in better transportation of amendments to subsurface. Similarly, addition of remedial amendments to 6g/l Guar gum solutions are desirable where decrease or increase in viscosity is not required.

At 30.6°C addition of Potassium Chloride to Guar gum solutions resulted in a decrease in the apparent viscosity for low to mid concentration Guar gum solutions (Figures 2.8d and 2.9d). Slight decrease in the viscosity was observed for a higher concentration of Guar gum with the addition of Potassium Chloride at both 5°C (Figures 2.8c and 2.9c) and 30.6 °C (Figure 2.8d and 2.9d). In contrast, at 5°C low to mid Guar concentrations containing Potassium Chloride manifested an increase in viscosity whereas at 30.6 °C a decrease in viscosity was observed.

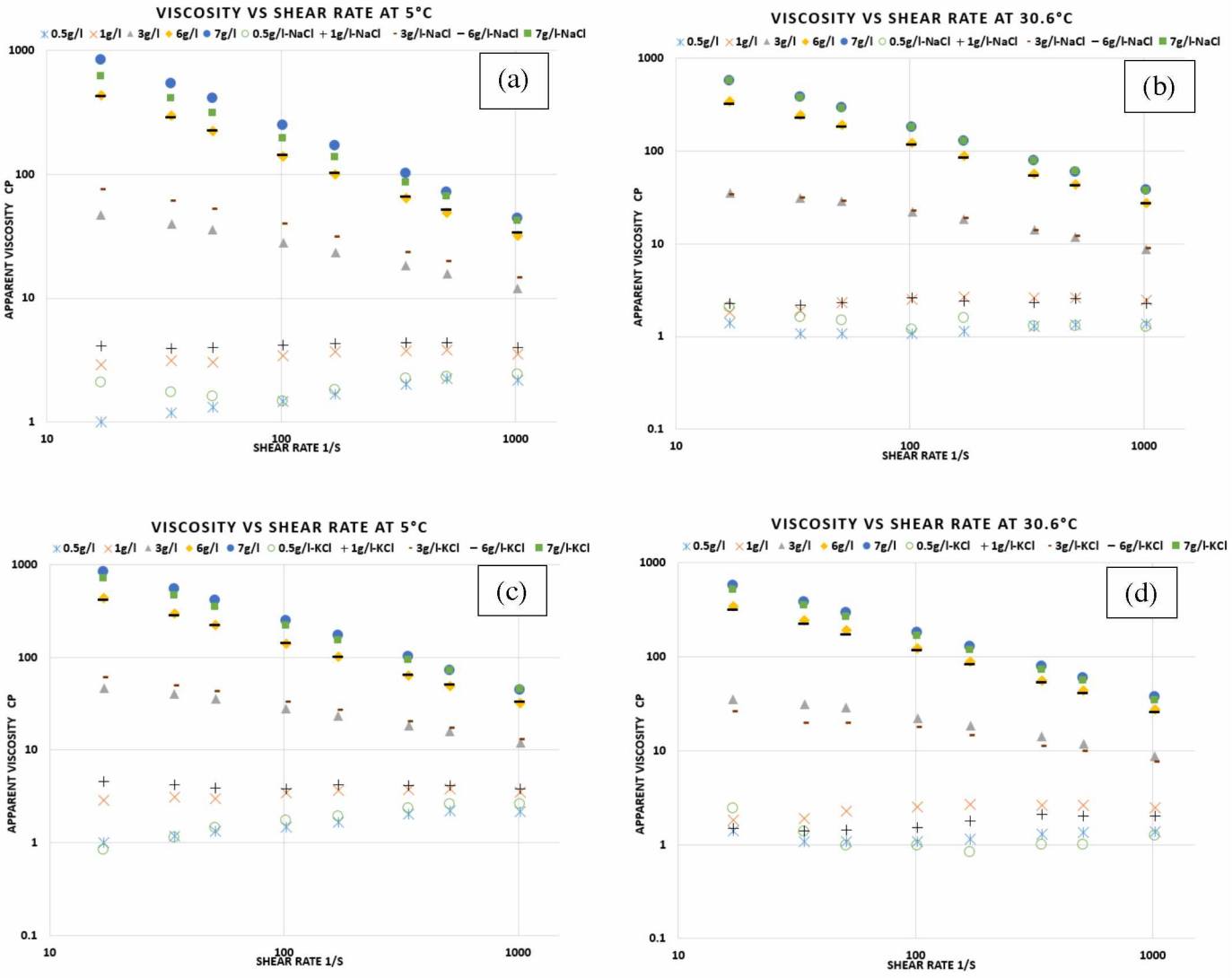

Figure 2.8. Viscosity vs shear rate for Guar gum solutions and Guar gum saline solutions at 5°C and 30.6°C. (a) Different concentrations of Guar gum solutions and Guar gum with 10g/l Sodium Chloride solutions at 5°C (b) Different concentrations of Guar gum solutions and Guar gum with 10g/l Sodium Chloride solutions at 30.6°C (c) Different concentrations of Guar gum solutions and Guar gum with 10g/l Potassium Chloride solutions at 5°C (d) Different concentrations of Guar gum solutions and Guar gum with 10g/l Potassium Chloride solutions at 30.6°C

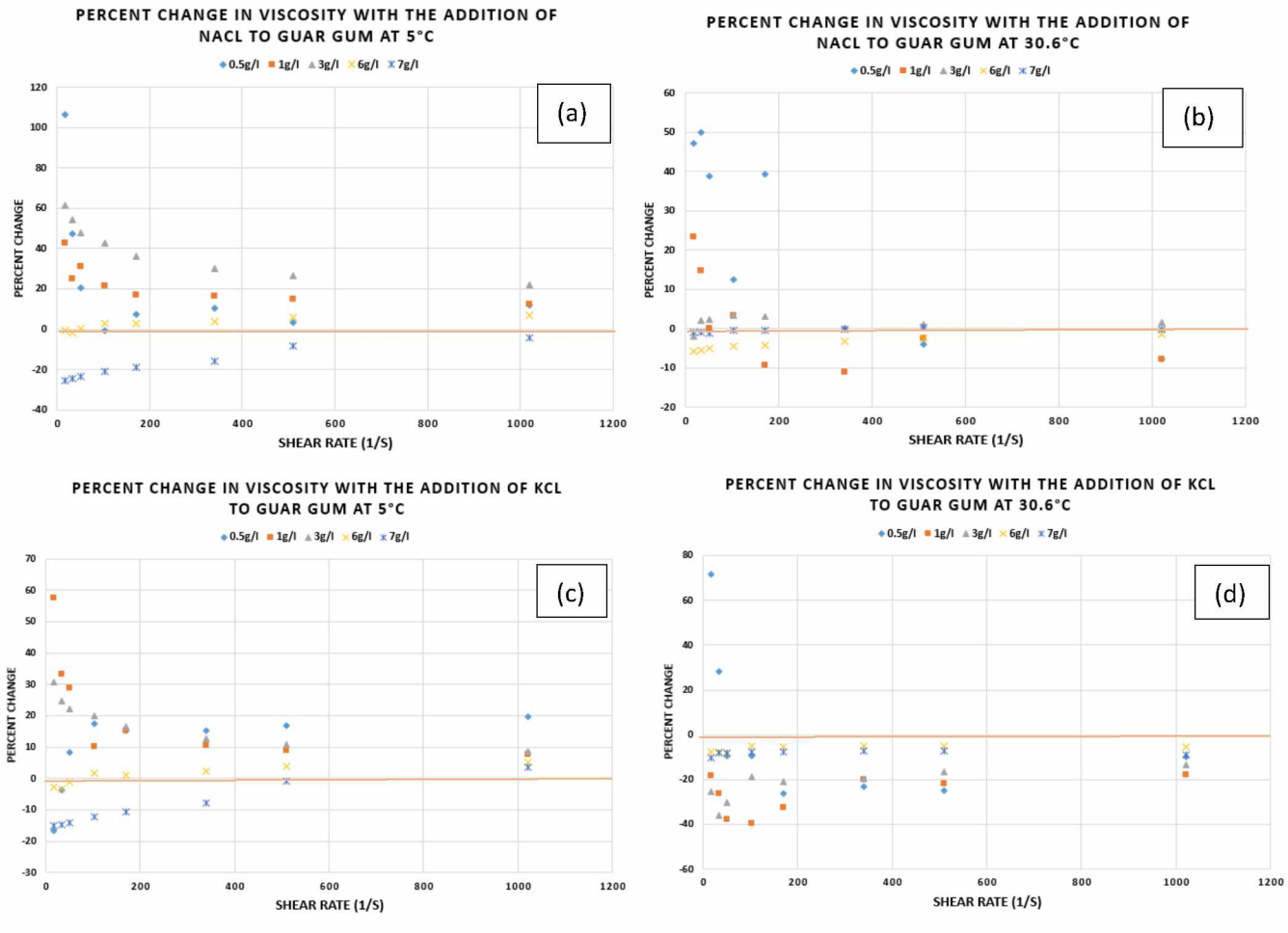

Figure 2.9. Percent change in viscosity of Guar gum with addition of 10g/l salt at 5°C and 30.6°C. (a) Addition of 10g/l Sodium Chloride at 5°C (b) Addition of 10g/l Sodium Chloride at 30.6°C (c) Addition of 10g/l Potassium Chloride at 5°C (d) Addition of 10g/l Potassium Chloride at 30.6°C

The possible explanation for decrease in the viscosity with salt is that the salts are hydrophilic molecules that strongly interact with water (Srichamroen, 2007). The presence of salt ions in the solution disrupts the covering of water molecules around the Guar chain resulting in decreasing solubility of Guar gum (Gittings et al., 2001) and the addition of higher concentration of salt reduces the availability of water in the solution preventing expansion of the Guar networks, thereby decreasing the viscosity of the solution. The addition of the salt also restricts the hydration of Guar gum in solution (Srichamroen, 2007).

Apart from salts, temperature is another important factor that affects the covering of the water molecules around the Guar chain, resulting in a reduction of the viscosity. This is evident from the results of our experiments summarized in Figure A2 and Table 2.3. All concentration levels containing Sodium Chloride showed a decrease in viscosity with an increase in temperature from 5°C to 30.6°C (Table 2.3). Low to mid concentrations revealed a much greater decrease with increase in temperature as compared to higher concentrations.

Comparison of viscosity decrease by the addition of salts when temperature was increased from 5°C to 30.6°C displayed the higher impact of Potassium Chloride on viscosity compared to Sodium Chloride as seen in Table 2.3. The possible explanation might be that the bigger ionic radius of Potassium has a greater impact compared to that of Sodium. For same temperature change (i.e., 5°C to 30.6 °C), all investigated concentrations except 7g/l displayed much higher decrease in viscosity with addition of salt compared to salt free solutions. However, salt free 7g/l Guar gum solution displayed higher decrease in viscosity compared to Guar gum solutions containing salts. This indicates that the addition of salts offset the effect of temperature change on 7g/l solutions.

Table 2.3. Percentage decrease in apparent viscosity of Guar gum saline solutions when temperature was increased from 5°C to 30.6 °C

Shear rate(1/s)	Guar gum solutions with NaCl					Guar gum solutions with KCl				
	0.5g/l	1g/l	3g/l	6g/l	7g/l	0.5g/l	1g/l	3g/l	6g/l	7g/l
17.02	0±15%	-45±4%	-55±0%	-25±2%	-9±0%		-67±1%	-57±4%	-25±0%	-28±2%
34.05	-8±9%	-45±3%	-49±2%	-21±1%	-8±0%		-67±0%	-60±2%	-21±0%	-24±1%
51.07	-8±3%	-42±3%	-44±1%	-19±2%	-8±0%	-33±31%	-63±1%	-54±2%	-21±0%	-24±1%
102.14	-18±2%	-38±10%	-43±1%	-18±1%	-8±0%	-44±16%	-60±2%	-46±0%	-18±0%	-23±1%
170.23	-12±11%	-44±5%	-40±1%	-18±1%	-8±0%	-57±4%	-57±4%	-46±0%	-17±0%	-23±0%
340.46	-42±4%	-47±0%	-40±0%	-18±0%	-9±0%	-57±2%	-50±3%	-45±0%	-18±0%	-23±0%
510.69	-44±3%	-42±1%	-40±0%	-18±0%	-9±0%	-62±0%	-51±4%	-43±0%	-19±0%	-23±0%
1021.38	-48±0%	-43±1%	-39±0%	-21±0%	-11±0%	-53±2%	-46±3%	-41±0%	-22±0%	-25±0%

Figure 2.10 summarizes the shear stress and shear rate relationship for different Guar gum solutions with 10g/l salt at 5°C and 30.6°C. The power law model was fitted to consistency curves of Guar gum solutions containing salt and fitted parameters are listed in Table 2.4. Comparison of Table 2.2 and Table 2.4 revealed little change in the power index with the addition of salt to Guar gum solutions. This indicates that fitting parameters were not much impacted by the addition of salt, especially for higher concentrations. Which means the addition of salt has not changed the shear thinning of the Guar gum solutions.

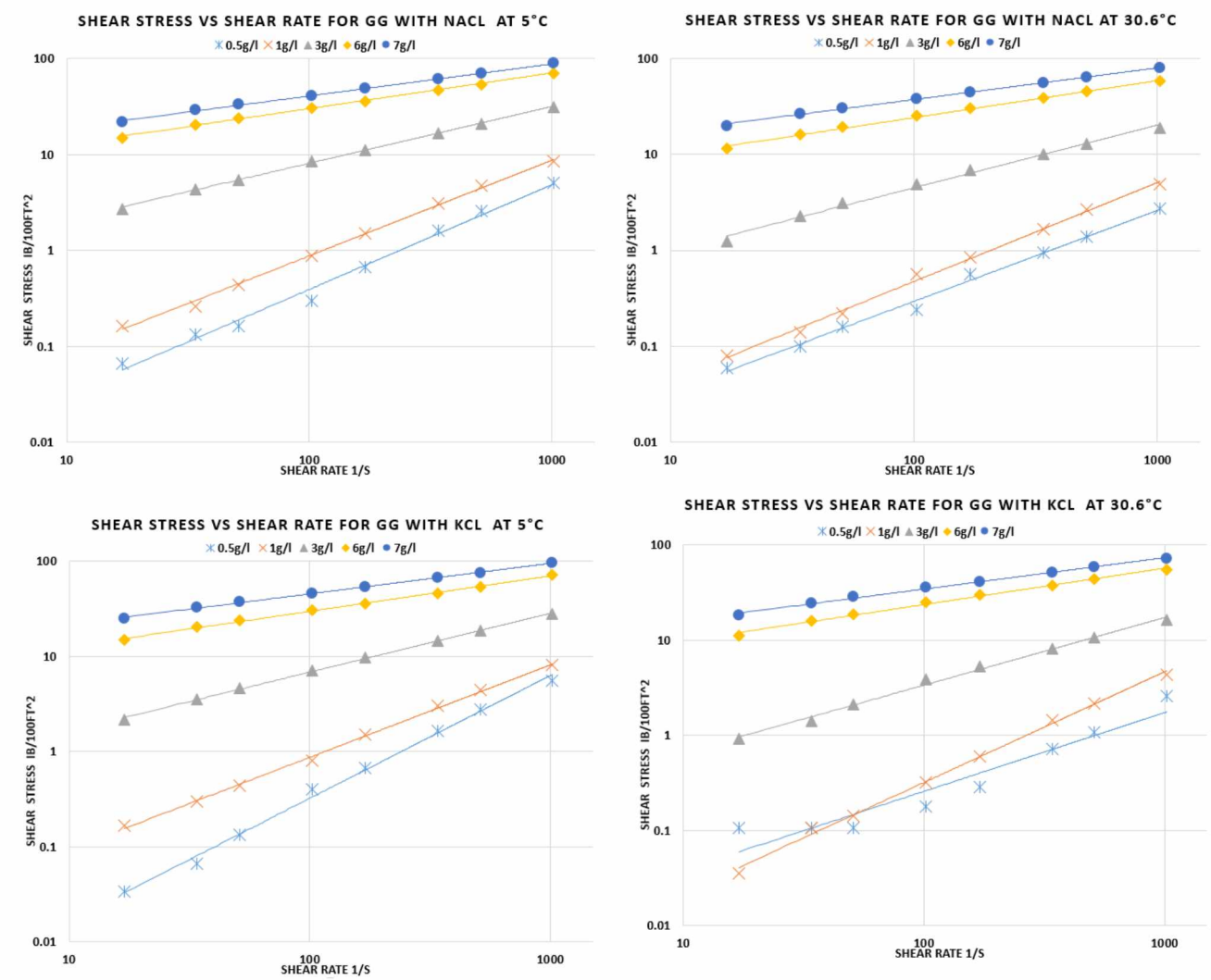

Figure 2.10. Shear stress and shear rate relationship for Guar gum with salts. Lines represent the Power law model fitting (a) Guar gum with 10g/l Sodium Chloride at 5°C (b) Guar gum with 10g/l Sodium Chloride at 30.6°C (c) Guar gum with 10g/l Potassium Chloride at 5°C (d) Guar gum with10g/l Potassium Chloride at 30.6°C

Table 2.4. Effect of salts on non-Newtonian behavior of Guar gum at 5°C and 30.6 °C. Fitting parameters K and n are according to power law relationship

Salts	Concentration, g/l	Temperature °C	Power law consistency index, K (Pa*s^n)	Power Law index, n	R^2
NaCl (10g/l)	3	5	2.545E-01	0.59	0.999
	6		2.606E+00	0.37	0.999
	7		4.206E+00	0.33	0.999
NaCl (10g/l)	3	30.6	1.061E-01	0.65	0.993
	6		1.955E+00	0.39	0.996
	7		3.907E+00	0.33	0.998
KCl (10g/l)	3	5	1.898E-01	0.62	0.999
	6		2.570E+00	0.37	0.999
	7		4.979E+00	0.32	0.999
KCl (10g/l)	3	30.6	6.100E-02	0.71	0.995
	6		1.944c+00	0.38	0.995
	7		3.624c+00	0.33	0.996

2.3.4 Rheological Study of Xanthan Gum

Figure 2.11 displays the effect of temperature on viscosity at different concentrations of Xanthan gum. The greatest effect of temperature was visible on 0.5g/l (Figure 2.11a). Highest viscosity was shown by the solution at 0.6°C and least at 30.6°C. A minimum of 28% viscosity decrease was observed when the temperature of 0.5g/l Xanthan gum solution increased from 5°C to 30.6°C.

Similar behavior was observed for 1g/l (Figure 2.11b) but the difference due to temperature was not as prominent as in 0.5g/l. The viscosity of 1g/l Xanthan gum solution decreased by 17% at a shear rate of 34.05 s^{-1} to maximum decrease of 30% at a shear rate of 1021.4 s^{-1} for a temperature increase from 5°C to 30.6°C (Table 2.5). The decrease in the viscosity due to increase in temperature was observed at all studied shear rates for low (i.e., 0.5g/l and 1g/l) concentrations of Xanthan gum.

An increase in viscosity was observed for mid (i.e., 3g/l) to high (i.e., 6g/l and 7g/l) concentration Xanthan gum solutions when temperature was increased from 5°C to 30.6°C. However, these increases were only limited to shear rates less than 170.23 s^{-1} while the viscosity decreased above this shear rate.

Table 2.5. Percentage change in apparent viscosity of different concentrations of Xanthan gum solutions for temperature increase from 5°C to 30.6 °C. Negative sign indicates decrease in viscosity.

Shear rate(1/s)	0.5g/l	1g/l	3g/l	6g/l	7g/l
17.02	-35±1%	-17±5%	5±2%	9±2%	5±3%
34.05	-34±1%	-14±4%	5±2%	8±4%	3±2%
51.07	-35±2%	-17±5%	5±2%	6±4%	4±3%
102.14	-35±1%	-18±2%	1±1%	4±4%	2±3%
170.23	-35±1%	-19±3%	-2±1%	1±4%	0±4%
340.46	-28±1%	-24±2%	-8±1%	-4±4%	-4±3%
510.69	-31±1%	-26±3%	-13±0%	-8±4%	-8±3%
1021.38	-32±2%	-30±3%	-19±1%	-13±3%	-13±2%

In terms of viscosity change, mid to high concentrations of Xanthan gum was less affected due to change in temperature (Figure 2.11) compared to same concentrations of Guar gum solution (Figure 2.4). The effect of temperature was more prominent on viscosity of Guar gum solution.

Xanthan gum aqueous solutions exhibited a shear thinning behavior, the apparent viscosity decreased with an increase in the shear rate for all concentrations and temperatures under consideration (Figure 2.11). The increase in the polymer concentration resulted in increase in viscosity. This increase in the viscosity with an increasing Xanthan gum concentration has been attributed to intermolecular interaction or entanglement that increases the effective macromolecule dimensions and molecular weight (Zhong et al., 2013).

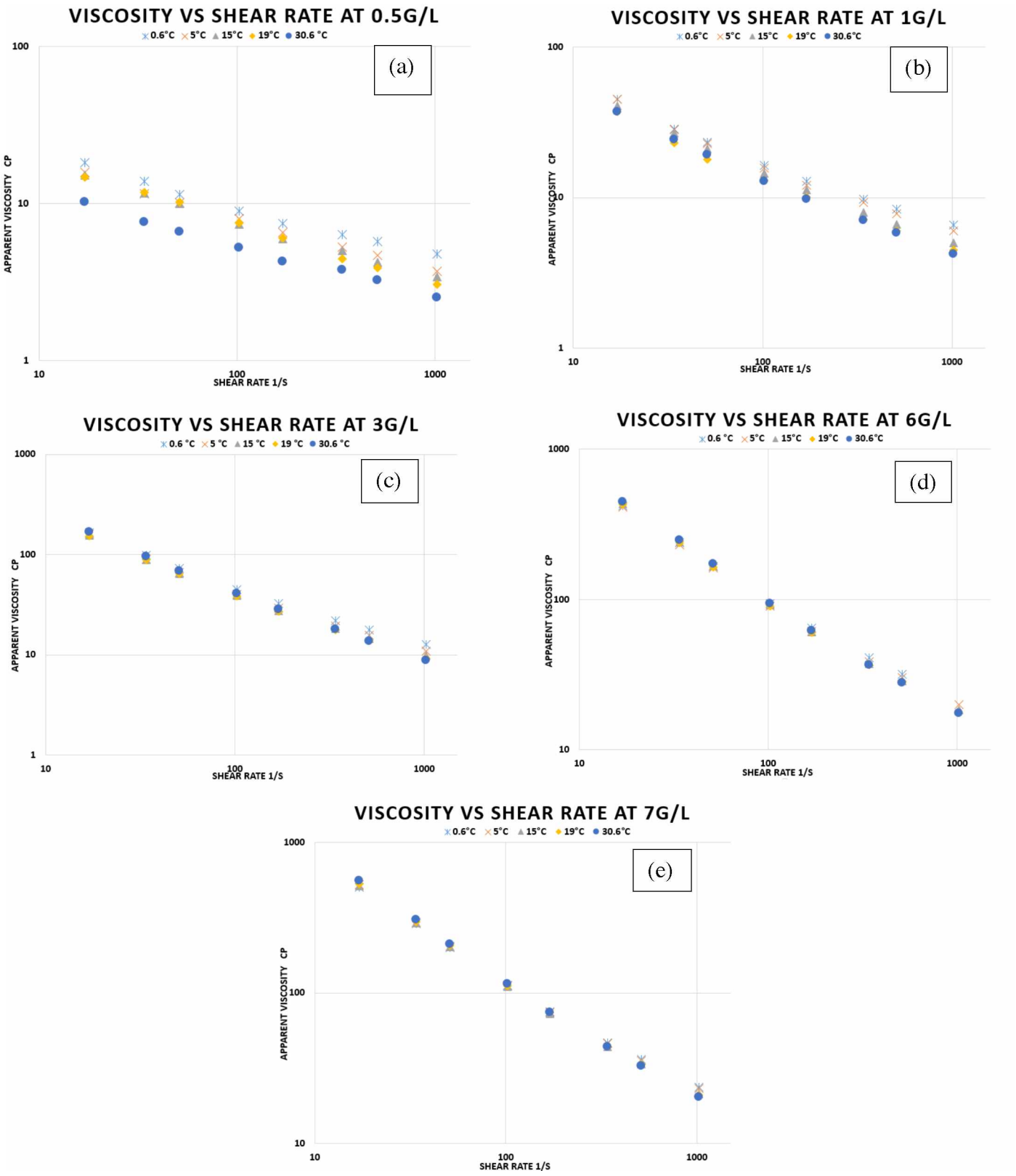

Figure 2.11. Variation of apparent viscosity with increase in the shear rate for Xanthan gum solutions at different temperatures

Figure 2.12 summarizes the effect of concentration and temperature on viscosity of both polymers. Low concentrations of Xanthan gum have a higher viscosity compared to same concentrations of Guar gum. At higher concentrations of polymers, Guar gum solutions manifested higher viscosity than Xanthan gum solutions for the temperature range involved in experiments. Interestingly, viscosity manifested by 0.5g/l Xanthan gum was greater than 1g/l Guar gum solution. Similarly, 6g/l Guar gum displayed much higher viscosity than 7g/l Xanthan gum. High coefficient of correlation exists for relationships between temperature and apparent viscosity for all investigated concentrations of both polymers except 7g/l.

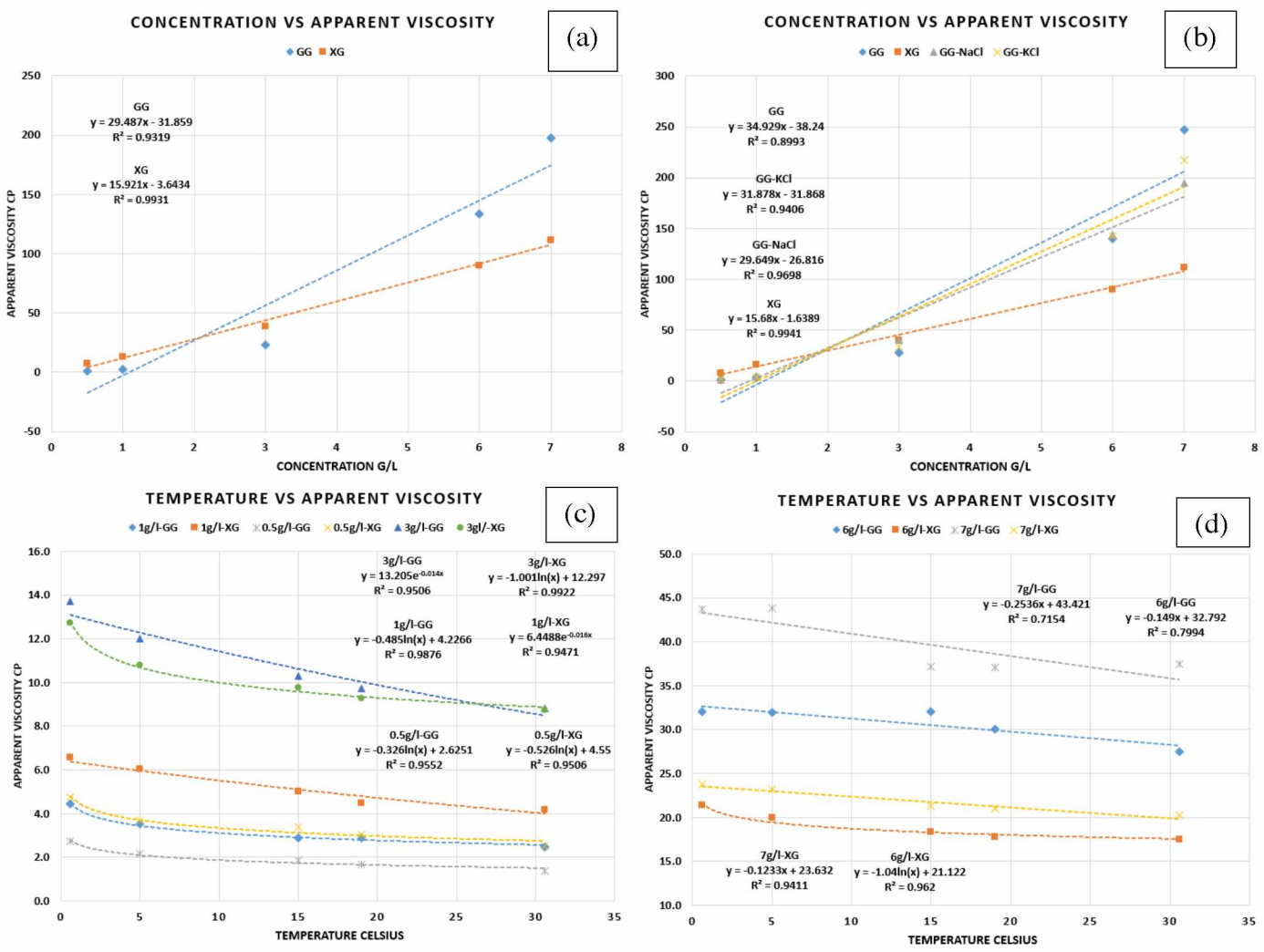

Figure 2.12. (a) Apparent viscosity vs concentration for Guar gum and Xanthan gum at shear rate of 102.14s^{-1} and 5 °C (b) Apparent viscosity of Guar gum, Guar gum with Sodium Chloride, Guar gum with Potassium Chloride and Xanthan gum at shear rate of 102.14s^{-1} and 5 °C (c) Apparent viscosity vs temperature for low to mid concentrations of Guar gum and Xanthan gum at shear rate of 1021.4 s^{-1} (d) High concentration of Guar gum and Xanthan gum at shear rate of 1021.4 s^{-1}.

The power law was fitted to the consistency curve of Xanthan gum solutions (Figure A4). The fitted K and n along with coefficient of determination for Xanthan gum are provided in Table 2.6.

The non-Newtonian shear thinning behavior for Xanthan gum was influenced by both concentration and temperature. Higher concentrations exhibited stronger shear thinning behavior (Table 2.6). Temperature increase did not affect shear thinning of 0.5g/l as power law index was almost constant at all investigated temperatures. However, for all other investigated concentrations of Xanthan gum, shear thinning behavior increased with the increase in the temperature.

The effect of temperature change on non-Newtonian shearing thinning behavior of Guar gum (Table 2.2) was not prominent like Xanthan gum (Table 2.6). Higher concentration of Guar gum has not shown any change in non-Newtonian shear thinning compared to Xanthan gum with change in temperature. As discussed earlier, strong shear thinning is desirable for hole cleaning operations in petroleum industry. Similarly, strong shear thinning can be more effective in contaminant remediation. Xanthan gum showed the improvement in shear thinning with increase in temperature.

Table 2.6. Effect of temperature and concentration on non-Newtonian behavior of Xanthan gum. Fitted K and n values according to power law relationship.

Concentration, g/l	Temperature, °C	Power law consistency index, K ($Pa*s^n$)	Power Law index, n	R^2
0.5	0.6	6.947E-02	0.615	0.994
	5	4.089E-02	0.696	0.998
	15	4.204c-02	0.631	0.999
	19	4.745E-02	0.615	0.999
	30.6	3.768E-02	0.623	0.996
1	0.6	1.598E-01	0.551	0.991
	5	1.573E-01	0.517	0.991
	15	1.610E-01	0.488	0.995
	19	1.377E-01	0.497	0.994
	30.6	1.618E-01	0.479	0.997
3	0.6	7.960E-01	0.371	0.974
	5	8.998E-01	0.347	0.976
	15	9.526E-01	0.326	0.979
	19	9.829E-01	0.314	0.982
	30.6	1.088E+00	0.285	0.990
6	0.6	3.356E+00	0.244	0.926
	5	3.096E+00	0.255	0.954
	15	3.601E+00	0.223	0.952
	19	3.641E+00	0.217	0.952
	30.6	3.710E+00	0.195	0.951
7	0.6	3.960E+00	0.245	0.959
	5	4.268E+00	0.231	0.947
	15	4.459E+00	0.215	0.957
	19	4.579E+00	0.211	0.966
	30.6	4.801E+00	0.186	0.950

2.3.5 Contact Angle

Wettability impacts the imbibition of liquid in the porous media and its understanding is crucial for non-Newtonian fluid flow and contaminant remediation. Contact angle is usually used for measurement of wettability. A smaller contact angle for fluid is the indication of better wettability, fluid can spread more on the surface compared to fluid with larger contact angle. The smaller contact angle allows liquid to establish a strong attraction (adhesive force) with solid surface, overcome the cohesive force of fluid, causing it to spread more on surface. For a fluid to be wetting, the contact angle between the fluid and solid surface must be less than 90°. Angle greater than 90° between the fluid and solid surface is indication of the non-wetting.

For attaining our broader goal of contaminant remediation, it was essential that both the non-Newtonian fluids must be wetting fluids so that they can reach the maximum surface area of porous media. The summary of contact angles is presented in Table 2.7 for all concentrations of both Guar and Xanthan gum solutions at all studied temperatures. All solutions of both polymers including Guar gum solutions containing salts (Table 2.8) have contact angle in wetting range.

At temperatures at or above 5°C, higher concentrations of Xanthan gum demonstrated larger contact angles. Low to mid concentrations of Xanthan gum demonstrated decrease in angle of contact with an increase in temperature up to 19°C then at 30.6°C increase in contact angle was observed. (Table 2.7).

All concentrations of Guar gum demonstrated either increase or decrease in contact angle with increase in temperature (Table 2.7) and addition of salts (Table 2.8). However, the pattern observed for the change of contact angle in Xanthan gum was missing in Guar gum.

Table 2.7. Contact angle for Guar gum and Xanthan gum at different temperatures. These contact angles were measured for glass.

Temperature	Polymer	0.5g/l	1g/l	3g/l	6g/l	7g/l
0.6 °C	Guar Gum	31.4°	27.2°	24.6°	33°	26°
5°C		20.8°	20.6°	22.4°	20.8°	25.4°
15°C		19.8°	21.2°	20.8°	22.8°	29.2°
19°C		29°	20°	19.6°	23°	20.8°
30.6°C		21.8°	18.4°	20.8°	27.4°	24.8°
0.6 °C	Xanthan Gum	28.4°	28.8°	28°	25.8	27°
5°C		20°	20.4°	21.4°	29	30.2°
15°C		20°	18.2°	20.4°	29.4	29°
19°C		17.4°	20.2°	22°	22.4	29°
30.6°C		27.2°	26.2°	28°	33.4	33.6°

Table 2.8. Contact angle for Guar gum solutions with salts at 5°C and 30.6°C. These contact angles were measured for glass.

Temperature	Salt (10g/l)	0.5g/l	1g/l	3g/l	6g/l	7g/l
5°C	NaCl	25°	20.4°	20.2°	22.2°	22°
30.6°C		18.8°	20.4°	22.4°	31.8°	32°
5°C	KCl	18.8°	19.8°	21.2°	25°	25°
30.6°C		25.6°	20.8°	20.8°	26.8°	30.4°

As mentioned earlier, smaller contact angle would allow the liquid to have greater contact with the solid surface which would affect the fluid flow. Greater contact (i.e., smaller contact angle) with solid surface would offer greater friction to flowing fluid and more energy is required to overcome this friction compared to the smaller contact (i.e., greater contact angle) of fluid with solid surface.

Understanding the relationship amongst the Contact angle, Power law parameters (i.e., n and k) and viscosity of each solution of Xanthan gum and Guar gum are crucial for flow and contaminant remediation (Figures 2.13 and 2.14). Smaller contact angle, low value of n and reasonable viscosity (i.e., not very viscous solution which can clog the tubes/pores of synthetic porous media) are desirable for fluid solution for contaminant remediation from synthetic porous media.

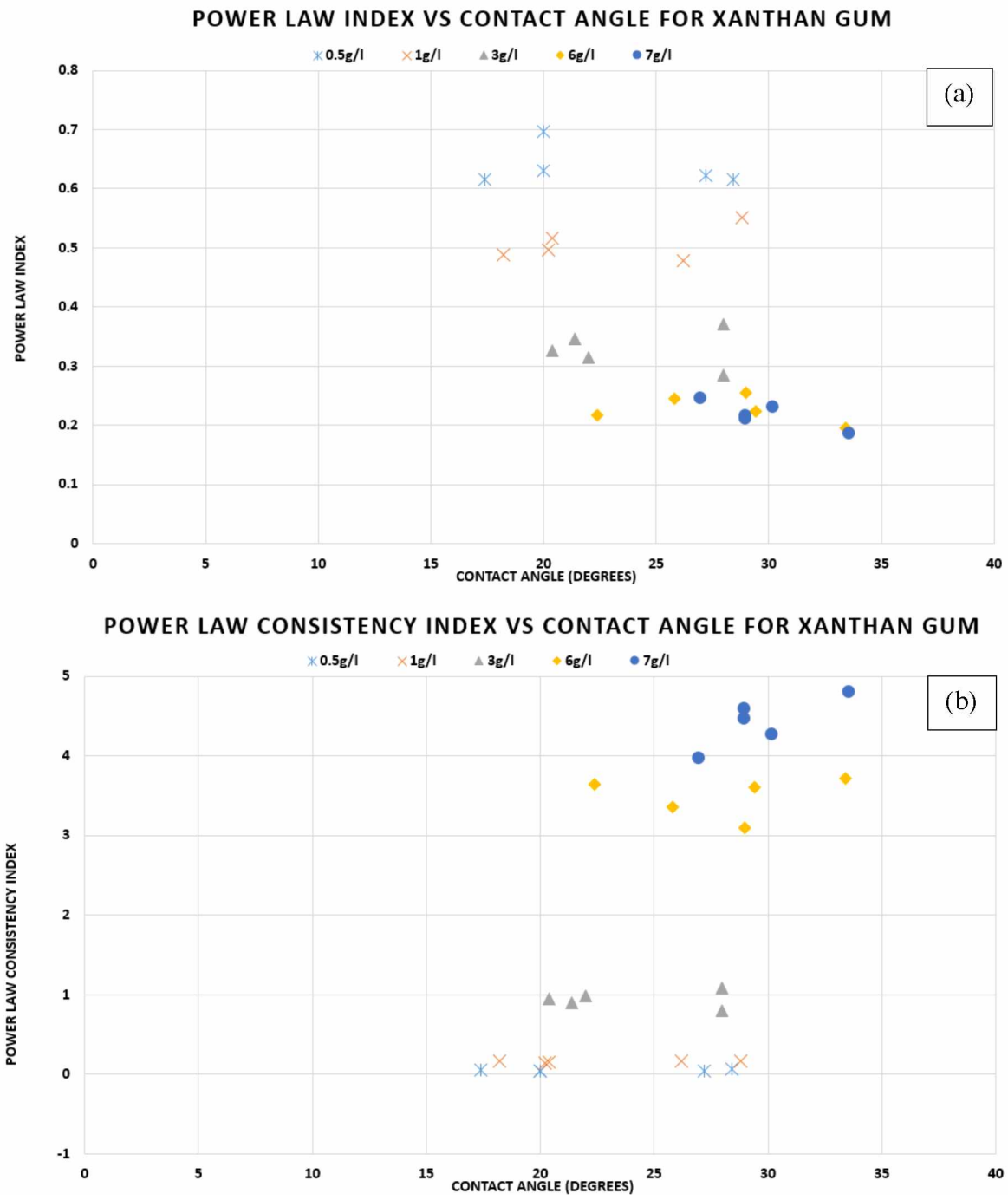

Figure 2.13. (a) Power law index n versus contact angle for all studied concentrations of Xanthan gum. (b) Power law consistency index k versus contact angle for all studied concentrations of Xanthan gum

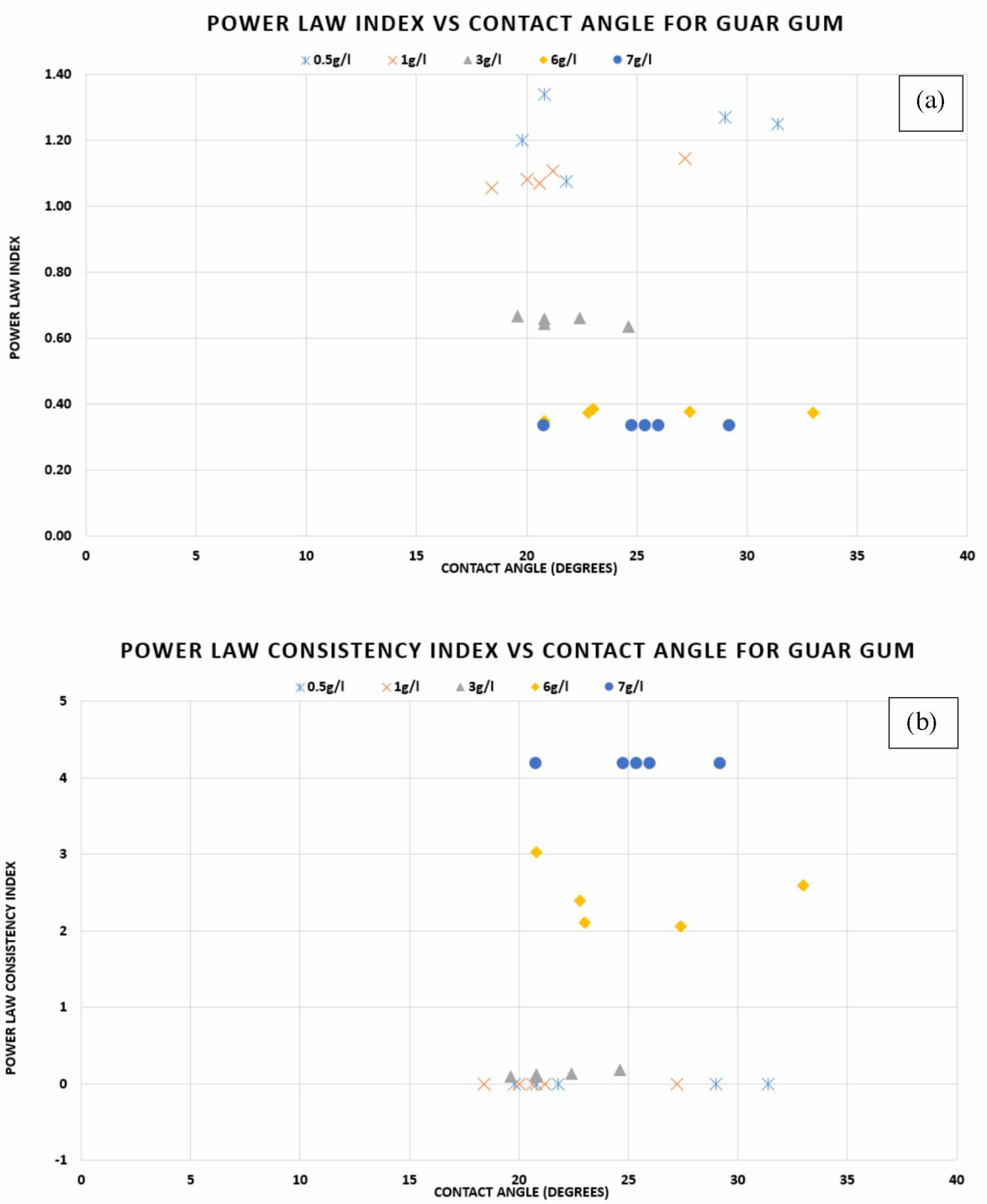

Figure 2.14. (a) Power law index n versus contact angle for all studied concentrations of Guar gum. (b) Power law consistency index k versus contact angle for all studied concentrations of Guar gum.

2.4 Conclusion

- In terms of viscosity, the effect of temperature change was higher on Guar gum than Xanthan gum, especially at mid to high concentrations. Both polymers displayed decrease in viscosity with increase in temperature apart from high concentrations of Xanthan gum at low shear rates.
- At any temperature used for the experiments, low to mid concentrations of Xanthan gum had higher viscosity compared to the same concentrations of Guar gum. However, at high concentration Guar gum displayed higher viscosity.
- Xanthan gum behaved as **non-Newtonian** shear-thinning fluid for all the selected range of temperature and concentration. Guar gum also displayed non-Newtonian shear thinning behavior only for mid to high concentrations but was asymptotic to Newtonian behavior for low concentrations.
- An increase in non-Newtonian shear thinning behavior was observed with increase in temperature for mid to high concentrations of Xanthan gum. However, non-Newtonian shear thinning behavior of mid to high concentration of Guar gum showed neither decrease nor increase with change in temperature. Both polymers displayed improvement in shear thinning behavior with increase in concentrations.
- Addition of salt did not significantly change the non-Newtonian shear thinning properties of Guar gum solutions.
- The 6g/l Guar gum solution showed no change in viscosity at 5°C and 30.6°C with the addition of salt. Guar gum concentrations less than 6g/l displayed an increase in viscosity, whereas concentrations greater than 6g/l exhibited decrease in viscosity with addition of salt at 5°C.
- Addition of salt offsets the effect of temperature change (i.e., 5°C to 30.6°C) on 7g/l Guar gum solution. Salt free 7g/l Guar gum solution displayed higher decrease in viscosity compared to Guar gum saline solution for same increase in temperature.
- Low to mid concentrations of Xanthan gum demonstrated decrease in angle of contact with an increase in temperature up to 19°C. All concentrations of Guar gum demonstrated either increase or decrease in contact angle with increase in temperature and addition of salts. However, the pattern observed for the change of contact angle in Xanthan gum was different from that of Guar gum, which demonstrated a lack of pattern.

2.5 References

Bourbon, A. I., Pinheiro, A. C., Ribeiro, C., Miranda, C., Maia, J. M., Teixeira, J. A., and Vicente, A. A., 2010. Characterization of galactomannans extracted from seeds of Gleditsia triacanthos and Sophora japonica through shear and extensional rheology: Comparison with Guar gum and locust bean gum. Food Hydrocolloids 24, 184-192.

Bradley, T. D., Ball, A., Harding, S.E., and Mitchell, J.R., 1989. Thermal degradation of Guar gum. Carbohydrate Polymers. 10,205-214.

Brunchi, C. E., Morariu, S., and Bercea, M., 2014. Intrinsic viscosity and conformational parameters of xanthan in aqueous solutions: Salt addition effect. Colloids and Surfaces B: Biointerfaces 122, 512-519.

Brunchi, C. E., Bercea, M., Morariu, S., and Dascalu, M., 2016. Some properties of Xanthan gum in aqueous solution: effect of temperature and Ph. J Polym Res. 23:123.

Casas, J.A., Mohedano, A.F., and Gracia-Ochoa, F., 2000. The viscosity of Guar gum and xanthan /Guar gum mixture solutions. Journal of the Science of Food and Agriculture 80:1722-1727.

Chenlo, R., Moreira, R., and Silva, C., 2010. Rheological Properties of an aqueous dispersion of Tragacanth and Guar gum at different concentrations. Journal of Texture studies 41, 396 - 415.

D'Cunha, N.J., and Misra, D., 2005: A Review of Enhanced Remediation Methods for Subsurface Dense Non-aqueous Phase Liquid Spills Employing Permeability Modification, World Journal of Engineering, 2(1): 69-80.

D'Cunha, N.J., Misra, D., and Thompson, A., 2009: An Investigation into the Applications of Natural Freezing and Curdlan Biopolymer for Permeability Modification to Remediate DNAPL Contaminated Aquifers in Alaska, Cold Regions Science and Technology, DOI: 10.1016/j.coldregions.2009.05.005, 59:42-50.

Ding, B., Ye, Y., Cheng, J., Wang, K., Luo, J., and Jiang, B., 2008. TEMPO-mediated selective oxidation of substituted polysaccharides-an efficient approach for the determination of the degree of substitution at C-6. Carbo hydr. Res. 343, 3112–3116

Gittings, M.R., Cipelletti, L., Trappe, V., Weitz, D.A., In, M., and Lal, J., 2001.The effect of solvent and ions on the structure and rheological properties of guar solutions.

Gupta, B.S., and Ako, J.E., 2005. Application of Guar gum as a flocculant aid in food processing and potable water treatment. Eur Food Res Technol 221:746-751.

Jung, J., Jang, J., and Ahn, J., 2016. Characterization of a Polyacrylamide Solution Used for Remediation of Petroleum Contaminated Soils, Materials, 9, 16: 1 – 13.

KÕk, M.S., Hill, S.E., and Mitchell, J.R., 1999. Viscosity of galactomannans during high-temperature processing: influence of degradation and solubilization. Food Hydrocolloids 13, 535-542.

Martin-Alfonso, J.E., Cuadri, A.A., Berta, M., and Stading, M., 2018. Relation between concentration and shear-extensional rheology properties of xanthan and Guar gum solutions. Carbohydrate Polymers 181, 63-70.

McCleary, B.V., Amado, R., Waibel, R., and Neukom, H., 1981. Effect of galactose content on the solution and interaction properties of guar and carob galactomannans. Carbohydr Res 92:269-285

Meuser, H., 2010. Contaminated Urban Soils; Springer Science & Business Media: Berlin/Heidelberg, Germany; Volume 18.

Mudgil, D., Barak, S., Khatkar, B.S., 2014. Guar gum: processing, properties, and food applications----A Review Food Sci Technol 51(3):409-418

Mukherjee, S., Mukhopadhyay, S., Zafri, M.Z.B., Zhan, X., Hashim, M.A., and Gupta, B.S., 2017. Application of Guar gum for the removal of dissolved lead from wastewater. Industrial Crops and Products 111, 261-269.

Naseer, F., O. Awoleke, D. Misra and M. Abou Najm, 2017. Effect of Temperature on Guar Gum Rheology of Different Concentrations, Paper#H43I-1768, Fall Meeting of the American Geophysical Union, December 11 – 15, New Orleans, LA.

Palaniappan, M., Gleick, P.H., Allen, L., Cohen, M.J., Christian-Smith, J., and Smith, C., 2010. Clearing the Waters: A Focus on Water Quality Solutions, United Nations Environmental Programme Publication, Nairobi, Kenya, pp. 89.

Patel, S.P., Patel, R.G., and Patel, V.S., 1987. Rheological properties of guar gum and hydroxyethyl guar gum in aqueous solution. Int. J. Biol. Macromol. 9, 314-320.

Sandolo, C., Matricardi, P., Alhaique, F., Coviello, T., 2009. Effect of temperature and cross-linking density on rheology of chemical cross-linked Guar gum at the gel point. Food Hydrocolloids 23, 210-220.

Srichamroen, A., 2007. Influence of Temperature and salt on viscosity property of Guar gum. Naresuan University Journal 15(2)55-62

Swann, B.M., 2017. Leveraging fluids with weak yield stress for directed alignment and distribution of magnetic disks in novel inks. Master Thesis, Chemical Engineering. Oregon State University. p. 82

Torres, M.D., Hallmark, B., and Wilson, D.I., 2014. Effect of concentration on shear and extensional rheology of Guar gum solutions. Food Hydrocolloids 40, 85-95.

Tosco, T., Gastone, F., Sethi, R., 2014. Guar gum solutions for improved delivery of iron particles in porous media (part 2): Iron transport tests and modeling in radial geometry. Journal of Contaminant Hydrology 166, 34-51.

Velimirovic, M., Tosco, T., Uyttebroek, M., Luna, M., Gastone, F., De Boer, C., Klaas, N., Sapion, H., Eisenmann, H., Lassson, P., Braun, J., Sethi, R., and Bastiaens, L., 2014. Field Assessment of Guar Gum Stabilized Microscale Zerovalent Iron Particles for In-situ Remediation of 1, 1, 1-Trichloroethane, Journal of Contaminant Hydrology, 164: 88 – 99.

Venugopal, K.N., and Abhilash, M. 2010. Study of hydration kinetics and rheological behavior of Guar gum. International Journal of Pharma Science and Research. 1, 28-39.

Wientjes, R.H.W., Duits, M.H.G., John Schaap, R.J.J., and Mellema, J., 2000. Linear Rheology of Guar gum solutions. Macromolecules 33, 9594-9605

Xu, L., Xu, G., Liu, T., Chen, Y., Gong, H., 2013. The comparison of rheological properties of aqueous welam gum and Xanthan gum solutions. 2013. Carbohydrates Polymers 92, 516-522.

Yang, L. K., Mukherjee, S., Pariatamby, A., 2015. Effective remediation of phenol, 2, 4-bis(1,1- dimethylethyl) and bis(2-ethylhexyl) phthalate in farm effluent using Guar gum-A plant based biopolymer. Chemosphere. 136, 111-117.

Yang, Z., Liu, Z., Zhang, Z., 2010. Drilling fluid technology. Peking: Petroleum Industry Press.

Zhang, L. M., Zhou, J. F., and Hui, P. S. (2005). A comparative study on viscosity behavior of water-soluble chemically modified Guar gum derivatives with different functional lateral groups. Journal of the Science of Food

Zhong, L., Oostrom, M., Truex, M.J., Vermeul, V.R., Szecsody, J.E., 2013. Rheological behavior of Xanthan gum solution related to shear thinning fluid delivery for subsurface remediation. Journal of Hazardous Material 244-245, 160-170.

Chapter 3 Porous Media Flow Characteristics of Newtonian and non-Newtonian Fluids under Different Thermal Regimes[2]

Abstract

Limited understanding exists in the flow characteristic of non-Newtonian fluids in porous media under low temperature (< 30°C) regimes such as those experienced in cold regions soils, per our knowledge. Most of the understanding has been developed for oil industry applications at very high temperature regimes. Understanding the flow characteristic of non-Newtonian fluids under low temperature conditions could help in developing methods to effectively remediate residual contaminants from soils in cold regions. In order to study the flow characteristic, we have studied the changes in rheological characteristics (viscosity and contact angle) of non-Newtonian fluids of different concentrations at low temperatures. The objective of this research is to study the flow characteristics of Newtonian and non-Newtonian fluids in porous media at 0.6°C, 5°C and 19°C. We used a glass-tube-bundle setup as a synthetic porous media to simulate an actual pore regime. De-ionized water, 0.5g/l Guar gum solution and 0.5g/l of Xanthan gum solution were used for the infiltration experiments carried out in cold room for four sets of synthetic porous media. Results obtained from the infiltration experiments using water and non-Newtonian fluid along with rheological parameters of fluids at different temperatures were used to obtain the representative radii and their corresponding percent contribution of flow. A software developed earlier in a different study was used to analyze the results of simulation in terms of maximum displacement distance versus percent flow for different sets of porous media at a certain temperature.

Keywords: Porous media, Non-Newtonian Flow, Guar gum, Xanthan gum, Temperature

[2] Naseer et al. Porous Media Flow Characteristics of Newtonian and non-Newtonian Fluids under Different Thermal Regimes. Unpublished Manuscript 2019.

3.1 Introduction

Improving spatial and temporal characterization of fluid flow and contaminant transport in soils is vital and significant to a wide range of fields including agricultural sciences, environmental engineering, hydrology, ecology, geomorphology as well as petroleum, chemical engineering. Non-Newtonian fluids are not uncommon to porous media applications, such as soil and groundwater remediation, hydraulic fracture, enhance oil recovery and cement injection in soils (Abou Najm and Atallah, 2016). Recently, use of non-Newtonian fluids are gaining interest for subsurface remediation.

Contamination of soil and groundwater by adsorbed contaminants such as phosphates, carbon tetrachloride, chlorinated aliphatic hydrocarbons (CAH), certain emerging contaminants, or certain heavy metals have been of major concern lately (e.g., Jung et al., 2016; Palaniappan et al., 2010; Barnes et al., 2007; Gillham and O'Hannesin, 1994). Quality of the water is increasingly threatened as human populations grow, industrial and agricultural activities expand, and as climate change threatens to cause major alterations of the hydrologic cycle. Inadequately treated sewage, industrial and agricultural or food wastes, dissolved metals and many emerging contaminants, enter through the soil to pollute the groundwater on a daily basis. A lack of understanding of fate and transport of contaminant within soil matrix and groundwater makes the situation worse. Preferential flow of contaminants through soil to groundwater is complicating the conceptual understanding of flow and transport through porous media. Adding to the complexity are the highly adsorbed contaminants that do not travel at a rate proportional to the flux rate of water in the porous media.

Experimental and field observations show that the infiltration of water does not necessarily move downward at a uniform rate. In reality, water and contaminants travel in wide range and at varying velocities. Moreover, contaminant trapped in the low permeability zones is difficult to be remediated by flushing water through the porous media because water bypasses the low permeability zone. These low permeability zones can be accessed by non-Newtonian fluids because these fluids exhibit viscosity change with temperature and shear rate. Non-Newtonian shear thinning fluid exhibits decrease in viscosity with increase in rate of shear. Low permeability zones offer higher shear rates to fluid, which results in decrease of viscosity of non-Newtonian fluids to penetrate in low permeability zones (Zhong et al., 2013) and thus aid in removal of the trapped residual contaminant.

Understanding the flow of non-Newtonian fluids under low temperature conditions could help in providing methods to effectively remediate residual contaminants from soils in cold regions. In order to study the flow characteristic, we have studied the changes in rheological characteristics (viscosity and contact angle) of two non-Newtonian fluids Guar gum and Xanthan gum of different concentrations at low temperatures. Prior rheological tests exhibit the ability of these polymers to form highly viscous aqueous solution at low concentrations. Rheological properties of Guar gum and Xanthan gum for temperature range of 0.6°C to 30.6°C showed higher viscosities for mid (i.e.,3g/l) to high (i.e., 6g/l and 7g/l) concentration of both polymers. Low (i.e., 0.5g/l) concentration showed relatively low viscosities compared to higher concentration for both polymers. This makes low concentrations more ideal to use in porous media because higher concentration can clog the porous media, especially low permeability zones, at low temperatures. Moreover, viscosity of higher concentrations are least affected by temperature, while the impact of temperature on the viscosity of low concentrations for both polymers is significant. This will allow the low concentrations to adjust their viscosity according to the temperature and shear rate.

From our rheological experiments, it is evident that viscosity and contact angle of non-Newtonian fluids were temperature sensitive. Both these properties are most important aspect associated with non-Newtonian fluids that affect flow in porous media. Environmental factors like temperature of soils can significantly influence the flow characteristics of fluid. Proper understanding of the relationship between the flow characteristics of fluid and temperature could help in providing methods to effectively remediate residual contaminants from soils.

Most of the flow understanding of non-Newtonian fluids have been developed at high temperature and pressure to fit their application in hydraulic fracturing or hole cleaning for oil and gas industry. However, at low temperature and zero applied pressure no such understanding has been developed, per our knowledge. To develop a preliminary understanding of low temperature effect on the fluid flow in porous media we have conducted infiltration experiments by using a glass-tube-bundle setup as synthetic porous media (Figure 3.1) to simulate an ideal pore regime. These experiments helped us to attain our objective of studying flow characteristics of Newtonian and non-Newtonian fluids in synthetic porous media at low temperatures that are experienced in cold region soils. The primary question this research intended to address was, how does the temperature impact the flow of Newtonian and non-Newtonian fluid in porous

media? The answer to this question is critical to understand for effective design of remedial system in soils.

3.2 Method and Material

3.2.1 Design of Synthetic Porous Media

Four sets of synthetic porous media were constructed by using different combinations of 0.5mm and 0.9mm diameter standard capillary tubes (Table 3.1). Eight 10 cm diameter perforated acrylic discs were used for construction of four sets of synthetic porous media. Two perforated discs were installed on a single metallic rod separated by a distance of 10 cm. Capillary tubes of 10cm length, 0.5mm and 0.9mm diameters were installed between two perforated acrylic discs (Figure 3.1). Silicon was used to fix them tightly. Total volume of each set of synthetic porous media was 785.40 cm^3.

Table 3.1. Synthetic Porous Media Characteristics

Set	Radii (cm)	Length(cm)	Number of tubes	Porosity	% of Total Porosity
1	0.025	10	53	0.001649	80.35
	0.045		4		19.65
2	0.025	10	53	0.001568	84.50
	0.045		3		15.50
3	0.025	10	53	0.001487	89.11
	0.045		2		10.89
4	0.025	10	53	0.001406	94.24
	0.045		1		5.76

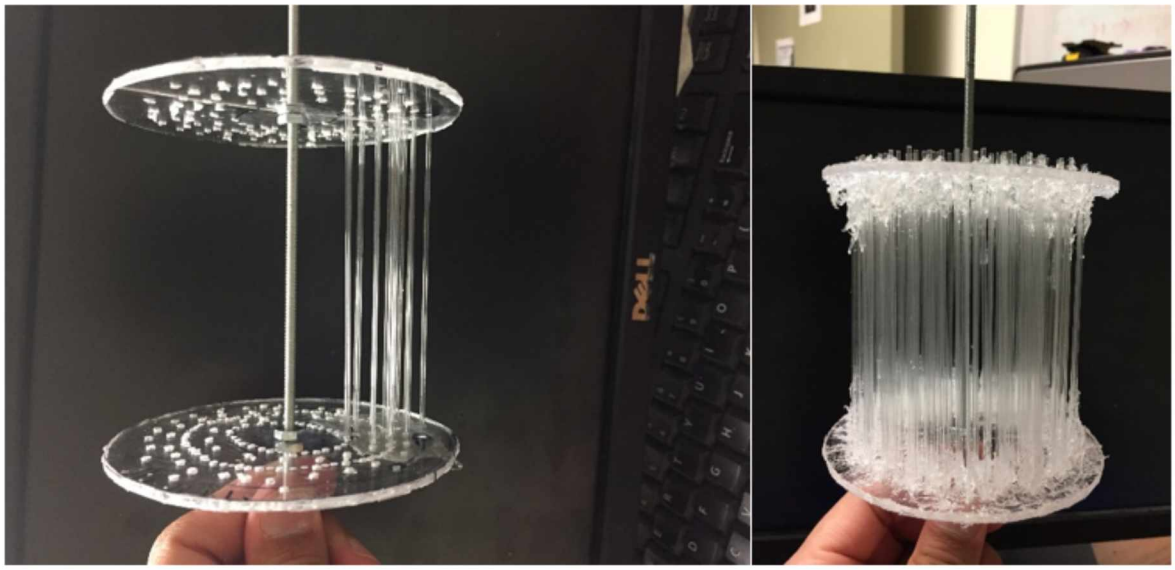

Figure 3.1. Construction of synthetic porous media

3.2.2 Fluids

Fluids used for the experiments were deionized water, 0.5g/l Guar gum solution and 0.5g/l Xanthan gum solution. Here, water represented the Newtonian fluid, while Guar gum and Xanthan gum solutions were non-Newtonian fluids. Only 0.5 g/l concentration of both polymers were used for flow experiments. As stated before, the higher concentration solutions have high viscosities that can clog the capillary tubes especially at low temperature and hence were determined to be inadequate for characterizing flow in porous media.

Guar gum and Xanthan gum solutions were prepared as described in chapter 2. Three 10ml samples were taken from every liter of prepared Guar gum or Xanthan gum solution. Samples were dried in the oven at 70°C and their weights were measured to ensure that the required amount (i.e., 0.5g) of polymers were dissolved in a liter of deionized water.

3.2.3 Experimental Setup

Each set of the synthetic porous media was installed in a permeameter chamber by using the silicone (Figure 3.2) to affix the structure to the wall of the permeameter and to prevent water to seep through the wall of the permeameter. Water proofing spray was used to stop any leakages and making sure fluids don't bypass the capillary tubes.

Fluids were filled in the reservoir at higher head and allowed to pass through the synthetic porous media. Synthetic porous media was completely saturated before recording any reading.

The outflow of each experiment was collected downstream in a beaker. For different fluid types, volumetric flow rate was recorded while maintaining a constant upstream head. A similar procedure was deployed for all experiments with each fluid type and each synthetic porous media set.

Figure 3.2. Experimental setup at 5°C in cold room

3.2.4 Temperatures

Temperatures selected for the flow experiments were 19°C, 5°C and 0.6°C. The desired temperature for experimental setup (Figure 3.2) was attained by keeping it in the cold chamber prior to each experiment. Fluids were also kept in the cold chamber to get the desired temperature. FLIR (Front Looking Infrared) thermal camera and thermometers were used to record the temperatures at different positions of experimental setup (Figures 3.3 and 3.4).

Despite all efforts to establish a uniform temperature regime, variation in temperature was recorded while conducting the experiments.

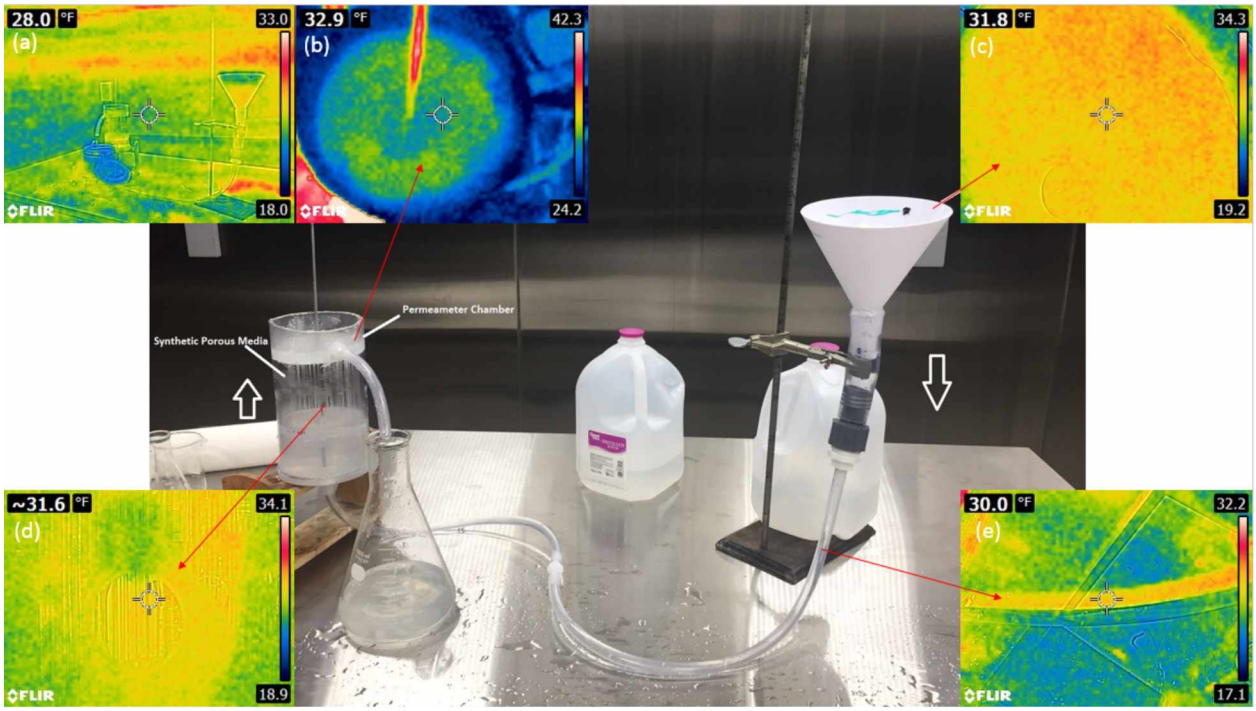

Figure 3.3. Thermal images displaying the temperature at different positions of experimental setup. Images are taken for flow experiment conducted at 0.6 °C. Image (a) covers the entire experimental setup in the cold room at 0.6°C /33°F.

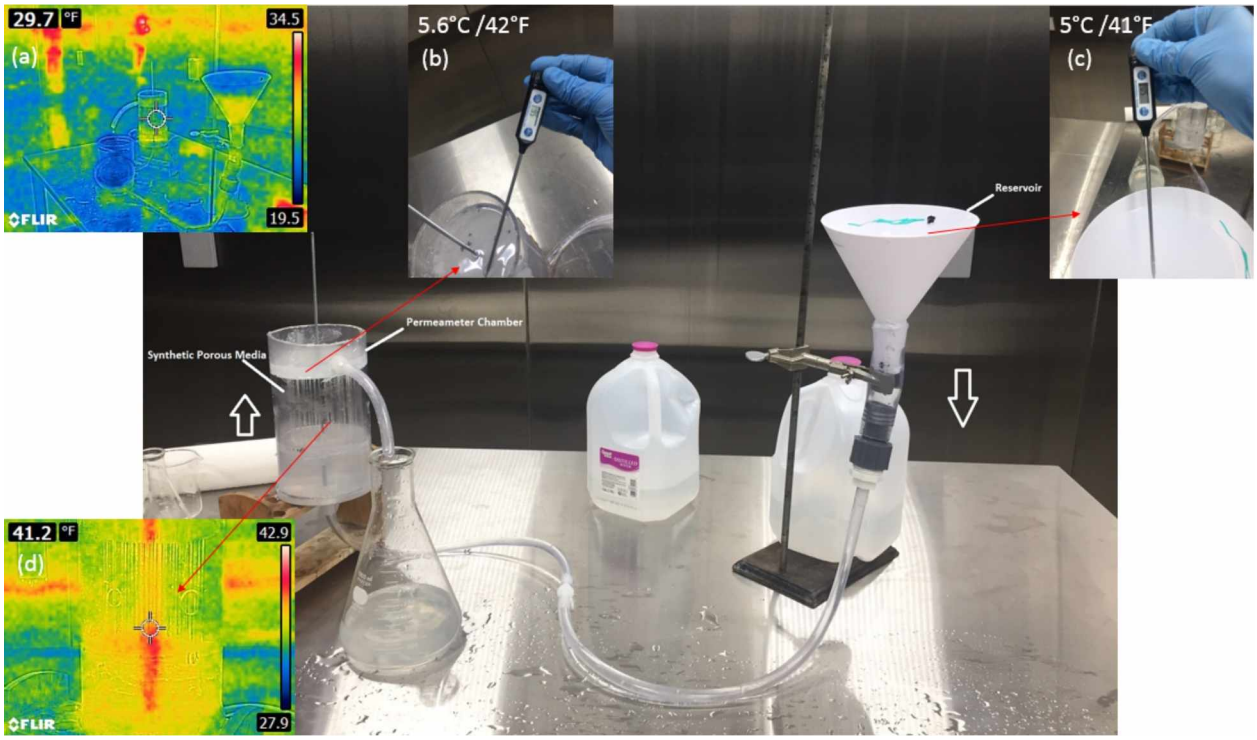

Figure 3.4. Temperatures at different locations of experimental setup for experiment conducted at 5 °C/41°F.

3.2.5 Background Theory

A theoretical framework presented by Abou Name and Atallah (2016) using combination of water and non-Newtonian fluid to estimate the pore structure of porous media was used to determine the flow characteristics obtained from our experiments. Their framework is based on an analog geometry of parallel capillary tubes that has the same functional behavior of real porous media in terms of saturated flow and porosity. The equivalent pore structure is formed by transforming the results from N saturated infiltration experiments using water and N-1 non-Newtonian fluids into a system of equations that yields N representative pore radii (R_i) (size distribution of tubes) and their corresponding percent contribution (weights) to flow (w_i) (Atallah, 2015; Abou Najm and Atallah, 2016). Their method used the following three problem types to characterize infiltration using a Matlab solver developed by Atallah (2015).

Problem Type 1: Obtaining weight (flow contributions) from pre-defined radii.

In problem type 1, the total number of distinct radii types of tubes are used to determine the contribution of flow by each radii type. In our experiments we have used two sizes, viz. 0.5mm and 0.9mm radii tubes. Therefore number of distinct radii types, N = 2. This N = 2 information is

fed to the Matlab solver (explanation is provided in section 3.2.6), which calculates the percent contribution of flow by the tubes of a particular radii type.

Problem Type 2: Obtaining radii from pre-defined weights (flow contributions)

Problem type 2 provides the option of inputting the weights in the Matlab solver for which it will generate the radius that has contributed to the percent of flow contribution or weight. Through this, the understanding of typical pore structures responsible for flow of any fluid is developed.

Problem Type 3: Obtaining both radii and weights (flow contributions) within a pre-defined range and minimum inter-radial spacing.

For problem type 3, Matlab solver requires the values of d_{adj} (i.e., minimum ratio between the ith and (i+1) th representative radius) and d_{range} (maximum ratio between the largest and smallest radius) to calculate both radii and weights. The requirement for problem type 3 is d_{range} must be equal to or greater than the $d_{adj}^{(N-1)}$ (we have two radii (N=2) in the synthetic porous media which have reduced the $d_{adj}^{(N-1)}$ to d_{adj}). The ratio of the two radii of the porous media would provide the value of d_{adj} to be 1.8 and to satisfy the condition of problem type 3 ($d_{range} \geq d_{adj}^{(N-1)}$) 10 was selected for the d_{range}.

3.2.6 The Matlab Solver

The Matlab based solver developed by Atallah (2015) was used to solve the three problem types, stated in sub-section 3.2.5, at three different temperatures of 19 °C, 5°C and 0.6 °C by using L2 norm objective function. The solver required the flow, viscosity and soil inputs to generate the simulation results. Flow inputs consist of flow (L^3 /T) generated by our infiltration experiment, density (M/L^3) of the liquid and head gradient. Solver provided the option of selecting between power law and cross law model for shear rate vs shear stress relationship of the fluids. For our simulation purposes, power law model was used for both water and non-Newtonian fluid. Power law model inputs consist of power law index (i.e., n) and consistency index (i.e., K) as provided in Table 2.6. Either Guar gum or Xanthan gum was needed for the simulation along with water. Based on prior conducted rheological experiments (Chapter 2), we have selected the 0.5g/l Xanthan gum over 0.5g/l Guar gum as low concentration of Xanthan gum showed the clear shear thinning behavior while 0.5g/l Guar gum displayed behavior asymptotic to Newtonian flow. Prior conducted rheological test of Xanthan gum at different

temperatures had provided the power model parameters (Table 2.6). Densities for Xanthan gum at different temperatures were calculated experimentally (Table 3.2). These densities of Xanthan gum along with densities and dynamic viscosities of water were used for simulation.

Table 3.2. Densities of water and Xanthan gum at different temperatures.

Fluid Type	Temperature (°C)	Density (kg/m3)	Dynamic Viscosity ($N.s/m^2$)
Water	19	998.38	1.03E-03
Water	5	1000	1.52E-03
Water	0.6	999.824	1.78E-03
0.5g/l Xanthan gum	19	929.75	-
0.5g/l Xanthan gum	5	941	-
0.5g/l Xanthan gum	0.6	966	-

Soil inputs in solver required the porosity, total sample volume and saturated depth. The length of the synthetic porous media was 0.1m, same as the saturated soil depth. The solver manual and other details may be accessed from Atallah (2015).

Equation 2 represents the flow in a single capillary tube.

$$Q = 2\pi \int_0^R r \times v_z dr \qquad (2)$$

For the power law model, flow is given by equation 3.

$$Q = 2\pi \int_0^R r \times v_z dr = \pi * \frac{\alpha}{1+3\alpha} \left[\frac{-H}{2\beta}\right]^{\frac{1}{\alpha}} R^{\frac{1}{\alpha}+3} \qquad (3)$$

Here, Q (m^3 /s) is the flow, R (m) is the representative radius, v (m/s^2) is the velocity for fluid, α is dimensionless exponent (power law index), which for water is 1.0. β is the consistency index in $Pas.s^{\alpha}$. For vertical flow H is given by following equation

$$H = \rho g\left(\frac{\partial h}{\partial z} - 1\right) \qquad (4)$$

Here, ρ (kg/m^3) is the density, g ($m/s^{2)}$ is gravitational acceleration and $\frac{\partial h}{\partial z}$ represents the head gradient per unit length.

After solving for three problem types, generated flow through synthetic porous media was represented by maximum displacement distance (MDD) in kilometers or meters. The MDD was calculated by using the equation D_z=qt. D_z represents the infiltration depth, q is velocity obtained by dividing the flow by area and t is time.

3.2.7 Goodness of Fit Tests

The Nash-Sutcliffe efficiency coefficient (NSE), the Absolute percent relative error (APRE) and the percent bias (PBIAS) statistics were used to compare the efficiency of the model predictability as compared to the theoretically computed MDD. Nash-Sutcliffe efficiency (NSE) is a normalized statistic that determines the relative magnitude of the residual variance ("noise") compared to the measured data variance ("information"). NSE indicates how well the plot of observed versus simulated data fits. NSE ranges between negative infinity and 1 (optimal value). NSE values between 0 and 1 are considered acceptable levels of performance (Moriasi et al., 2007).

$$\mathrm{NSE} = 1 - \left[\frac{\sum_{i=1}^{n}(Y_i^{obs} - Y_i^{sim})^2}{\sum_{i=1}^{n}(Y_i^{obs} - Y^{mean})^2}\right] \qquad (5)$$

Y_i^{obs} is the ith observation value and Y_i^{sim} is the simulated value. Y^{mean} is the mean of the observed data and n is the total number of observations.

Absolute percent relative error measures the total relative error between simulated and observed data. The optimal value for the APRE is zero.

$$\mathrm{APRE} = \frac{\sum_{i=1}^{n}(Y_i^{sim} - Y_i^{obs})}{\sum_{i=1}^{n} Y_i^{obs}} \qquad (6)$$

Percent bias measures the average tendency of the simulated data to be larger or smaller than their observed counterparts. Zero represents the optimal value for PBIAS. Positive values indicate model underestimation bias, and negative values indicate model overestimation bias (Moriasi et al., 2007).

$$\mathrm{PBIAS} = \left[\frac{\sum_{i=1}^{n}(Y_i^{obs} - Y_i^{sim}) * 100}{\sum_{i=1}^{n} Y_i^{obs}}\right] \qquad (7)$$

3.3 Results and Discussion

3.3.1 Problem Type 1

Maximum displacement distance (MDD) for problem type 1 for the four synthetic porous media sets (Table 3.1) were plotted against cumulative percent flow at 0.6 °C, 5 °C and 19°C (Figure 3.5). MDD plots were generated for single pore (N=1 model), two representative pores (N model) and theoretical infiltration of water at 3600 seconds. The N model used the combination of the Newtonian (i.e., water) and a non-Newtonian fluid (0.5g/l Xanthan gum) according to the method proposed by Abou Najm and Atallah (2016) to simulate the theoretical

infiltration of water in the synthetic porous media. The theoretical infiltration is based on the flow obtained for water from equation 3 using radii (0.025 cm and 0.045 cm) of capillary tubes involved in synthetic porous media. The N model used the flow obtained for both water and 0.5g/l Xanthan gum from the synthetic porous media infiltration experiments conducted at different temperatures in cold room. Plots in Figure 3.5 represents the depth of the water infiltration in every pore category. Percentage of water contributed by corresponding pore is represented by the area under each part of the curve (Atallah, 2015).

Plots for MDD versus percent flow were generated at same radii for N model at 0.6 °C, 5 °C and 19°C to compare the effect of temperature on infiltration depth for each of the four synthetic porous media sets (Table 3.3 and Figure 3.5). For problem type 1, Matlab solver provides the option of selecting the radius (pores), for which it will generate the weights (contribution to flow) and number of pores (Table 3.3). The infiltration depth of two representative pores (N model) increases with the increase in the temperature (Figure 3.5). This observation was noticed for all the synthetic porous media set involved in the experiment.

Table 3.3. Result summary of problem type 1 at different temperatures. Weights and number of pores are the results of simulation solved for the given inputted radii.

N	Temperature (°C)	Set	Radii(m)	weights	Number of pores
2	19	1	2.20E-04	0.593	64.58
			4.40E-04	0.407	2.77
		2	1.80E-04	0.470	95.88
			5.00E-04	0.530	1.82
		3	2.00E-04	0.645	73.18
			4.60E-04	0.355	1.44
		4	1.80E-04	0.620	84.32
			4.10E-04	0.380	1.92
1	19	1	2.49E-04	1.000	66.64
		2	2.34E-04	1.000	71.73
		3	2.21E-04	1.000	76.12
		4	2.02E-04	1.000	86.51
2	5	1	2.20E-04	0.552	66.40
			4.40E-04	0.448	3.37
		2	1.80E-04	0.443	97.90
			5.00E-04	0.557	2.07
		3	2.00E-04	0.633	77.04
			4.60E-04	0.367	1.60
		4	1.80E-04	0.611	89.12
			4.10E-04	0.389	2.11
1	5	1	2.61E-04	1.000	60.30
		2	2.43E-04	1.000	66.21
		3	2.29E-04	1.000	70.93
		4	2.09E-04	1.000	80.63
2	0.6	1	2.20E-04	0.474	63.47
			4.40E-04	0.526	4.40
		2	1.80E-04	0.378	96.46
			5.00E-04	0.622	2.67
		3	2.00E-04	0.532	74.15
			4.60E-04	0.468	2.33
		4	1.80E-04	0.506	84.83
			4.10E-04	0.495	3.08
1	0.6	1	2.76E-04	1.000	54.21
		2	2.62E-04	1.000	57.33
		3	2.45E-04	1.000	62.02
		4	2.24E-04	1.000	70.14

Results of APRE, NSE and PBIAS statistical tests were conducted on the MDD of single pore model and N model for each plot of problem type 1 and are summarized in Table 3.4. Results of statistical tests depict that there was no significant effect on the N model (two representative pores) performance at different temperatures. Each statistical test has more or less same value at all three studied temperatures.

Comparison of the two models demonstrates better performance of N model at all three studied temperatures with PBIAS of N model being 8% , -6% , 5% and 24% for synthetic porous media set 1, set 2, set 3 and set 4, respectively. While for N=1 model, PBIAS ranged between 42% to 69%. In term of NSE, only the value of set 01 at 0.6°C and 5°C and set 02 at 0.6°C resides under the acceptable range of NSE for N=1 model. While for N model NSE values for all four sets at all three temperature resides in the acceptable range of 0 to 1. Similarly, in terms of APRE, N model outperform the N=1 model for all synthetic porous media sets at all three studied temperatures. Even the worst performance of N model which was for set 04 performed better compared to the single pore (N=1) model.

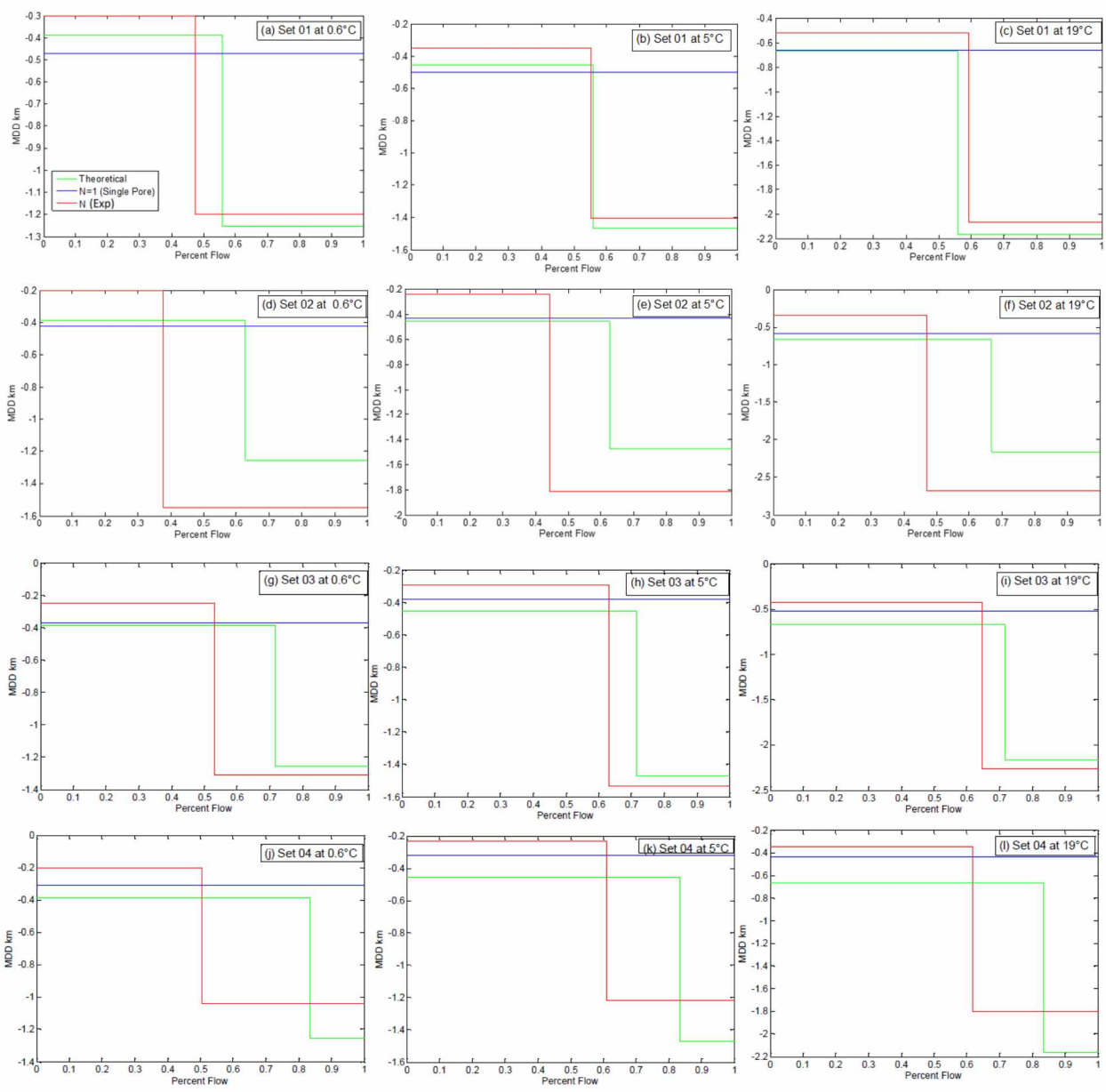

Figure 3.5. Maximum displacement distance versus percent flow for problem type 1 at 0.6 °C (1st Column), 5 °C (2nd Column) and 19°C (3rd Column) for four synthetic porous media sets at t = 3600 secs.

Table 3.4. Statistical test on MDD for Problem type 1

Problem Type 1						
Model	Temperature (Celsius)	Statistical Measure	Set 01	Set 02	Set 03	Set 04
N (2radii)	0.6	PBIAS (%)	8.63	-6.63	5.00	24.30
		NSE	0.97	0.68	0.94	0.79
		APRE (%)	8.63	29.33	11.96	24.30
	5	PBIAS (%)	8.68	-6.43	5.18	24.44
		NSE	0.97	0.68	0.94	0.78
		APRE (%)	8.68	29.17	11.84	24.44
	19	PBIAS (%)	8.68	-6.57	5.06	24.34
		NSE	0.97	0.68	0.94	0.79
		APRE (%)	8.68	29.28	11.92	24.34
N=1 (Single pore)	0.6	PBIAS (%)	42.58	48.36	54.74	62.16
		NSE	-0.65	-0.84	-1.07	-1.38
		APRE (%)	52.83	52.83	54.74	62.16
	5	PBIAS (%)	48.41	55.37	60.49	67.14
		NSE	-0.84	-1.10	-1.31	-1.62
		APRE (%)	52.83	55.37	60.49	67.14
	19	PBIAS (%)	53.31	58.75	63.14	69.33
		NSE	-1.02	-1.24	-1.43	-1.72
		APRE (%)	53.31	58.75	63.14	69.33

Experimental flow rates obtained from the infiltration experiments at different temperatures were used to plot the maximum displacement distance against the percent flow for deionized water, 0.5g/l Xanthan gum solution and 0.5g/l Guar gum solution at 900 seconds (Figure 3.6). At 19°C, all fluids have greatest infiltration depth in comparison to same fluid type at 0.6°C and 5 °C. This can be explained by considering the viscosity for each fluid type at particular temperature. For example, viscosity of Xanthan gum is higher than both water and Guar gum at all studied temperature. This results in lesser infiltration of Xanthan gum compared to Guar gum and water.

Prior experiments conducted for contact angle showed 0.5g/l Xanthan gum has lower angle of contact compared to 0.5g/l Guar gum solution at all the three studied temperatures, which means Xanthan gum solution has better wettability compared to Guar gum solution. The larger area of contact of Xanthan gum with solid surface also contributed to lesser infiltration by offering higher resistance to flow.

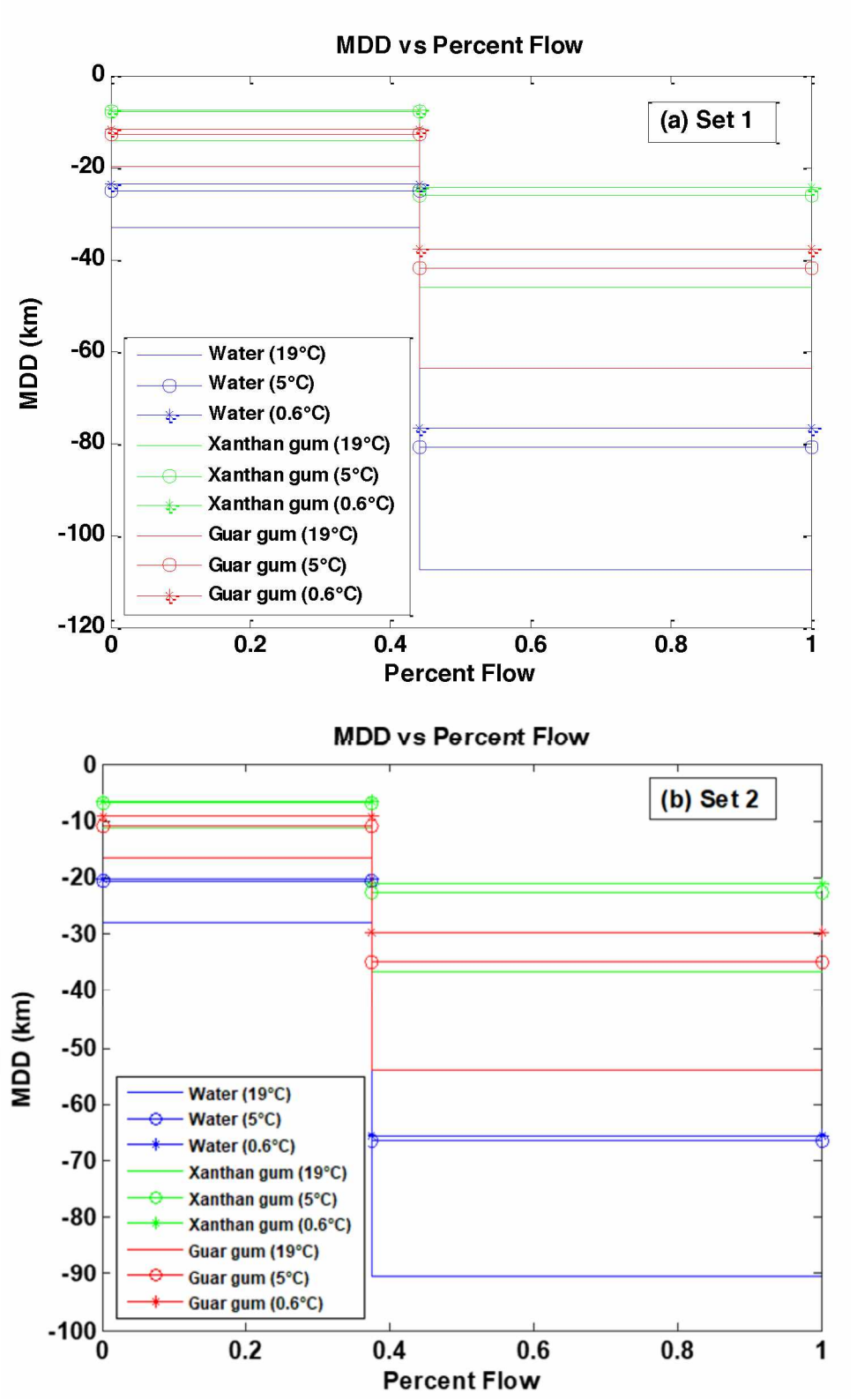

Figure 3.6. Infiltration depth of the water, Xanthan gum and Guar gum at 0.6°C, 5°C and 19°C for synthetic soil set 1 (a) and set 2

3.3.2 Problem Types 2 and 3

Maximum displacement distance (MDD) for problem type 2 (Figure 3.7) and problem type 3 (Figure 3.8) for the four synthetic porous media sets were plotted against cumulative percent flow at 0.6 °C, 5 °C and 19°C. For both problem types the result of the simulation (N model) was not representative of the theoretical infiltration of water. This observation was noticed for all sets of synthetic porous media at all studied temperatures.

To further investigate the causes of difference between the simulated N model and theoretical flow, FLIR thermal camera was used to record the temperature of experimental setup (Figure 3.3 and Figure 3.4). Thermal images showed that there was significant variation of temperature at different position of the experimental setup. Perhaps, this variation in temperature is the cause of the difference between the simulated N model and theoretical infiltration.

The variation in temperature at different position of the experimental setup would impact the flow (i.e., Q) of the infiltration experiments. To test this assumption, we have simulated N model using two different flows (Figure 3.9), simulation N (Exp) used the flow (i.e., Q) obtained from the infiltration experiments conducted in the cold room for both Newtonian and non-Newtonian fluid at 0.6°C and 19°C and simulation N (Est) used the flow obtained by using the equation (3) for both Newtonian and non-Newtonian fluid. Parameters (density, dynamic viscosity, etc.) required in the equation (3) were used according to the temperature at which the flow was calculated.

The performance of the simulation N (Est) was much better than N (Exp). The results obtained from N (Est) were much closer to the theoretical infiltration and thus bolsters our assumption that the values of N (Exp) were affected by the variation in temperature within the flow set up that affected the simulation results as shown in Figures 3.7 and 3.8.

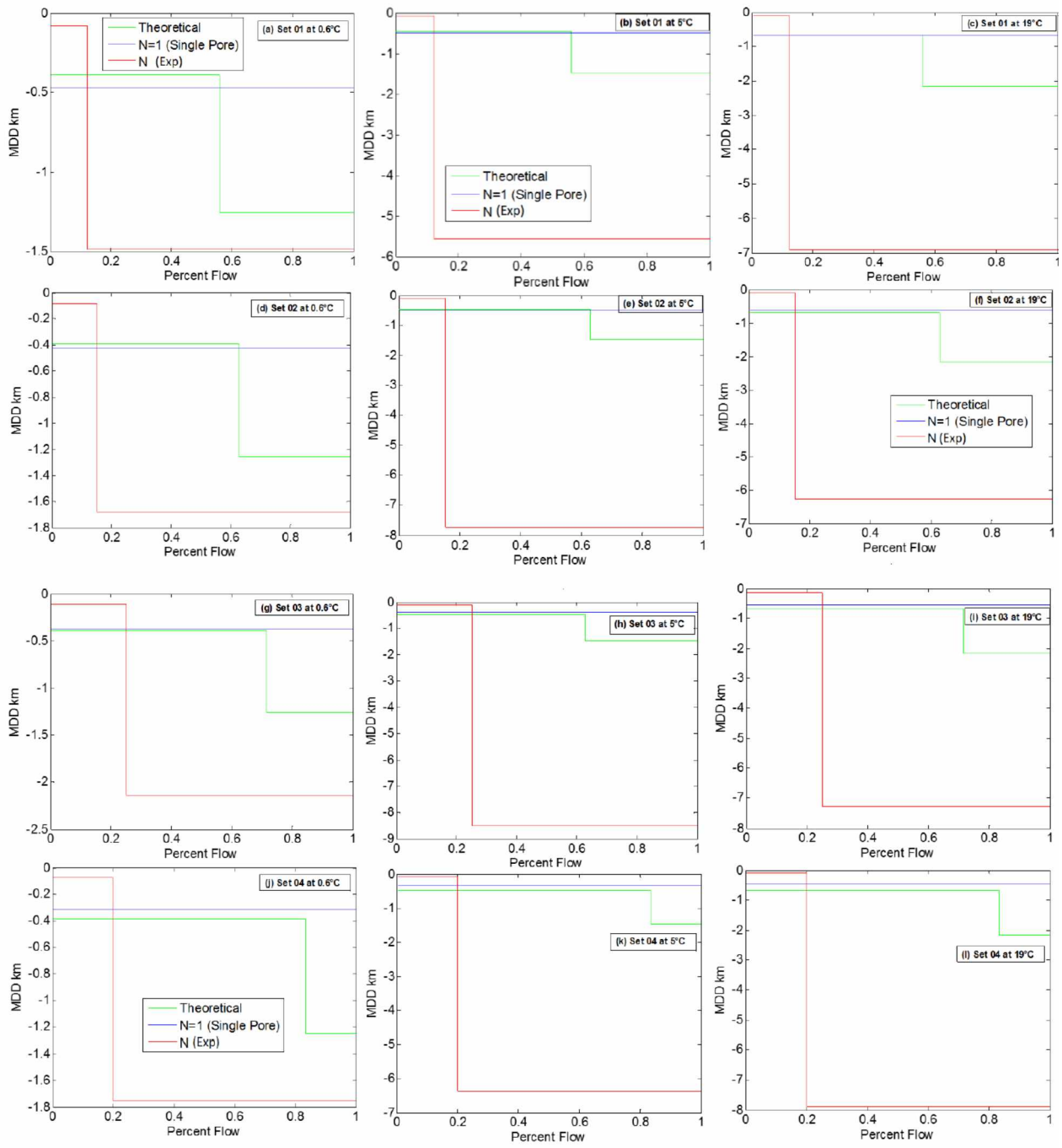

Figure 3.7. Maximum displacement distance versus percent flow for problem type 2 at 0.6 °C (1st Column), 5 °C (2nd Column) and 19°C (3rd Column) for four synthetic porous media sets at t = 3600 secs

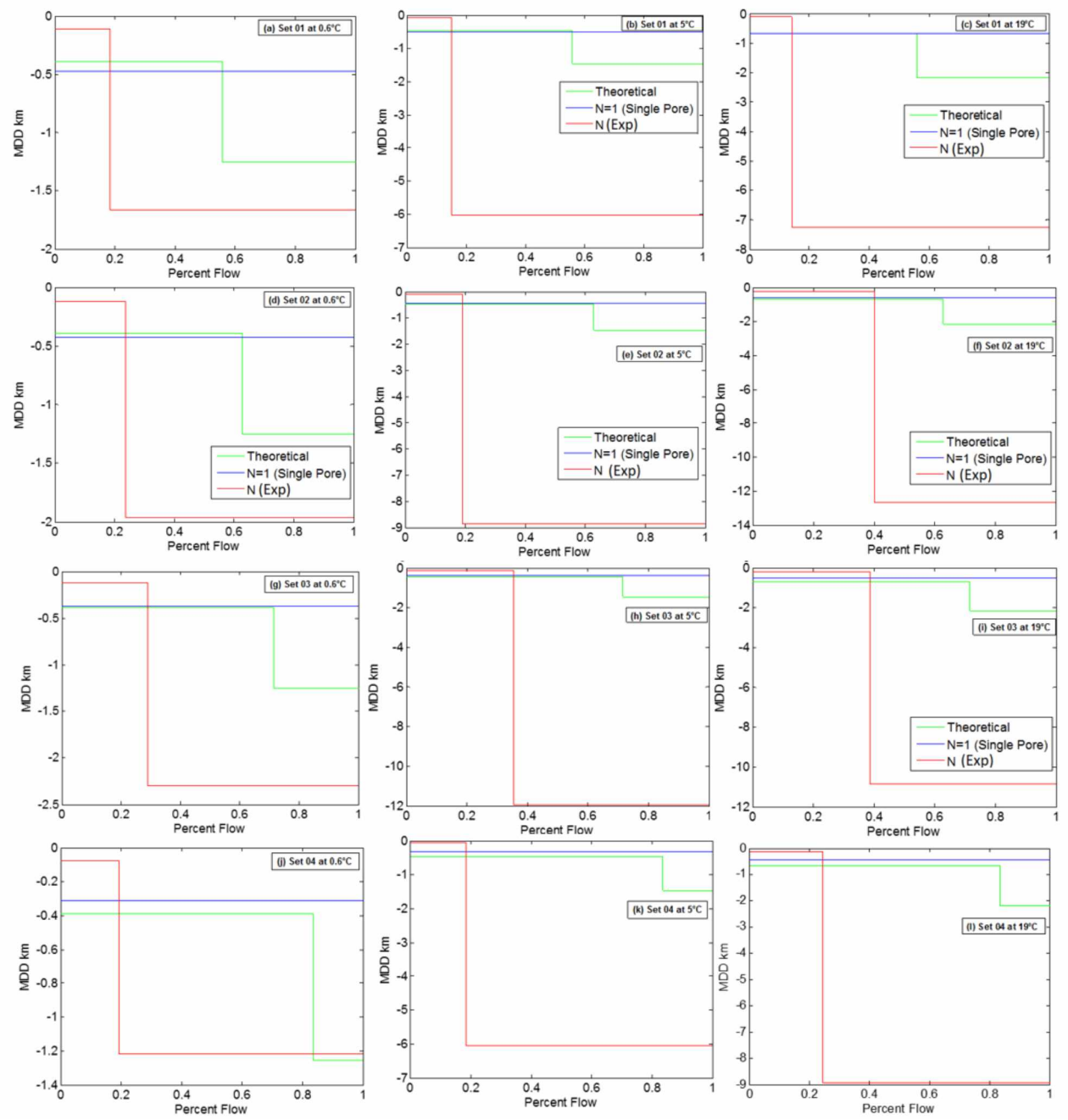

Figure 3.8. Maximum displacement distance versus percent flow for problem type 3 at 0.6 °C (1st Column), 5 °C (2nd Column) and 19°C (3rd Column) for four synthetic porous media sets at t = 3600 secs

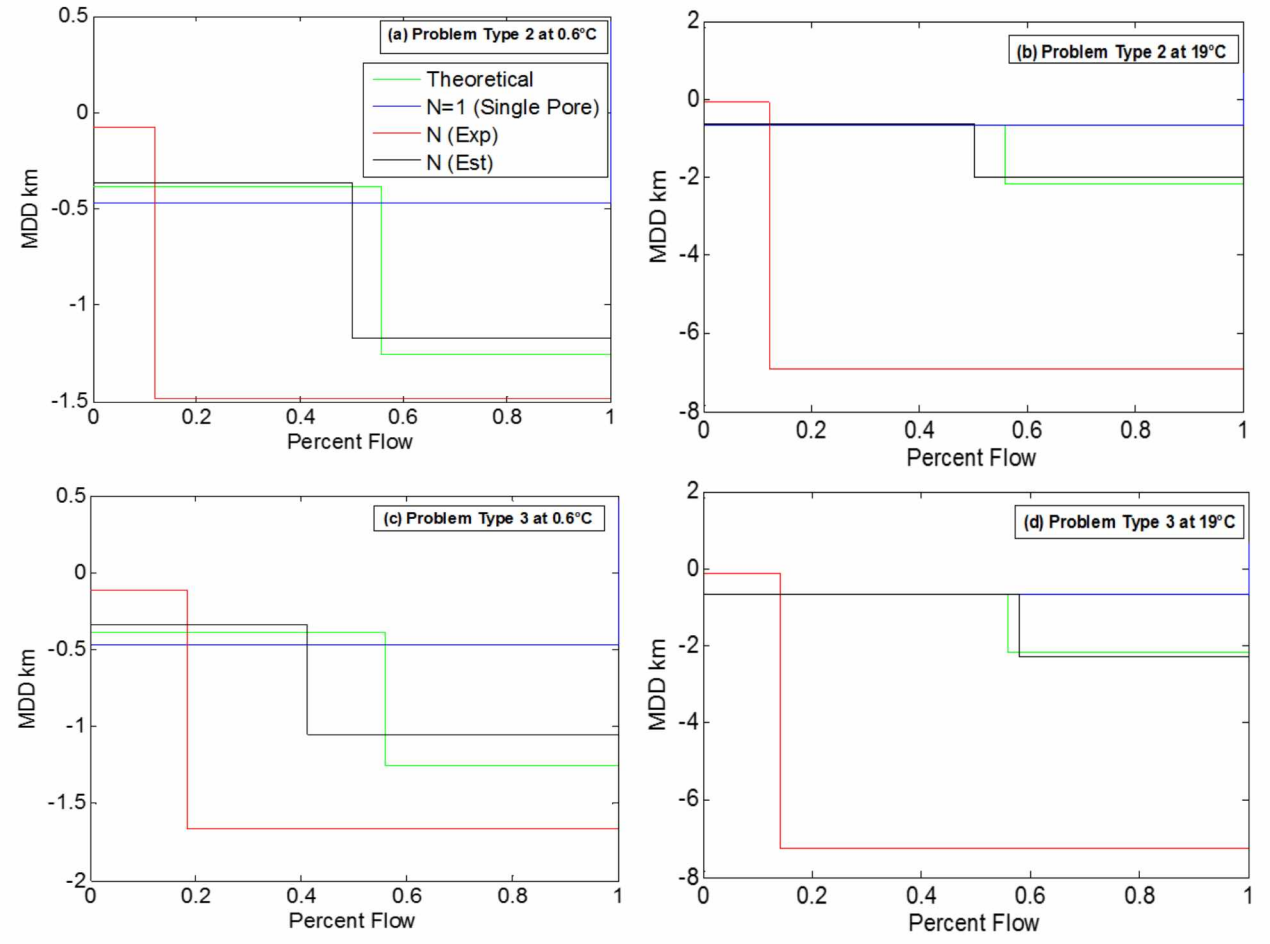

Figure 3.9. MDD versus percent flow for problem type 2 and 3 for set 1 at 3600s

Once variation of temperature was noted at different position of experimental setup (Figures 3.3 and 3.4), efforts were made to bring the entire experimental setup to uniform temperature. Despite all the efforts to maintain constant temperature, solid surfaces (Figures 3.3d, 3.3e and 3.4d), flowing fluid (Figures 3.3b, 3.3c, 3.4b and 3.4c) and ambient air (Figures 3.3a and 3.4a) are at different temperatures. It was observed during experiments that even handling of the experimental setup and flowing fluid would impact the temperature change. The difference in temperature between the solid surface, flowing fluid and ambient air would cause heat transfer by convection in the presence of moving fluid and by conduction in the absence of motion. The rate of heat transfer in a moving fluid is much higher by convection than by conduction and convection process is greatly influenced by fluid properties such as dynamic viscosity, density, thermal conductivity, and fluid velocity (Cengel, 2004). These fluid properties including the contact of fluid with solid surfaces (contact angle) are temperature sensitive and would be impacted by heat transfer, which would influence fluid flow through tubes resulting in difference between theoretical flow and experimental flow, N (Exp).

The temperature difference between the flowing fluid (Newtonian or non-Newtonian), solid surfaces (pipes and tubes) and ambient air would cause heat transfer until both bodies (liquid and solid or liquid and air) attain the same temperature at the point of contact. Despite keeping the experimental setup and fluids in the cold room for longer duration of time. This thermal equilibrium was never achieved because for experimental setup shown in Figure 3.2 it was very difficult to completely achieve the thermal equilibrium. The reason was moving fluid kept on changing the contact from ambient air at reservoir to tubes in synthetic porous media, both ambient air and tubes were at different temperatures, thus changing the reference temperature (i.e., temperature of ambient air or tubes) for flowing fluid to achieve.

Additionally, the concept of thermal profile is also important to consider. The difference in the temperature between flowing fluid and wall of the tubes would develop the thermal boundary layer (Cengel, 2004). The fluid particles near to the surface of the tube would get the energy from it. These fluid particles would exchange the energy with the particles in the adjoining fluid layer and particles in the adjoining fluid layer would pass it to the particles of the next layer. As a result, the temperature profile would be established in the flow field. Flow region over the surface of the tubes in which the temperature varies in the direction normal to the surface is the thermal boundary layer. The thermal boundary layer would impact the convective heat transfer

as the convective heat transfer rate along the surface depends on the temperature gradient at that location. (Cengel, 2004).

Fluid flowing through tubes would generate velocity and thermal profile. Velocity profile would generate in the hydrodynamic entrance length due to viscous forces arising between the layers of the flowing fluid. The velocity of the particles in the fluid layer close to the surface of the tube becomes zero because of the no-slip condition. Hydrodynamic entrance length is the minimum distance required to generate fully developed velocity profile for laminar flow and is dependent on the Reynolds number. Similarly, thermal entrance length is the minimum distance required to fully develop the thermal profile and is dependent on both Reynold number and Prandtl number (ratio of kinematic viscosity (dynamic viscosity/density) to thermal diffusivity).

For the fluids having Prandtl (Pr) number greater than 1.0, e.g., water has Pr number of 7.237 at 19°C, 11.2 at 5°C and 13.6 at 0.6°C, the hydrodynamic entrance length would be less than the thermal entrance length. Length of the capillary tubes used for construction of synthetic porous media is 10 cm, this length is sufficient for development of velocity profile. However, for fully developed stable thermal profile the length of the capillary tubes used in the synthetic porous media was not sufficient to meet the thermal entrance length requirement for 0.045 cm radius tubes.

No establishment of stable thermal profile and non-achievement of thermal equilibrium may be the cause of the error between experimental flow and theoretical flow. This needs to be investigated further by using longer insulated tubes of different diameters or lower than specified temperatures selected to achieve the maximum temperature level of that specified temperature in the experimental set up. Other factors that may be considered is using non-Newtonian fluids of slightly larger concentration, such as 1.0 g/l or 1.5 g/l.

3.4 Conclusion

- Infiltration depth of both Newtonian and non-Newtonian fluids would decrease with the decrease in temperature because of the change in their properties like dynamic viscosity, density and angle of contact. Infiltration of Xanthan gum solution is less compared to the Guar gum solution and water at a concentration of 0.5 g/l.
- Establishment of stable thermal profile and thermal equilibrium are critical for flow in synthetic porous media in non-isothermal flow conditions.

3.5 References

Abou Najm, M.R., and Atallah, N., M. 2016. Non-Newtonian fluid in action: Revisiting Hydraulic Conductivity and Pore Size Distribution of Porous Media. Vadose zone J. doi: 10.2136/vzj2015.06.0092.

Atallah, N.M., 2015. Solver for a new theory for revisiting Hydraulic Conductivity and pore size distribution of porous Media. Master Thesis, Department of Civil and Environmental Engineering American University of Beirut. p.116

Barnes, D.L., W. Rhodes, S. Frutiger, R. Ranft. 2007. Persistence of Herbicides in a Subarctic Environment. In proceedings of the 8th International Symposium on Cold Regions Development, Tampere, Finland, September 25-27.

Cengel, Y.A., 2004. Heat Transfer: a practical approach. New York, NY: McGraw-Hill

Gillham, R.W., and O'Hannesin, S.F., 1994. Enhanced degradation of halogenated aliphatics by zerovalent iron. Ground Water 32, 958–971.

Moriasi, D.N., Arnold, J.G., Van Liew, M.W., Bingner, R. L., Harmel, R. D., and Veith, T. L., 2007. Model Evaluation Guidelines for Systematic Quantification of Accuracy in Watershed Simulations. American Society of Agricultural and Biological Engineers, 50(3) :885-900.

Jung, J., Jang, J., and Ahn, J., 2016. Characterization of a Polyacrylamide Solution Used for Remediation of Petroleum Contaminated Soils, Materials, 9, 16: 1 – 13.

Palaniappan, M., Gleick, P.H., Allen, L., Cohen, M.J., Christian-Smith, J., and Smith, C., 2010. Clearing the Waters: A Focus on Water Quality Solutions, United Nations Environmental Programme Publication, Nairobi, Kenya, pp. 89.

Zhong, L., Oostrom, M., Truex, M.J., Vermeul, V.R., Szecsody, J.E., 2013. Rheological behavior of Xanthan gum solution related to shear thinning fluid delivery for subsurface remediation. Journal of Hazardous Material 244-245, 160-170.

Chapter 4 Comparison of Newtonian and non-Newtonian fluid for Remediation of Adsorbed Contaminant[3]

Abstract

The goal of this research was to compare the effectiveness of Newtonian and non-Newtonian fluids for effective remediation of adsorbed contaminant in porous media under non-isothermal flow regimes. Non-Newtonian fluids can adjust their viscosity according to the applied shear rate. This was useful parameter that was considered in contaminant remediation from the glass-tube-bundle setup, which acted as a synthetic porous media. Synthetic porous media consist of varying numbers and different diameters of standard capillary tubes. Small diameter capillary tubes behaved as low permeability zone and offered higher shear rate. This higher shear rate offered a decrease in the viscosity of non-Newtonian fluids, which facilitated fluid penetration through smaller diameter capillary tubes. Dichlobenil was used as a candidate contaminant, which was injected into the capillary tubes of the synthetic porous media until it filled all the pores. After that water, 0.5g/l Guar gum solution and 0.5g/l Xanthan gum solution were allowed to pass in separate experiments through the synthetic porous media to remediate Dichlobenil. Gas Chromatography-mass spectrometry (GCMS) analysis was conducted to find the amount of Dichlobenil removed by each fluid type from the porous media. Limited experiments conducted at 19°C showed water was the most effective fluid in remediating the contaminant from porous media in comparison to Guar gum and Xanthan gum.

Keywords: Guar gum, Xanthan gum, Contaminant remediation

4.1 Introduction

Contamination of soil and groundwater caused by human activities is turning into a major global problem. Contamination such as those caused by heavy metals through mining activities, use of pesticides in agricultural fields to enhance crop growth, industrial effluents from factories, and oil and gas spills are some diverse sources, which are adversely impacting soils and aquifers around the world. The impact of contaminant is not limited to human beings but has detrimental impacts on environment including wildlife and marine life. Growing population and climate change would worsen the problem of contamination. It is need of the hour to test and develop alternate and effective contaminant remediation techniques.

[3] Naseer et al. Comparison of Newtonian and non-Newtonian fluid for Remediation of Adsorbed Contaminant. Unpublished Manuscript 2019.

Non-Newtonian fluids are gaining interest in recent years for subsurface remediation. Guar gum solution was investigated for the treatment of drinking water, industrial effluent, and transportation of microscale zero-valent iron particles in porous media (Mukherjee et al., 2017, Gupta and Ako, 2005, Tosco et al., 2014). Xanthan gum solution was tested to deliver remedial amendments (e.g., phosphate, sodium lactate, ethyl lactate) for subsurface remediation (Zhong et al., 2013). Non-Newtonian shear thinning fluid viscosity decreases with increase in shear rate, which facilities the penetration of these fluids into low permeability zones as shear rate offered by low permeability zone is high. Through this attribute, non-Newtonian fluids offer effective remediation of contaminants from low permeable zones that would otherwise be bypassed by water. Additionally, these polymers are non-toxic, cheap and benign to environment. We have used two most common non-Newtonian shear thinning fluids, Guar gum and Xanthan gum, for studying their remediation capability of Dichlobenil as a candidate contaminant.

Dichlobenil was selected as a contaminant because it is less harmful when used in laboratory for experiments. Dichlobenil is herbicide used to control weeds and grass growth in agricultural and residential areas, it is commercially available in root killer products. Dichlobenil is strongly adsorbed to soils (Porazzi et al., 2005) and is also persistent in water (Cox, 1997).

A synthetic porous media was developed by using varying number and different diameter capillary tubes. Use of different diameter tubes (represents pores) offered different shear rate to fluid flow in the same synthetic porous media. Large diameter capillary tubes offered low shear rates and small diameter capillary tubes offered high shear rates to the flowing fluid. The non-Newtonian fluid flow might be uniform through the different diameter capillary tubes as fluid can adjust viscosity according to the applied shear rate. This can be useful in remediating the contaminant uniformly from both small and large tubes simultaneously.

The objective of this research work is to compare the effectiveness of water, 0.5g/l of Guar gum and 0.5g/l Xanthan gum for remediation of Dichlobenil (2,6-Dichlorobenzonitrile) surrogate contaminant from the synthetic porous media.

4.2 Methodology

Three hundred milligram of commercially available Roebic root killer with 0.55% active Dichlobenil (2, 6-Dichlorobenzonitrile) was dissolved in 100ml of water at 19°C to generate 16.5 ppm solution. The prepared contaminant solution was injected in the capillary tubes of synthetic porous media with the help of 10 microliter injections (Figure 4.1a). The total volume injected in

the synthetic porous media was 0.75ml. The total pore volume of synthetic porous media was 1.29 ml.

Fluids used for the contaminant remediation from porous media were deionized water, 0.5g/l Guar gum solution and 0.5g/l Xanthan gum solution at 19°C. Each fluid type was filled in the reservoir at higher head and allowed to pass through the synthetic porous media (already installed in a permeameter chamber) containing 0.75ml of contaminant (Figure 4.1b). For each experiment, 0.75ml of contaminant was first injected into the porous media and then each fluid type was allowed to pass through the porous media to collect the downstream effluent in separate beakers. The effluents were collected in three intervals 38.75 pore volume (PV, first 50ml), 38.75 PV (next 50ml), and 77.5 PV (last 100ml).

Ten grams of Sodium Chloride was added to the 38.75 PV (Twenty grams of Sodium chloride was added to 77.5 PV outflow) outflow generated from the experiments in the separatory funnel (Figure 4.1c). After the dissolution of Sodium Chloride in 38.75 PV outflow, 15ml of Methylene Chloride (Dichloromethane) was added to the funnel (Figure 4.1d). After mild shaking, the Methylene Chloride layer from the funnel was collected in the beaker (Figure 4.1 e). Addition of 15ml of Methylene Chloride to 38.75 PV outflow (water or Guar gum or Xanthan gum) in separatory funnel was repeated thrice for maximum extraction of Dichlobenil from outflow. Addition of Methylene Chloride facilitated the separation of Dichlobenil from effluent (water or Guar gum or Xanthan gum) inside separatory funnel. The 1ml of collected Methylene Chloride containing Dichlobenil from beaker was transferred to vials for Gas Chromatography-Mass Spectrometry (GC-MS) analysis (Figure 4.1f). Dichlobenil standard for GC-MS was also prepared in Methylene Chloride. To check the variability caused during the process of GC-MS analysis 10 microliters of Nitrobenzene-d5 was added to vials of samples and standard.

Figure 4.1. (a) Injection of Dichlobenil in capillary tubes of synthetic porous media. (b) Experimental set up (c) Separatory funnel containing salt and outflow (water or Guar gum or Xanthan gum (d) Addition of 15ml Methylene Chloride to separatory funnel (e) Layering of Methylene Chloride and outflow in separatory funnel (f) 1ml vials for GCMS analysis

To investigate the effectiveness of remediation of contaminant from the synthetic porous media using Newtonian and non-Newtonian fluids at 0.6°C and 5°C, 16.5 ppm Dichlobenil solution prepared at 19°C (Figure 4.2a) was cooled down to 8°C (Figure 4.2b). Cooling of the 16.5ppm Dichlobenil solution results in the precipitation of the Dichlobenil (Figure 4.2b). As a result of precipitation, the concentration of Dichlobenil solution was not sufficient for quantification. Less concentrated solution of the Dichlobenil was also prepared to conduct experiments at low temperature but after the extraction of Dichlobenil using Methylene Chloride in separatory funnel, final concentration of Dichlobenil was not sufficient for quantification.

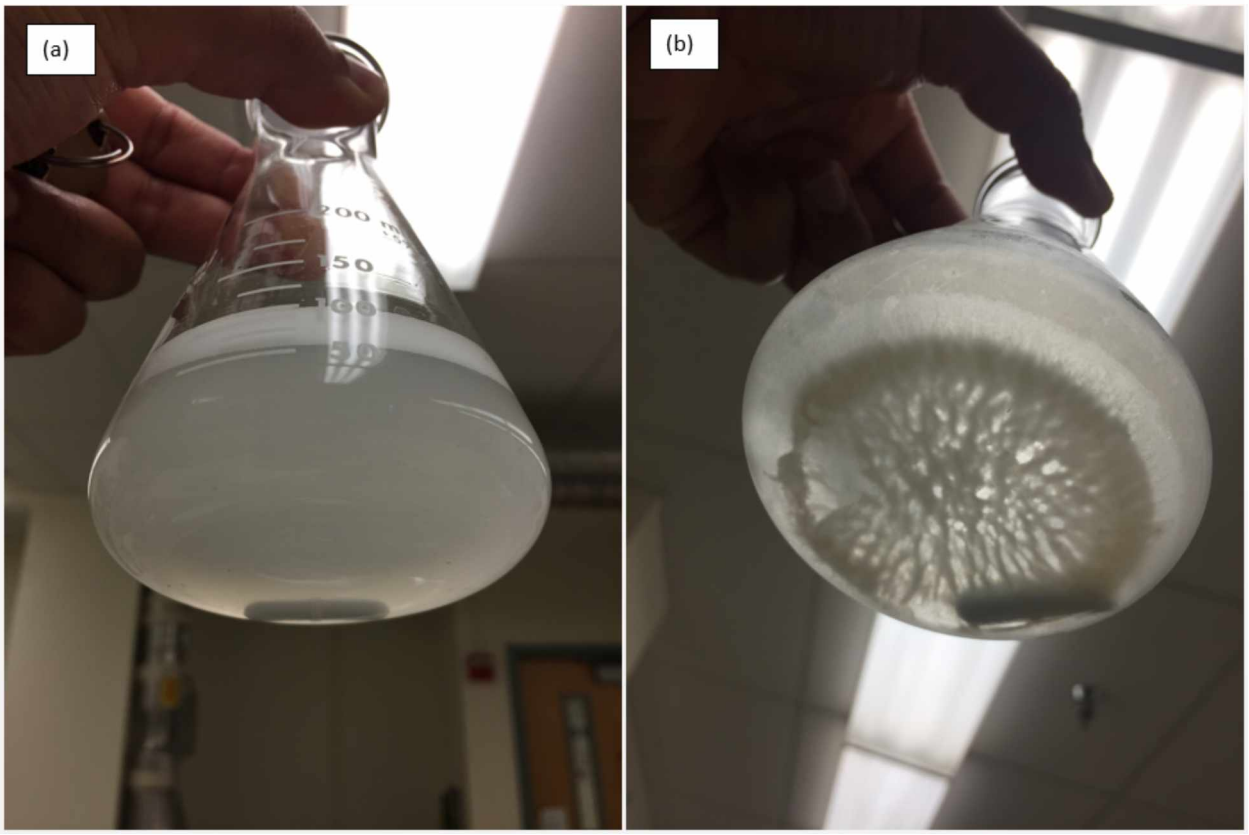

Figure 4.2. 16.5 ppm of Dichlobenil at (a) 19°C and (b) 8°C

4.3 Results

The GC-MS analysis of the samples collected from experiments conducted at 19°C showed the effectiveness of water, 0.5g/l Guar gum solution and 0.5g/l Xanthan gum solution for remediation of the surrogate contaminant, Dichlobenil, from the synthetic porous media (Figure 4.3). The part per billion concentrations of Dichlobenil were obtained from the chromatographs of water (Figures 4.4 and 4.5), 0.5g/l Guar gum (Figures 4.6 and 4.7) and 0.5g/l Xanthan gum (Figures 4.8 and 4.9). Result of the GC-MS analysis showed that water was the most effective fluid in remediating the herbicide from the capillary tubes of the synthetic porous media, as can be seen in Figure 4.3.

Remediation of Dichlobenil from the synthetic porous media using Guar gum was 33%, 41% and 53 % less than water for 1st 38.75PV, 2nd 38.75PV and 3rd 77.5 PV of effluent, respectively. Similarly, Xanthan gum remediated 58 %, 63 % and 59 % less Dichlobenil compared to water for 1st 38.75PV, 2nd 38.75PV and 3rd 77.5 PV of effluent, respectively. The least removal of herbicide from the synthetic porous media was observed for the Xanthan gum. Comparison between the two polymers showed the Xanthan gum remediation of contaminant was 37%, 38% and 14% less than Guar gum for 1st 38.75PV, 2nd 38.75PV and 3rd 77.5 PV of effluent, respectively. The total herbicide removed by all the fluids from porous media demonstrated the highest contribution of water (51 %), than Guar gum (28 %) and lastly Xanthan gum (20%). From our rheological experiments, we know the 0.5g/l Xanthan gum have the highest viscosity compared to 0.5g/l Guar gum and water having the least viscosity. This comparison showed that the fluid having highest viscosity is least effective for contaminant remediation from the synthetic porous media.

Water might have removed the contaminant from the large diameter tubes. This is because water flow through the path of least resistance and larger diameter tubes offer least resistance to flow of water compared to small diameter tubes. This might have prevented the water to remove the contaminant from small diameter tubes. On the other hand, Guar gum and Xanthan gum might have removed the contaminant from both diameter tubes simultaneously. This needs to be further investigated by modifying the methodology of experiments to keep track of contaminant removal from each tube of specific diameter for each fluid type.

The use of higher concentration of polymers and longer tubes in synthetic porous media would be important for the remediation experiments. Higher concentration would provide the

better shear thinning and higher viscosity (better scouring). Both these properties are desirable for contaminant remediation from capillary tubes. Longer tubes in the synthetic porous media not only hold more contaminant for quantification purposes but also helps to observe the effectiveness of shear thinning of non-Newtonian fluids in removing contaminant from small diameter tubes.

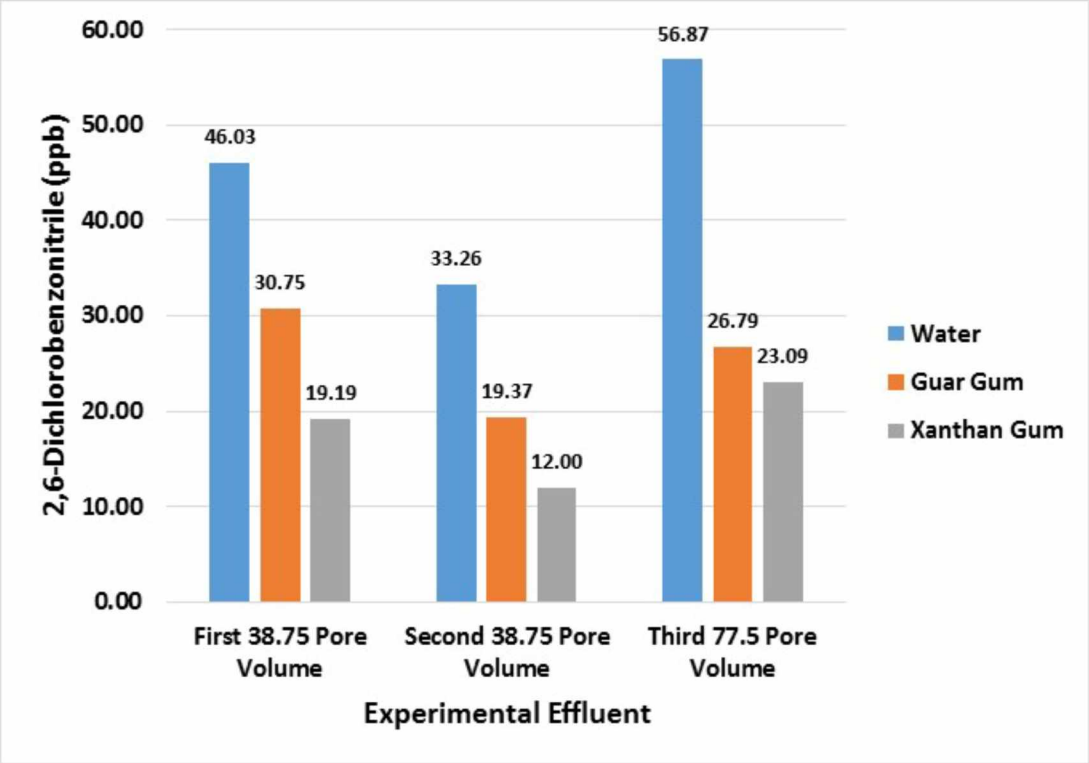

Figure 4.3. Comparison of water, Guar gum and Xanthan gum for removal of 2, 6-Dichlorobenzonitrile from synthetic porous media.

Chromatographs of deionized water (Figures 4.3 and 4.4), 0.5g/l Guar gum (Figures 4.5 and 4.6) and 0.5g/l Xanthan gum (Figures 4.7 and 4.8) showed multiples peaks. The peaks before and at 6 minutes represented Nitrobenzene-d5 that was added to the samples to check the variability caused in detection during the process of analysis. Peaks close to 8 minutes represented detection of 2, 6-Dichlorobenzonitrile in samples.

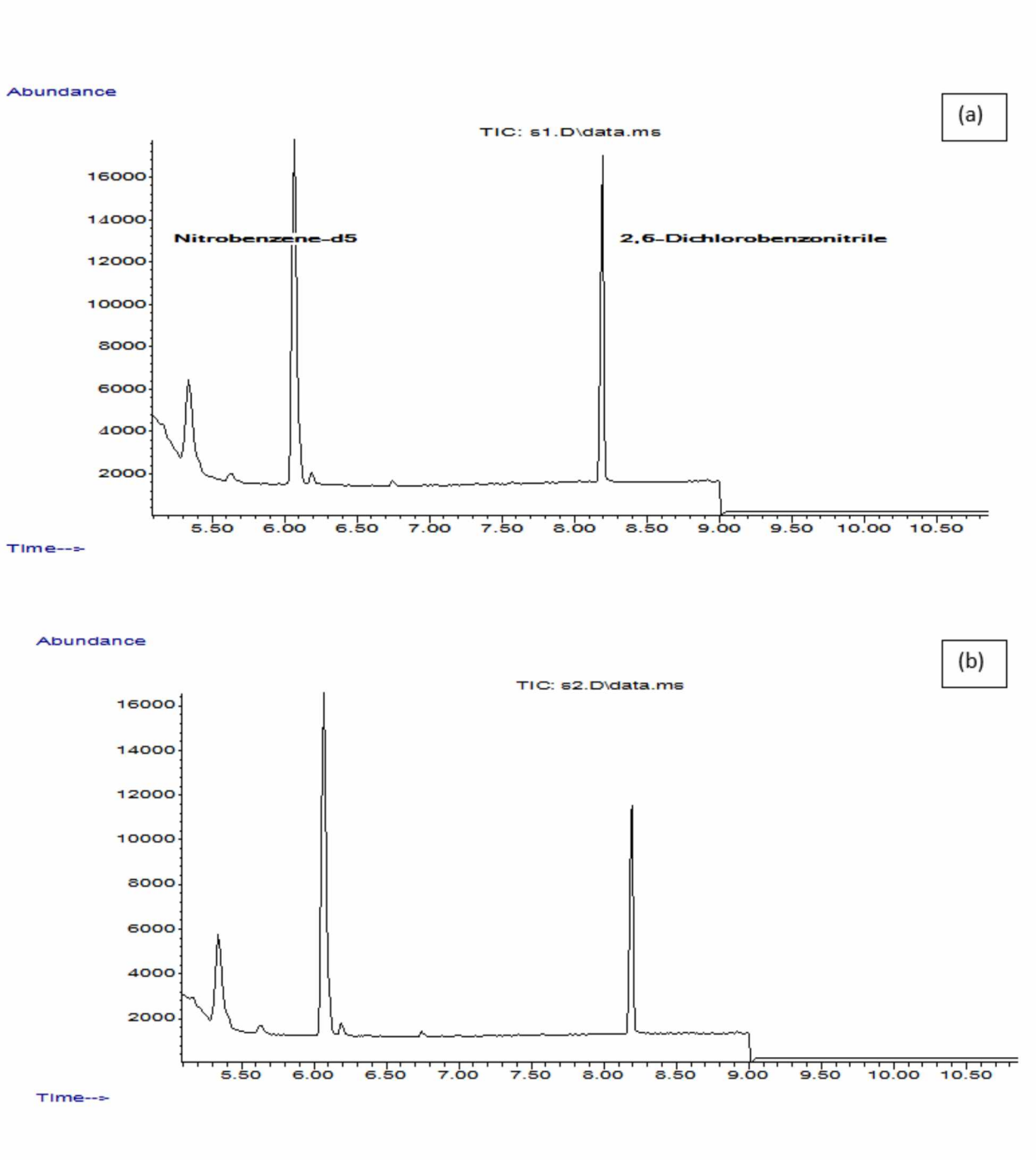

Figure 4.4. Time is in minutes and abundance is in counts. (a) Chromatograph for first 38.75PV (i.e., 50ml) of water outflow. (b) Chromatograph for second 38.75PV (i.e., 50ml) of water outflow.

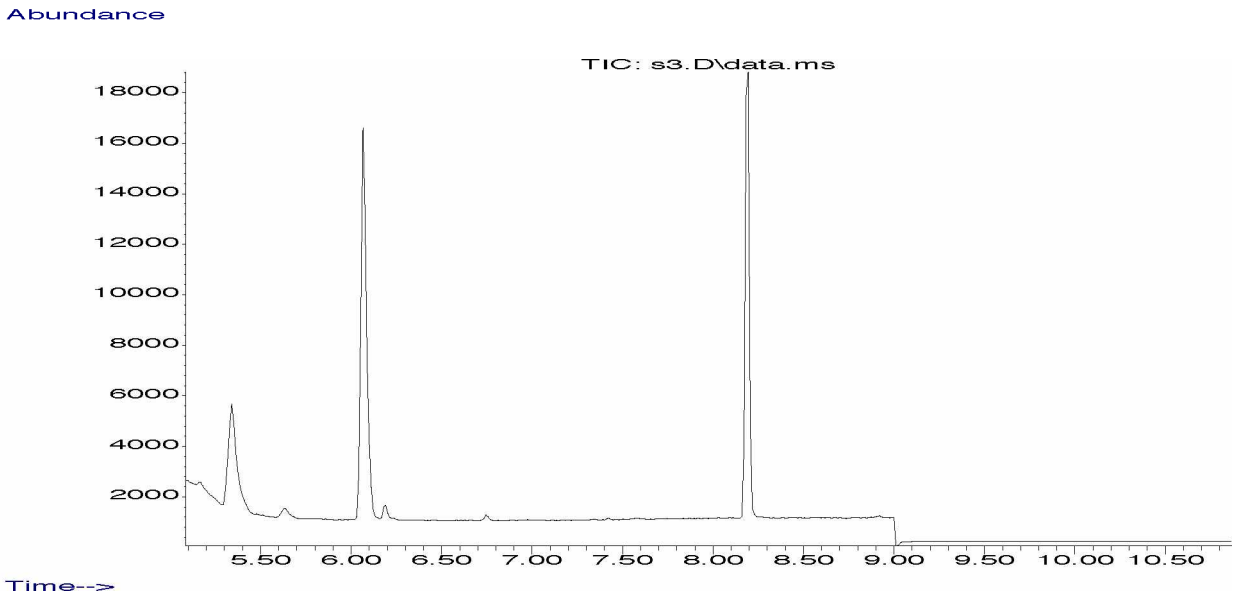

Figure 4.5. Chromatograph for third 77.5PV (i.e., 100ml) of water outflow

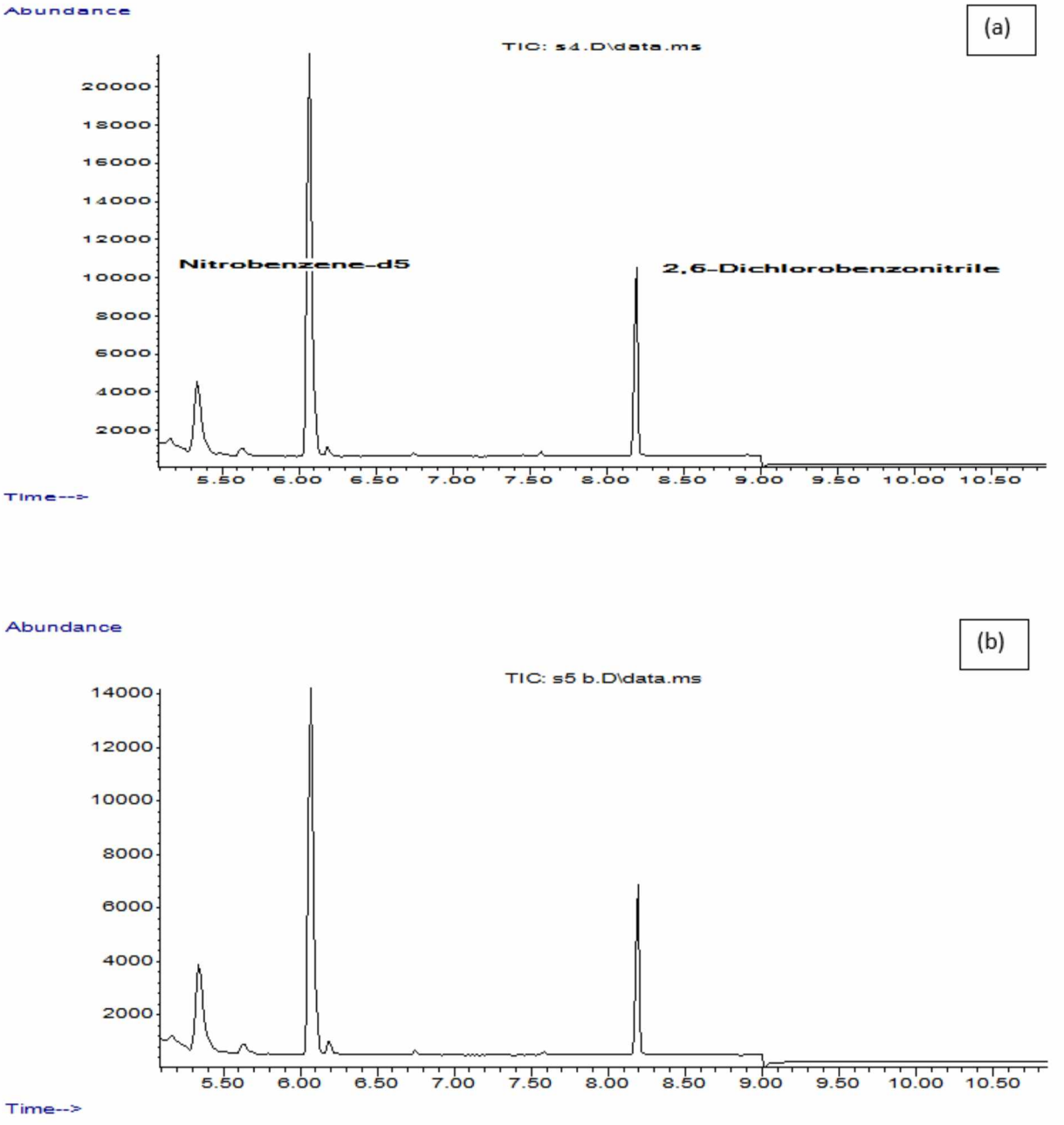

Figure 4.6. (a) Chromatograph for first 38.75PV of Guar gum outflow. (b) Chromatograph for second 38.75PV of Guar gum outflow.

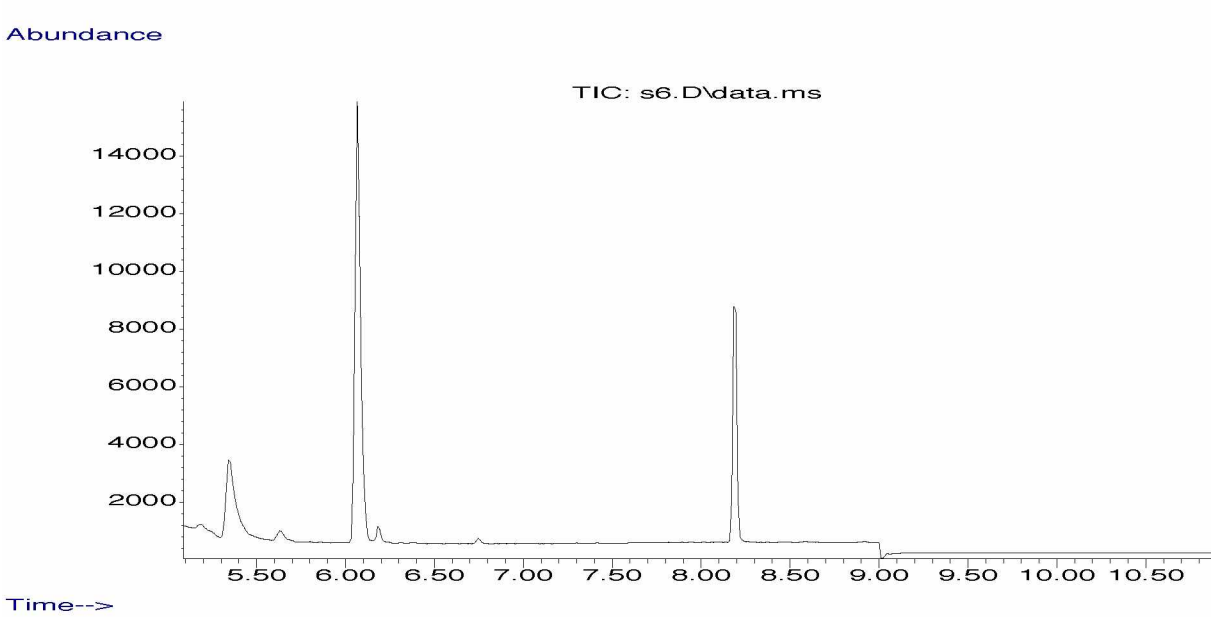

Figure 4.7. Chromatograph for third 77.5PV of Guar gum outflow

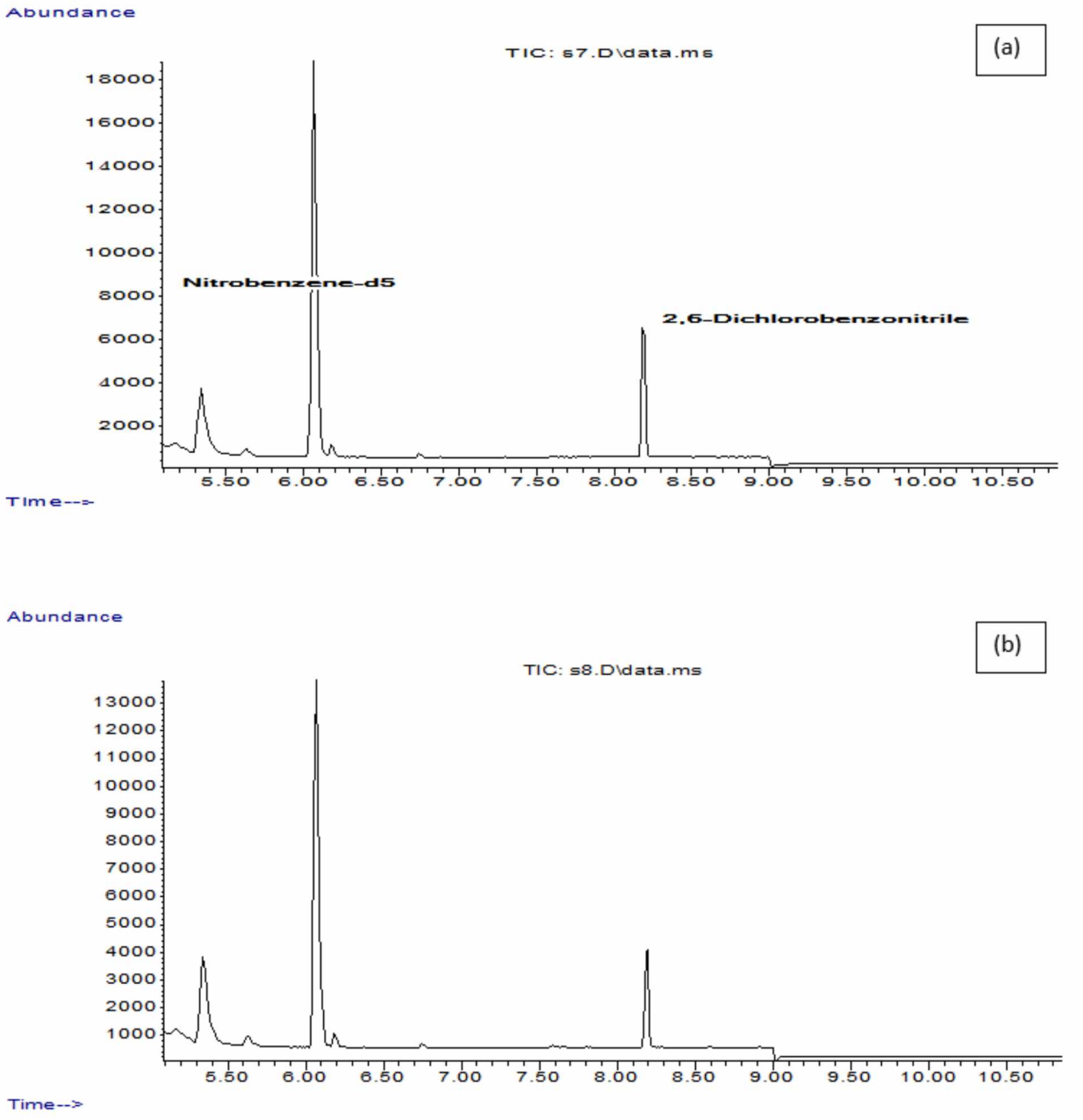

Figure 4.8. (a) Chromatograph for first 38.75PV of Xanthan gum outflow. (b) Chromatograph for second 38.75PV of Xanthan gum outflow.

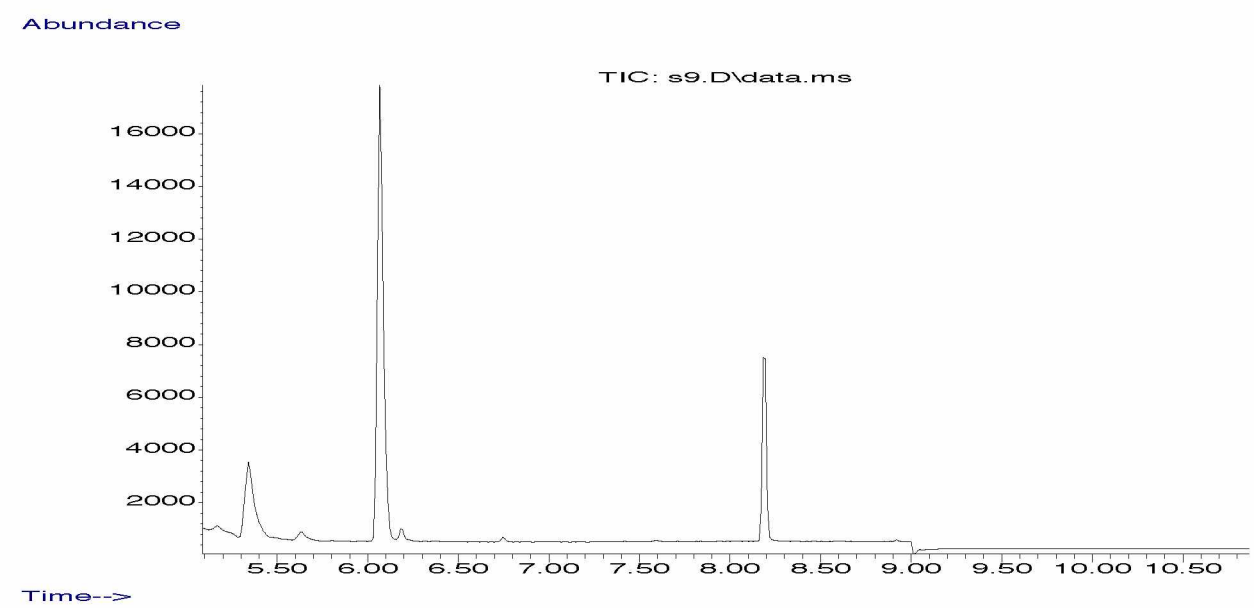

Figure 4.9. Chromatograph for third 77.5PV of Xanthan gum outflow.

4.4 Conclusion

With the limited set of experiments conducted at 19°C, water was most effective in remediating the 2, 6-Dichlorobenzonitrile from synthetic porous media in comparison to 0.5g/l Guar gum and 0.5g/l Xanthan gum.

4.5 References

Cox, C., 1997. Dichlobenil. Journal of pesticide reform.17, 14-20.

Gupta, B.S., and Ako, J.E., 2005. Application of Guar gum as a flocculant aid in food processing and potable water treatment. Eur Food Res Technol 221:746-751.

Mukherjee, S., Mukhopadhyay, S., Zafri, M.Z.B., Zhan, X., Hashim, M.A., and Gupta, B.S., 2017. Application of Guar gum for the removal of dissolved lead from wastewater. Industrial Crops and Products 111, 261-269

Porazzi, E., Martinez, M.P., Fanelli, F., Benfenati, E., 2005. GC-MS analysis of dichlobenil and its metabolites in groundwater. Talanta. 68, 146-154

Tosco, T., Gastone, F., Sethi, R., 2014. Guar gum solutions for improved delivery of iron particles in porous media (part 2): Iron transport tests and modeling in radial geometry. Journal of Contaminant Hydrology 166, 34-51.

Zhong, L., Oostrom, M., Truex, M.J., Vermeul, V.R., Szecsody, J.E., 2013. Rheological behavior of Xanthan gum solution related to shear thinning fluid delivery for subsurface remediation. Journal of Hazardous Material 244-245, 160-170.

Chapter 5 Conclusion

Rheological Analysis Results

- In terms of viscosity, the effect of temperature change was higher on Guar gum than Xanthan gum, especially at mid to high concentrations. At any temperature used for the experiments, low to mid concentrations of Xanthan gum have higher viscosity compared to same concentrations of Guar gum. However, at high concentration Guar gum displayed higher viscosity.
- Xanthan gum behaved as **non-Newtonian** shear-thinning fluid for all the selected range of temperature and concentration. Guar gum also displayed non-Newtonian shear thinning behavior only for mid to high concentrations with an approximation to Newtonian behavior for low concentrations.
- An increase in non-Newtonian shear thinning behavior was observed with increase in temperature for mid to high concentrations of Xanthan gum. However, non-Newtonian shear thinning behavior of mid to high concentration of Guar gum showed neither decrease nor increase with change in temperature. Both polymers displayed improvement in shear thinning behavior with increase in concentrations.

Flow Experiments results

- Infiltration depth of both Newtonian and non-Newtonian fluids would decrease with the decrease in the temperature because of the change in their properties like dynamic viscosity, density and angle of contact. Infiltration of Xanthan gum solution is less compared to the Guar gum solution and water.
- Establishment of stable thermal profile and thermal equilibrium are critical for flow in synthetic porous media in non-isothermal flow conditions.

Contaminant remediation result

- With the limited set of experiments conducted at 19°C, water was most effective in remediating the 2, 6-Dichlorobenzonitrile from synthetic porous media in comparison to 0.5g/l Guar gum and 0.5g/l Xanthan gum.

Future Work

- Flow experiments in tight temperature-controlled chamber with low heat transfer material needs to be investigated. Other factors that may be considered is using non-Newtonian fluids of slightly larger concentration, such as 1.0 g/l. Use of Xanthan gum as a non-Newtonian fluid needs to be considered because of its less sensitivity towards the change in temperature.
- Contaminant remediation at different temperatures from hierarchical porous media using higher concentration of polymer needs to be investigated. Non-Newtonian fluids having higher concentration of polymers provide better shear thinning (lower value of n) and higher viscosity (better scouring). The hierarchical porous media must be constructed using longer tubes of different diameters. Longer length tubes not only hold higher quantity of contaminant in each tube for quantification purposes but also assist in observing the effectiveness of shear thinning of non-Newtonian fluid in remediating contaminant from smaller diameter tubes.

  Comparison of effectiveness of non-Newtonian fluid with water may be done by observing the amount of contaminant removed from each tube of specific diameter. For example, for first 200 pore volume water may remove the contaminant faster from larger diameter tubes compare to smaller tubes. Whereas, non-Newtonian fluid may remove contaminant simultaneously from both larger and smaller tubes. Comparison of residual contaminant in each tube may provide the effectiveness of each fluid type in remediating the contaminant from smaller diameter tubes.

References

Balhoff, M.T., and K.E. Thompson. 2006. A macroscopic model for shear thinning flow in packed beds based on network modeling. Chem. Eng. Sci. 61(2):698–719. doi:10.1016/j.ces.2005.04.030.

Barnes, D.L., W. Rhodes, S. Frutiger, R. Ranft. 2007. Persistence of Herbicides in a Subarctic Environment. In proceedings of the 8th International Symposium on Cold Regions Development, Tampere, Finland, September 25-27.

Blokker, N., 2014. Analysis of Alginate-Like Exopolysaccharides for the Application in Enhanced Oil Recovery. Master Thesis, Delft University of Technology, Delft, The Netherlands, 18 September 2014.

D'Cunha, N.J., and D. Misra, 2005: A Review of Enhanced Remediation Methods for Subsurface Dense Non-aqueous Phase Liquid Spills Employing Permeability Modification, World Journal of Engineering, 2(1): 69-80.

D'Cunha, N.J., D. Misra and A. Thompson, 2009: An Investigation into the Applications of Natural Freezing and Curdlan Biopolymer for Permeability Modification to Remediate DNAPL Contaminated Aquifers in Alaska, Cold Regions Science and Technology, DOI: 10.1016/j.coldregions.2009.05.005, 59:42-50.

Di Federico, V., Pinelli, M., and Ugarelli, R., 2010. Estimates of Effective Permeability for non-Newtonian Fluid Flow in Randomly Heterogeneous Porous Media, Stoch Envirn Res Risk Assess, 24: 1067-1076.

Gillham, R.W., and O'Hannesin, S.F., 1994. Enhanced degradation of halogenated aliphatics by zerovalent iron. Ground Water 32, 958–971.

Hove, K.; Pedersen, O.; Garmo, T.H.; Hansen, H.S.; Staaland, H. Fungi, 1990. A major source of radiocesium contamination of grazing ruminants in Norway. Health Phys., 59, 189–192.

Jung, J., Jang, J., and Ahn, J., 2016. Characterization of a Polyacrylamide Solution Used for Remediation of Petroleum Contaminated Soils, Materials, 9, 16: 1 – 13.

Lake, P.S., 2008. Flow-Generated disturbances and Ecological Responses: Floods and Droughts. In Hydroecology and Ecohydrology: Past, Present and Future; Wiley Press: New York, NY, USA; pp. 75–92.

Palaniappan, M., Gleick, P.H., Allen, L., Cohen, M.J., Christian-Smith, J., and Smith, C., 2010. Clearing the Waters: A Focus on Water Quality Solutions, United Nations Environmental Programme Publication, Nairobi, Kenya, pp. 89.

Pollock, T.J.; Thorne, L.; Yamazaki, M.; Mikolajczak, M.J.; Armentrout, R.W., 1994. Mechanism of bacitracin resistance in gram-negative bacteria that synthesize exopolysaccharides. J. Bacteriol., 176, 6229–6237.

Sorbie, K., 1991. Polymer-Improved Oil Recovery; Springer Science Business Media: Berlin, Germany, 1991; Chapter 1; pp. 1–5.

Velimirovic, M., Tosco, T., Uyttebroek, M., Luna, M., Gastone, F., De Boer, C., Klaas, N., Sapion, H., Eisenmann, H., Lassson, P., Braun, J., Sethi, R., and Bastiaens, L., 2014. Field Assessment of Guar Gum Stabilized Microscale Zerovalent Iron Particles for In-situ Remediation of 1,1,1-Trichloroethane, Journal of Contaminant Hydrology, 164: 88 – 99.

Zhong, L., Oostrom, M., Truex, M.J., Vermeul, V.R., Szecsody, J.E., 2013. Rheological behavior of Xanthan gum solution related to shear thinning fluid delivery for subsurface remediation. Journal of Hazardous Material 244-245, 160-170.

Appendix

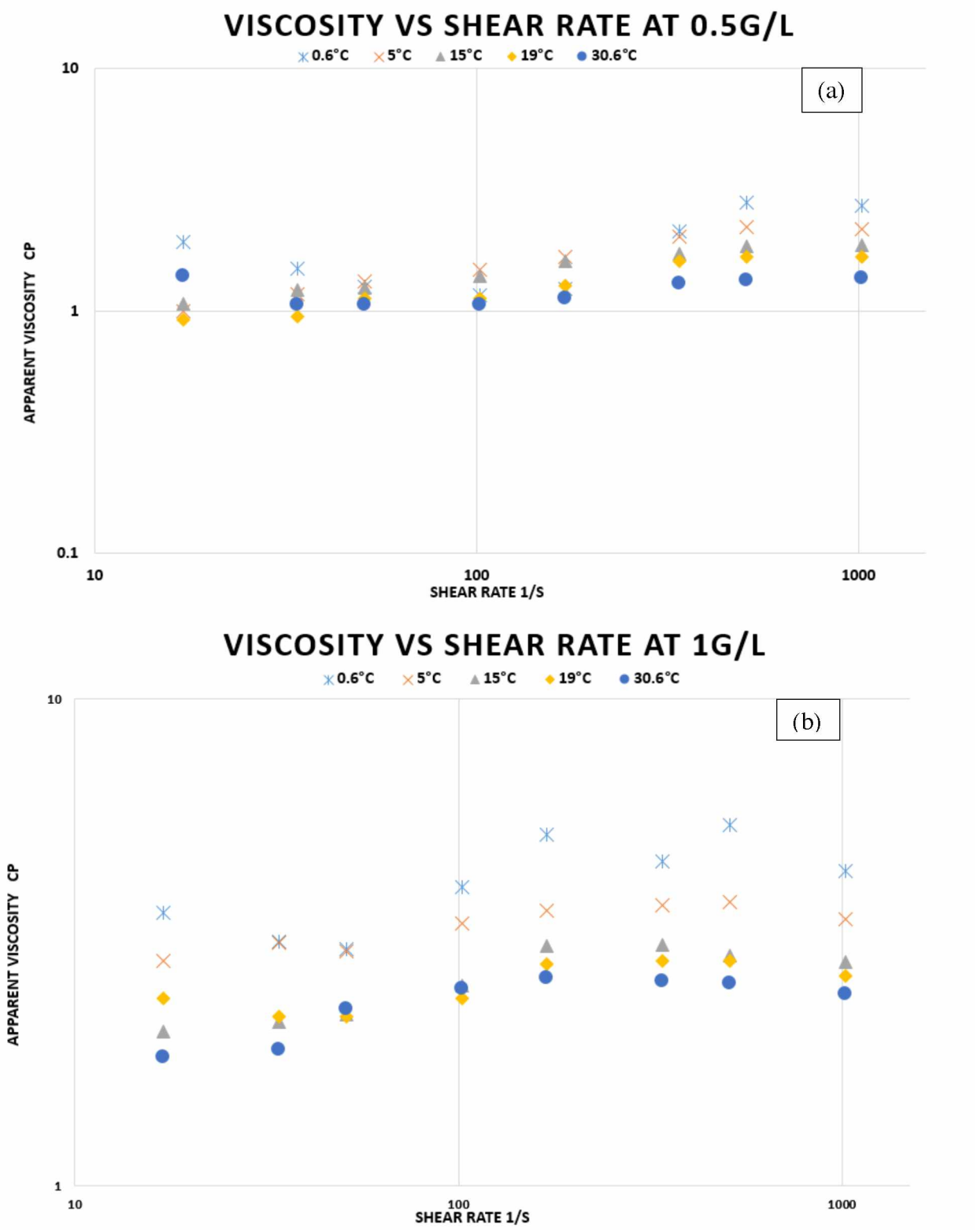

Figure A1. Viscosity vs Shear rate for Guar gum concentrations of 0.5g/l (a) and 1g/l (b).

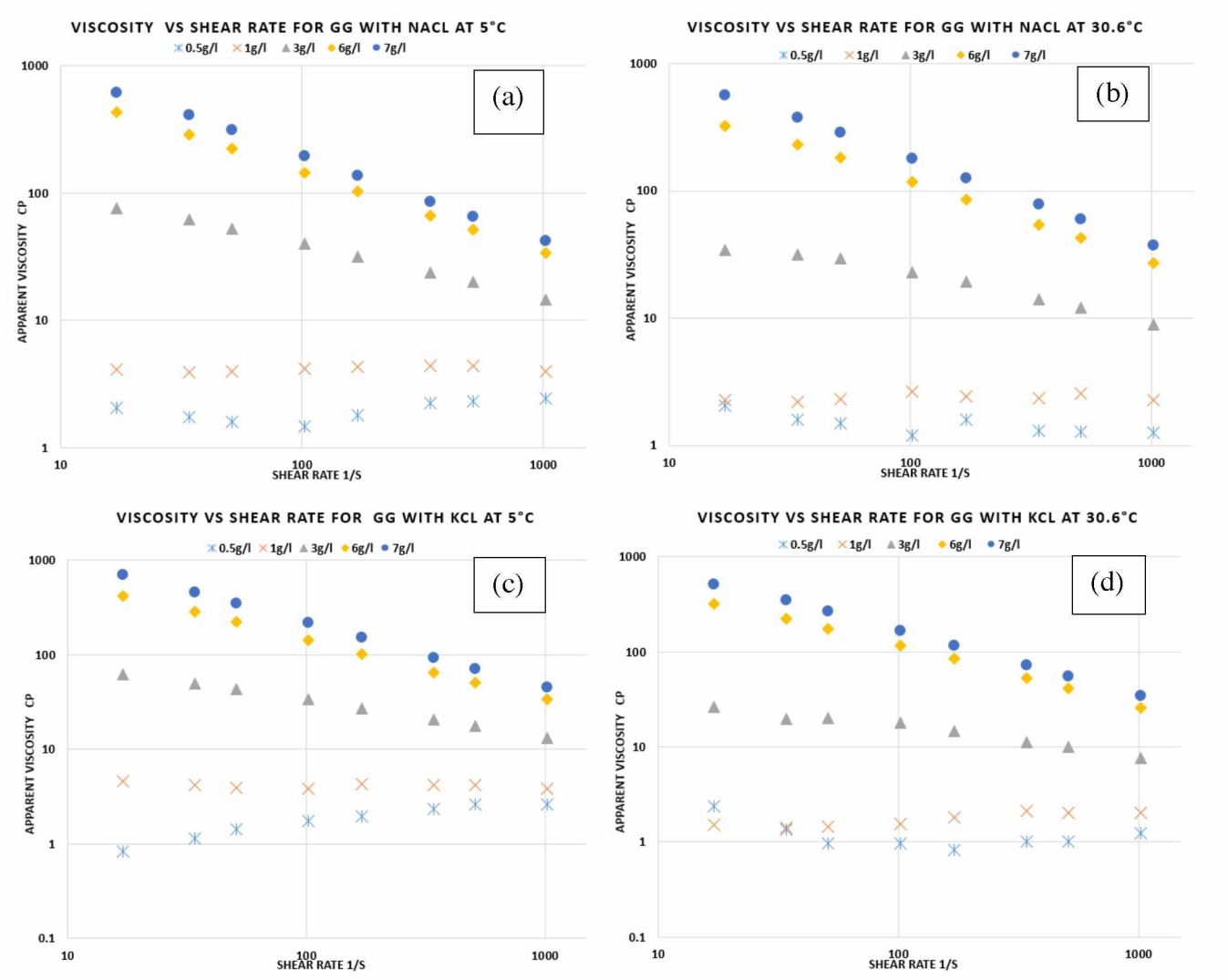

Figure A2. Viscosity vs shear rate for Guar gum with salts at 5°C and 30.6°C. (a) Different concentrations of Guar gum with 10g/l Sodium Chloride at 5°C (b) Different concentrations of Guar gum with 10g/l Sodium Chloride at 30.6°C (c) Different concentrations of Guar gum with 10g/l Potassium Chloride at 5°C (d) Different concentrations of Guar gum with 10g/l Potassium Chloride at 30.6°C

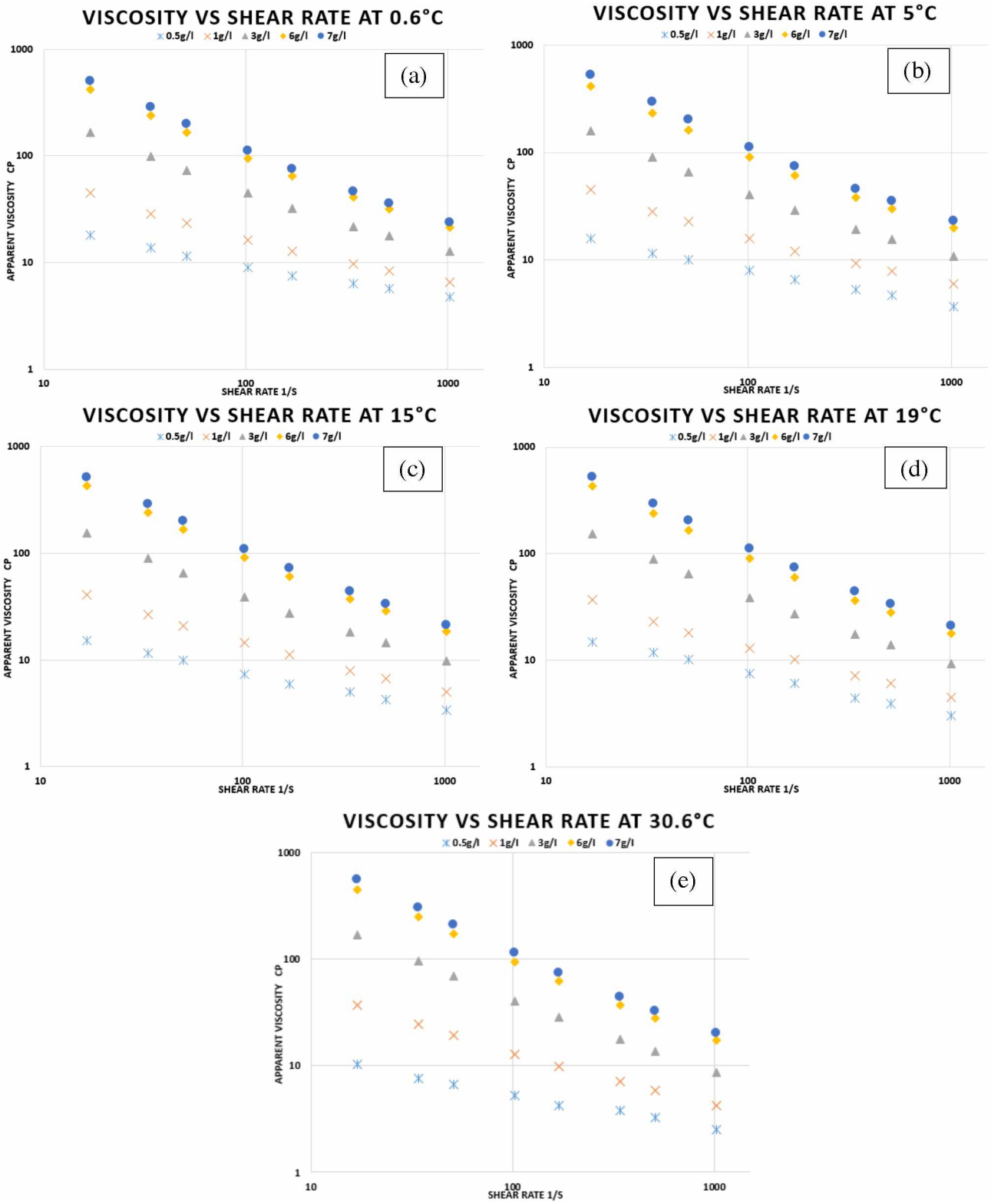

Figure A3. Variation of apparent viscosity with the increase in shear rate for different concentrations of Xanthan gum at different temperatures

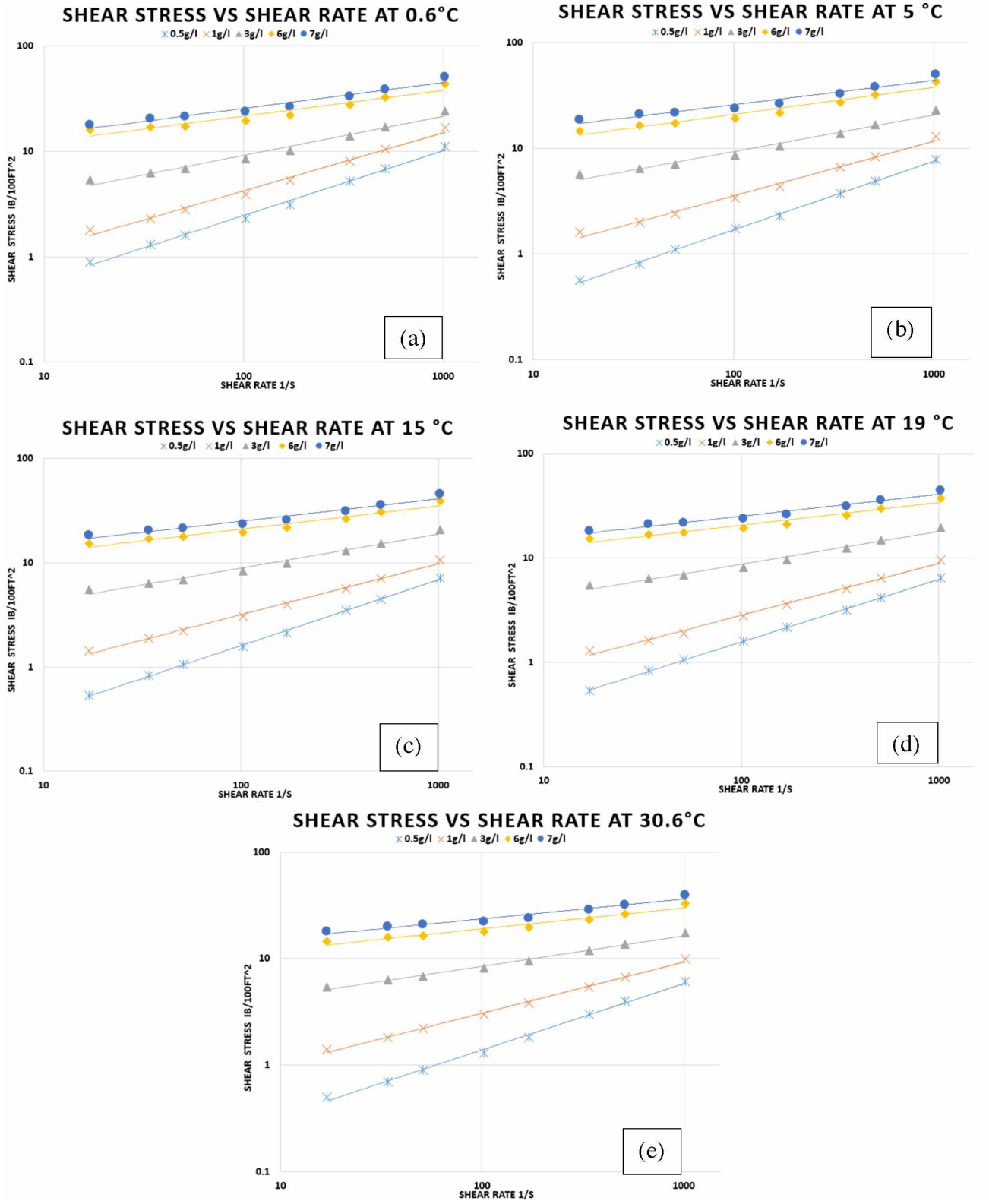

Figure A4. Consistency curves for different concentration of Xanthan gum at different temperatures